Investigation of Sampling Techniques for Drug Delivery

by

Heidi Jo Holovics
B.A., University of Minnesota, Morris, MN, 2002

Submitted to the Department of Chemistry and the Faculty of the
Graduate School of the University of Kansas in partial fulfillment of
the requirements for the degree of Doctor of Philosophy

_____
(Committee Chair)

_____

_____

_____

_____
(Committee Members)

Date defended:_____

The Dissertation Committee for Heidi Jo Holovics certifies
that this is the approved version of the following dissertation:

Investigation of Sampling Techniques for Drug Delivery

_____
(Committee Chair)

_____

_____

_____

_____
(Committee Members)

Date approved:_____

Abstract

Heidi Jo Holovics, Ph.D.
R.N. Adams Institute of Bioanalytical Chemistry
Department of Chemistry, May 2007
University of Kansas

Suitable techniques for monitoring drug delivery are essential for drug screening and determination of proper dosing regimens. Current *in vivo* dermal sampling techniques are not optimal for drug delivery studies as they are not able to determine true dermal concentrations and do not provide continual sampling in the same skin region. The focus of this research has been to utilize microdialysis sampling for the determination of drug delivery following dermal applications and as a novel *in vitro* drug transport design.

Initial work focused on an application of microdialysis by determining lidocaine flow around an incision under both passive and iontophoretic conditions in the CD hairless rat. Compared to traditional dermal sampling techniques, cutaneous microdialysis was an ideal technique for this application as it allows continual sampling in site specific regions. The use of iontophoresis on a sutured incision was found to enhance drug flow through the incision.

One of the difficulties with microdialysis is it is limited to the laboratory setting. Ultrafiltration is a promising alternative to microdialysis, as sampling can occur while the animal is freely moving. This study compared dermal microdialysis and ultrafiltration sampling in the Sprague Dawley rat and the Göttingen minipig. The use of cutaneous ultrafiltration sampling was determined to an insufficient

sampling technique as it extracted extracellular fluid from both the dermal and subcutaneous regions resulting in delayed drug responses and underestimation of the true drug concentration.

The osmotic pump is a potential alternative to the traditional infusion pump used for microdialysis sampling as it is implanted internally and allows the animal to be freely moving. Overall, the use of an osmotic pump proved to be an effective pumping device for cutaneous microdialysis sampling. Large variations in flow rates were found however the use of an internal standard reduced the variation to an acceptable range.

Finally, an investigation into the use of a new drug transport design that utilizes a cell-coated linear microdialysis probe. Several cell culture parameters including sterilization, substrate coating, and seeding densities were explored. The results from this study suggest that the reliability of this design was insufficient for determining drug penetration.

Acknowledgements

Foremost, I would like to thank my advisor, Dr. Craig Lunte, for his infinite wisdom and guidance during my time at KU. I still recall the conversation we had at a BBQ on his deck when I was an REU student. It was because of him that I decided to pursue my doctorate in chemistry. It was only fitting that I completed it in his group. I could have not asked for a better advisor! I would also like to thank the remaining analytical faculty at the University of Kansas for their open door policies and willingness to chat. I would like to thank my committee Dr. Heather Desaire, Dr. Robert Dunn, Dr. Paul Hanson, and Dr. Kenneth Audus for their valuable time and encouragement.

A special thanks for all the collaborators that have contributed to my research and scientific knowledge. I would especially like to thank Dr. Kenneth Audus and Dr. Ronald Borchardt and their groups for being able to use their lab facility and cell cultures lines and for the great advice they were able to offer. I also want to acknowledge Dr. Mike Thompson, a pathologist from Lawrence Memorial Hospital, who processed all of my histology samples throughout the years. Thanks to Dr. Carter Anderson and Dr. Barry Levine who collaborated with me for the iontophoresis project. They have allowed me to gain some invaluable experiences and given me an insight into the industrial setting. Finally, thanks to Dr. Malcolm Smyth and Dr. Tony Killiard for allowing me to work in their labs when I was in Ireland and for their assistance and support while I was in Dublin.

Many thanks are owed to the prior and current Lunte group members. Their advice and suggestions were always appreciated. In particular, I would like to thank Dr. Shannon Vandaveer for her hard work and dedication on the pig project. She made those long hours in the basement of Malott fly by!

Finally I would like to thank my family and friends. To the volleyball and softball teams I have played on over the years. What better way to relieve some aggression than smacking some balls around! Erin, I will never forget our Sex in the City nights! To Holly, I appreciate the words of encouragement during my undergraduate degree and now my doctorate degree. You have never given up on me and I really appreciate it! To my parents, Orrin and Yolanda, I can't thank you enough for you continual love and guidance throughout my life. My new parents-in-laws, David and Connie, for their added support and encouragement. To my siblings, Randy, Erica, Twyla, and Tanya, who have been great role models! Each one of them has inspired me with their dedication, hard work, and tenacity. Last but not least, I am forever grateful to my husband Tom. He has given me the drive to continue to work each day. His love and patience is never ending. I can't thank him enough for his continued support and am excited to spend the rest of my life with him!

Table of Contents

Chapter One: Microdialysis as a Tool for Drug Permeability Studies

Chapter Two: Investigation of Drug Delivery by Iontophoresis in a Surgical Wound Utilizing Microdialysis

Chapter Three: Ultrafiltration and Microdialysis Sampling in the Göttingen Minipig and Sprague Dawley Rat

Chapter Four: Osmotic Pump as the Pumping Device for Microdialysis Sampling

Chapter Five: Investigation of the Optimization of Cell-Coated Linear Microdialysis Probes for *In Vitro* Drug Penetration Studies

Chapter Six: Conclusions and Future Work

List of Tables

List of Figures

Chapter One

Microdialysis as a Tool for Drug Permeability Studies

1.1 Drug Administration Methods

Prescription drug sales are a continually expanding market that accounted for nearly $275 billion in sales for the U.S. and almost $650 billion in worldwide sales for the year 2006 [1, 2]. The onset of new types of dosage forms, pharmaceutical advertisements, and consumer awareness has resulted in an expanded market. Traditionally, dosage forms consisted of injections, oral formulations, and topical cream. Current delivery methods have expanded to additional delivery routes and are generally divided into the following categories: parental, oral, buccal and sub-lingual, vaginal, transdermal, nasal, pulmonary, and ocular [3].

As the emergence of new potential drug entities or delivery methods are developed, proper testing procedures need to assess the efficacy and bioavailability of these test compounds. Microdialysis is an ideal technique as it has multiple functionalities that range from *in vitro* drug binding studies to *in vivo* drug monitoring, allowing for full pharmacokinetics data. Therefore, this research focused on utilizing microdialysis for several applications that include the determination of drug delivery in an incised skin system, the evaluation of an alternative dermal model, the use of a non-restricted pumping device, and its application as a pre-screening drug permeability device.

1.2 Dermal Drug Delivery

Since the approval of the first motion sickness patch in 1979, transdermal drug delivery has continued to thrive as a viable delivery route. In 2004, the U.S. market for transdermal patches was reported to be more than $3 billion [4, 5]. Transdermal delivery is an ideal route for patients as it is a relatively pain free route of administration and has extended release properties, eliminating multiple dosing schemes. In addition, dermal administration allows for a direct delivery route and avoids the harsh environment of the gastrointestinal tract and metabolism in the liver.

One of the major drawbacks to dermal delivery is the limited number of drugs that can be delivered via this route. As described in Section 1.2.1, the structured nature of the skin restricts the passage of the majority of molecules. Generally dermal delivery is limited to compounds that have a small molecular weight, are highly lipophilic, or are extremely potent [5, 6]. To overcome these difficulties numerous chemical and physical methods have been developed.

1.2.1 Skin Structure

Mammalian skin is a versatile tissue that serves primarily as a protective entity and as a contributor in thermoregulation. In addition, it provides several secondary functions for the body that include sensation and a route for excretions. It is a highly organized unit composed of multiple layers which help to maintain its structure and functionality (Figure 1.1). The skin can be divided into the two main layers of the epidermis and the dermis [6-10].

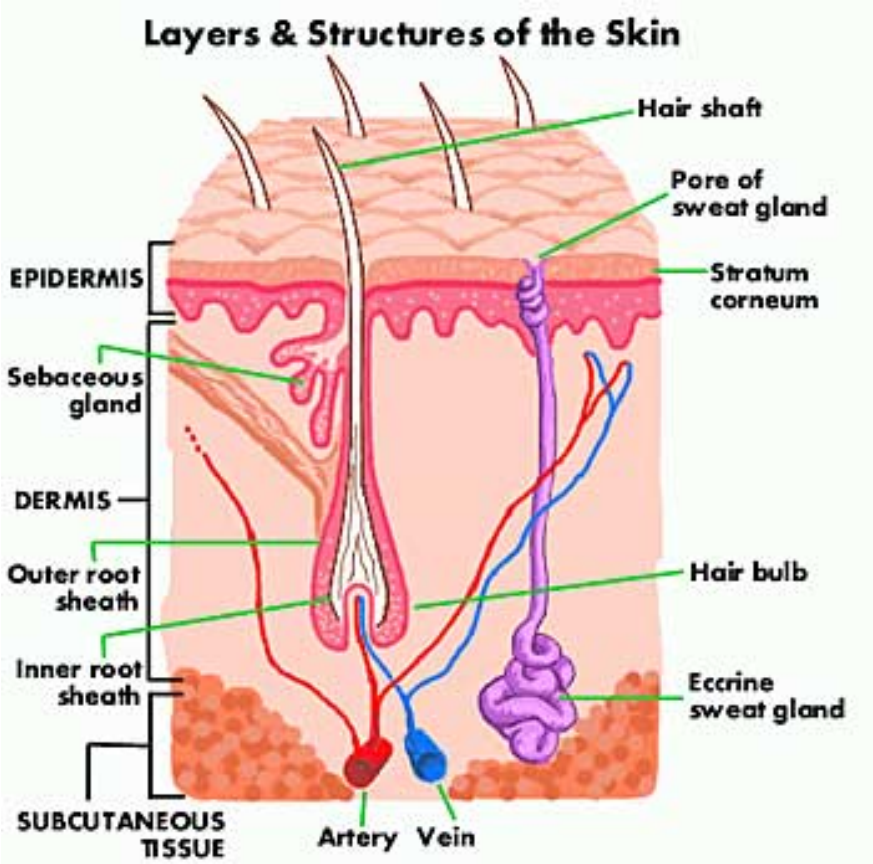

Figure 1.1. Diagram of the skin. Picture from http://www.healthy-skin-guide.com/skin-diagram.html

The epidermis is comprised of four distinct layers, listed in order from the inside to the outside, of the stratum basale or germinativum, stratum spinosum, stratum granulosum, and the stratum corneum. Approximately 95% of the epidermis is constituted of keratinocytes. The various layers represent the stages of differentiation of keratinocytes until the final layer of the stratum corneum which is composed of dead, flattened keratinized cells called corneocytes. The stratum corneum is a highly organized layer best described by Peter Elias as the brick and mortar organization, where the protein rich corneocytes signify the bricks and the lipid layers that form the unified formation as the mortar. This cohesive structure helps regulate water loss from the body and maintains a defensive barrier for the body [7-11].

The dermis constitutes the majority of the skin layer and is composed of connective tissue, more specifically collagen and elastin, which provides support and elasticity. It is highly vascularized to approximately 0.2 mm below the skin surface. This blood supply is crucial for temperature regulation, nutrient supply, and wound repair. In addition, the vascular system serves as a sink for drug penetration which sets up a concentration gradient from the drug source, one of the driving forces for drug delivery. Finally, three appendages originate within the dermis and include hair follicles, sebaceous glands, and eccrine glands [7-11].

Drug delivery through the dermis is limited due to the highly restrictive nature of the stratum corneum. Permeation across the skin can occur either by the skin appendages or through the stratum corneum. Skin appendages compose

approximately 0.1 percent of the total skin surface area. The amount of drug penetration through these pores is generally insignificant but is largely dependent on the size and charge of a molecule. Penetration through the stratum corneum occurs by either the intercellular or the transcellular pathways. The major penetration route is intercellular or through the continuous intertwining lipid layer while transcellular penetration is generally limited as partitioning has to occur between both the hydrophilic corneocytes and the hydrophobic lipids [9, 10].

1.3 Current Methods for Monitoring Dermal Penetration

To gain a better understanding of dermal penetration, an appropriate method of evaluation is required. There are a variety of techniques that have been developed for the determination of drug penetration through the dermis. The following section presents a short review of the past and present dermal sampling techniques.

1.3.1 In Vitro Calibration Techniques

In vitro dermal penetration studies are generally performed using either Franz diffusion cells or Side-by-Side diffusion cells. Ideally, the use of human cadaver skin is preferred; however, several animal skin models and artificial membranes have been previously used [10, 12, 13]. Diffusion studies offer the benefit of sampling directly below the skin membrane, allow for high throughput, maintain a well controlled experimental setting, and allow testing of potentially toxic compounds. Some of the major drawbacks to *in vitro* sampling are a change in skin organization after a freeze-

thaw cycle and the lack of a circulatory system [8, 14]. Previous studies have shown that *in vitro* transdermal studies often overestimate the drug penetration in comparison to the *in vivo* studies [14, 15].

1.3.2 Skin-Sandwich Flap

The skin sandwich flap or isolated tissue model is a unique method for the determination of percutaneous absorption, as it contains an isolated blood supply to a skin section that allows for both local and systemic drug determination. For these studies, a flap of skin (ideally human) is grafted onto a laboratory rodent and used for *in vivo* absorption studies. Data collection is of the drug plasma concentration from the isolated region, the overall plasma concentration, and the concentration remaining in the skin flap. This technique has been utilized for dermal penetration studies of benzoic acid and β-estradiol [16-18]. This technique is limited however as it is a procedure that is time-consuming, costly, and has limited survival rates [10].

1.3.3 Pharmacological Response

An alternative method to monitor drug absorption through the dermis is by indirectly measuring the pharmacological response. These responses could include changes in blood pressure, more commonly vasoconstriction as a drug response. One major disadvantage to this method is that it is limited to compounds that illicit a biological response and often lack methods to monitor the response [10, 12, 19].

1.3.4 Surface Recovery and Disappearance

These two related techniques monitor the applied drug concentration on the surface of the skin. Surface recovery measures transdermal absorption by removing the drug residue on the surface and determining the drug loss. The difference in the initial concentration and the drug recovered is assumed to be the amount of drug absorbed. Alternatively, surface disappearance monitors the loss of a compound on a skin surface. The use of x-ray fluorescence and ATR/FT-IR are two techniques that have demonstrated uses for surface disappearance measurements. Disadvantages to these particular methods are that the subject is exposed to external radiation and the compound must have a characteristic spectra within the range needed for measurements [20, 21]. Surface recovery and disappearance lack in their ability to provide information about drug concentrations in different regions of the skin [10, 13, 22, 23]. Both techniques assume that the difference in drug concentration is due to absorption into the skin and don't take into account other means of loss such as evaporation or metabolism.

1.3.5 Absolute Topical Bioavailability

Another more common determination of transdermal delivery is the measurement of the compound in either blood or urine after administration. Using this technique, the drug levels can be monitored throughout the course of application. The major drawback with this method however is that drug concentrations are generally extremely low in blood or urine after dermal application and often require

extremely sensitive assays. Also measurements are limited to the total drug concentration and do not provide information about the actual dermal concentration [10, 13, 22, 23].

1.3.6 Skin Punch Biopsy

The skin punch or shave biopsy is one of the most invasive techniques but is also one of few that allows for the determination of drug concentrations at specific locations within the skin layers. Shave biopsies contain mainly the epidermis and parts of the dermis while the punch biopsy retrieves tissue up to part of the subcutaneous layer. These specific layers can easily be separated mechanically or by heating techniques [12]. Besides being quite invasive, another disadvantage to this technique is that it measures the total drug concentration and not the pharmacologically active unbound drug quantity [10, 13, 22, 23].

1.3.7 Suction Blister

Another well established method for the determination of transdermal drug distribution is the suction blister technique. This method employs the creation of a blister by the application of a vacuum which separates the epidermis from the dermis. Following drug administration, the suction blister fluid and the stratum corneum-epidermis sheets can utilized for drug concentration. In order to obtain complete pharmacokinetics data, the formation of multiple blisters is required [10, 13, 22, 23]. Some of the difficulties encountered from blister fluid sampling are variations in

blister size, amount of inflammation and, proper timing for the formation of the blister. In addition, delayed response and lower drug concentration in the blister fluid have been reported in comparison to plasma data [24, 25].

1.3.8 Tape Stripping

One of the more commonly used methods for the determination of percutanous absorption is tape stripping. Drug concentrations of the stratum corneum are obtained by first removing the stratum corneum using adhesive tape strips and then determining the amount of total drug present. Overall, drug content in only the top regions of the skin is determined. One of the disadvantages for this technique is that the amount of stratum corneum removed by tape stripping is variable as it is dependent on both the adhesive properties and the regional location of the body. In addition, to obtain full pharmacokinetics data multiple regions need to be evaluated which enhances the variability of the data. [10, 13, 22, 23, 26-28].

1.3.9 Microdialysis

Finally, cutaneous microdialysis is a relatively new technique that has been under review in the literature [29-34]. Its use for cutaneous sampling was first demonstrated in 1991 for the determination of ethanol absorption across human skin [35]. Ault et al. further verified cutaneous microdialysis by directly comparing microdialysis results of a probe placed in an excised skin sample to that of the Franz cell receptor [36]. Two years later he illustrated the importance of using an *in vivo*

skin model as the dermal concentration from *in vitro* excised skin was 40-fold greater compared to *in vivo* intact skin [14].

In general, a small microdialysis probe is implanted into the dermis and perfused with a solution that is physiologically equivalent to its surrounding tissue. Due to a concentration gradient, small analytes will diffuse across the membrane and be collected for further analysis. A more extensive review of this technique can be found in Section 1.4. It offers several advantages over the previously mentioned techniques. Microdialysis is minimally invasive and allows for the determination of pharmacokinetics data within the same skin region. The use of multi-probe experiments can be completed to determine drug concentrations at different penetration depths [37]. Cutaneous microdialysis also extends beyond the determination of drug profiles following oral or topical administration. Microdialysis is capable of a continuous drug delivery to a localized area. This can be utilized for further understanding of some conditions, for example sweat gland dysfunction [38].

1.4 Microdialysis Sampling

Microdialysis sampling, a subset of the more traditional dialysis, is a site specific sampling technique that has transformed the way drug delivery and distribution studies are conducted. Since its origin in the 1960s, the use of microdialysis has become widespread and integrated for the use in many studies. Its use for bioavailability has been demonstrated in numerous regions of the body that include brain, heart, liver, muscle, bone, stomach, subcutaneous tissue, cutaneous

tissue, lung, and eye [32, 39-46]. In addition, its use has been explored in drug-protein interactions and in bioprocess monitoring [47, 48].

1.4.1 Principles of Microdialysis

Microdialysis is a sampling technique used in the determination of drug concentrations at site specific locations. In general, a small dialysis fiber is implanted in the tissue of interest. This fiber possesses a molecular weight cut-off which limits the size of the compounds that can diffuse across the membrane. Due to a concentration gradient, small compounds diffuse across the membrane. If placed under static conditions equilibrium will be obtained, where the concentration of drug within the probe is equivalent to the drug surrounding the membrane. However in microdialysis, a solution that is physiological similar to the extracellular fluid within the sampling region is flushed through the probe, sweeping the drug to the outlet of the probe for analysis (Figure 1.2). Initially, this physiological solution is termed the perfusate, while the collected sample is termed the dialysate. Since the probe is not in a static environment, only a fraction of the drug outside the dialysis fiber is able to diffuse through the membrane. After some time, a steady state exchange rate is achieved. Therefore, to accurately determine the drug concentration in the selected sampling region, probe calibration is required and will be discussed in Section 1.4.3.

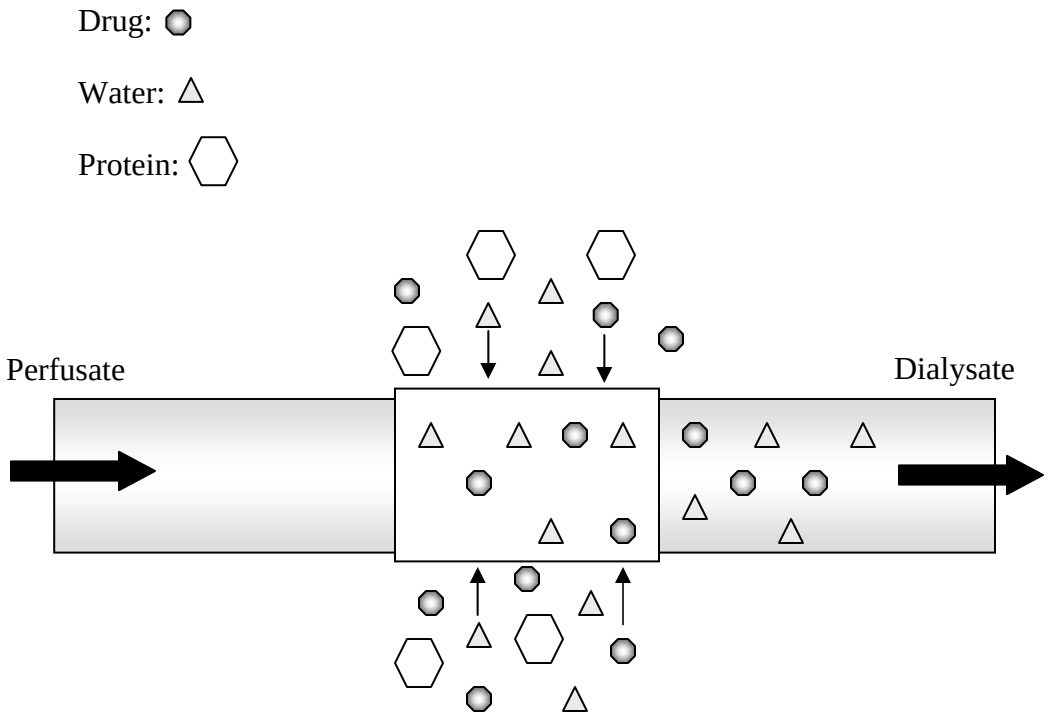

Figure 1.2. Schematic of microdialysis sampling.

1.4.2 Probe Design

As previously mentioned, microdialysis has been utilized in a variety of tissues throughout the body. Several different probe designs have been developed for different regions of the body. The three most common microdialysis probes, linear, flexible cannula, and rigid cannula designs, can be seen in Figure 1.3. The linear microdialysis probe is a flexible design that has been used in multiple tissue regions including subcutaneous, liver, heart, and cutaneous. It consists of a dialysis fiber positioned between the inlet and outlet tubing generally composed of Teflon, PEEK, polyethylene, fused silica, or polyimide. The flexible concentric microdialysis probe is an alternative design that is generally implanted in a blood vessel for the determination of the free blood concentrations. In comparison to the linear microdialysis probe design it is less invasive as it allows for a single point of entry. In comparison to the linear probe however, it is slightly larger in dimension. A third probe design consists of a rigid concentric cannula design. The general design consists of a piece of stainless steel tubing within a shorter piece of stainless steel tubing. The internal tubing is covered with the dialysis membrane. Due to its rigidity, this probe is limited in the tissue locations and is generally used for brain microdialysis for the monitoring of neurotransmitters [43, 46, 49].

The dialysis fiber is one of the most important features of the microdialysis probe. A variety of membrane compositions are commercially available and include polycarbonate, cellulose acetate, regenerated cellulose, and polyacrylonitrile [43, 49, 50]. Traditionally, molecular weight cut-offs utilized for microdialysis experiments

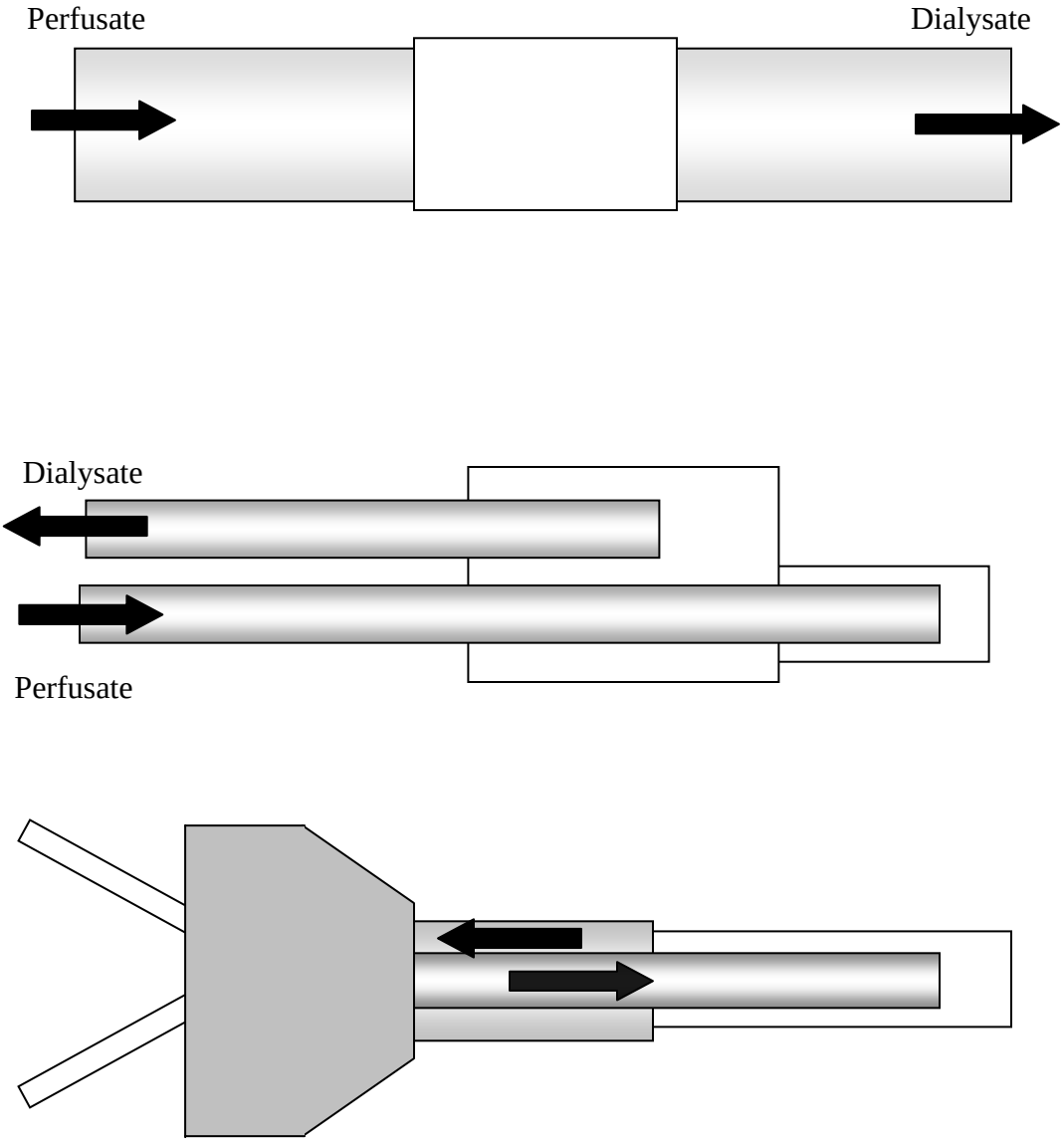

Figure 1.3. Schematic of three probe designs from top to bottom: linear, flexible cannula, rigid cannula.

ranged from 5 – 30 kDa. However with continued interest in sampling macromolecules and proteins, dialysis fibers with molecular weight cut-offs of 100 – 3000 kDa are becoming available [50, 51].

1.4.3 Calibration

To get a better estimation of the drug concentration in a specific tissue, the calibration of each individual probe needs to be completed for every experiment. Several different calibration techniques have been developed. A brief summary of each technique with the positive and negative aspects will be discussed.

1.4.3.1 *In Vitro*

Prior to the start of a microdialysis experiment, probe response for each analyte should be completed *in vitro* to verify proper behavior of the analyte and the microdialysis system. This can be completed by comparing results between both delivery and recovery experiments. For a recovery experiment, the microdialysis probe is placed into a warmed Ringer's bath (37 ˚C) with a known concentration of analyte. The microdialysis probe is perfused with a Ringer's solution and the dialysate is collected and analyzed. The probe extraction efficiency for recovery (EE_R) is then calculated using the following relationship:

$$EE_R = \frac{C_d}{C_s} \quad (1)$$

where C_d is the concentration of the dialysate and C_s is the concentration of the sample. Results obtained from a recovery experiment should then be compared to delivery experiments. To complete these experiments, a known concentration of analyte is perfused through a microdialysis probe placed in a warmed Ringer's solution (37 ˚C). The delivery extraction efficiency (EE_D) can then be calculated using the following equation:

$$EE_D = \frac{C_p - C_d}{C_p} \quad (2)$$

where C_d is the concentration of the dialysate and C_p is the concentration of the perfusate. In a well behaved system, the extraction efficiency by recovery should be equal to the extraction efficiency by delivery ($EE_R = EE_D$) [52]. Possible deviations to this relationship could indicate possible adhesion of the analyte to either the inlet or outlet tubing or to the microdialysis fiber [53, 54].

Generally extraction efficiencies determined *in vitro* are higher than results determined *in vivo* due to differences in the probe environment. In most tissue, the drug diffusion pathway is hindered by cellular structures, resulting in lower extraction efficiencies [55, 56]. However in hydrodynamic regions like the blood vessel, the extraction efficiency determined *in vivo* should be equal to *in vitro* results. This

relationship can be useful in refining surgical techniques [56]. Efforts have been made to improve the agreement between *in vitro* and *in vivo* extraction efficiencies. For instance, *in vitro* recovery experiments performed in serum are more comparable to the *in vivo* calibration results [57, 58].

1.4.3.2 No-Net-Flux

The ultimate calibration method for microdialysis is the no-net-flux method. Using this method, several different concentrations which encompass the expected drug concentration of the analyte is perfused through the microdialysis probe. If the analyte concentration in the tissue is greater than the perfusate, then the drug will diffuse through the membrane into the dialysate. However, if the drug concentration in the perfusate is greater than the surrounding tissue, then the drug within the microdialysis fiber will diffuse into the tissue. The difference in the dialysate and perfusate concentrations (C_p-C_d) can be plotted against the concentration of the perfusate. When the concentration in the tissue is equal to the concentration in the perfusate, no overall flux of drug across the membrane occurs. Therefore, the intersection of the x-axis of the no-net-flux plot is the tissue concentration. In addition, the slope of the line is the extraction efficiency determined by the no-net-flux. Although this is the ideal calibration technique, it is a time consuming method that requires the concentration in the tissue to remain constant during the calibration procedure [59, 60].

1.4.3.3 Delivery

A less time consuming alternative to the no-net-flux method that is commonly performed is an *in vivo* delivery of the analyte of interest. A comparison between the no-net-flux and *in vivo* delivery methods was completed by Song and Lunte in both muscle and adipose tissue. Similar extraction efficiencies were found for both calibration techniques [55]. As previously described, the extraction efficiency by delivery of an analyte can be determined by perfusing a known concentration of an analyte through the microdialysis probe. After steady state has been achieved, the extraction efficiency by delivery can be calculated using Equation 2. Since the extraction efficiency by delivery is equal to the extraction efficiency by recovery, this calculated fraction can be used to determine the concentration within the tissue [43, 49, 52]. One of the major disadvantages to this technique is that it assumes the extraction efficiencies remain constant following dosage. Depending on the nature of the administered drug, this is not always true. As demonstrated by Song and Lunte, blood flow is an important factor in extraction efficiency [55]. Therefore, administration of a vasodilator or vasoconstrictor can dramatically affect the established delivery value.

1.4.3.4 Retrodialysis

Retrodialysis is a calibration technique that augments the calibration by delivery method. This particular method introduces a calibrator to the perfusate which can be used to monitor the extraction efficiency throughout the experiment [61,

62]. At the start of an experiment the extraction efficiency of both the analyte of interest and the calibrator are determined. This phase is termed the reference period and the ratio of the analyte of interest and the calibrator are determined. The probe is then perfused with just the calibrator until the analyte of interest is cleared from the surrounding tissue. The drug is then administered while the extraction efficiency of the calibrator is determined throughout the collection time [61, 62]. The extraction efficiency of the analyte of interest can be calculated using the following relationship:

$$EE_R = \left(\frac{C_p - C_d}{C_p} \right)_{calibrator} X \quad \left(\frac{EE_{R,drug}}{EE_{R,calibrator}} \right)_{\mathrm{Re}\, f} \tag{3}$$

where the extraction efficiency of the calibrator determined throughout the course of the experiment is multiplied to the ratio of the extraction efficiency of the drug and calibrator during the reference period [61]. When selecting an appropriate internal standard, it should have similar diffusion properties as the analyte of interest, not induce any physiological effect, and have greater than 20% extraction efficiency in order to reduce variability [61, 63].

1.4.3.5 Slow Perfusion

The flow rate in microdialysis is an important factor for extraction efficiencies. One relationship that has been used to relate flow rate to extraction efficiency is:

$$EE = \left(1 - e^{-rA/F}\right) x\, 100 \qquad (4)$$

where r is the mass transport coefficient, A the surface area of the microdialysis membrane, and F the flow rate [41]. Therefore, at low flow rates the extraction efficiency becomes large. To eliminate the need for calibration, ultraslow flow rates (less than 0.5 μL/min) can be used to achieve near 100% recovery of the analytes [41, 64]. However, this technique limits the sample volume of each sample and can be challenging for many analytical systems.

1.4.3.6 Endogenous Reference

Finally, the use of an endogenous species as a recovery marker for microdialysis sampling has been evaluated as an alternative calibration technique. Ideally, this method of calibration would be less time-consuming as no prior calibration is required and it would not require steady-state conditions prior to sampling. The use of urea and glucose has been studied as an endogenous marker. Thus far, conflicting results on their effectiveness as a marker have been reported and further work needs to be established prior to using it as a standard calibration procedure [65-67].

1.4.4 Additional Considerations

1.4.4.1 Lipophilic Compounds

One of the difficulties encountered with microdialysis sampling is the poor recovery of lipophilic compounds. This is generally due to the high protein binding efficiencies of these compounds and their ability to stick to plastic and glass commonly associated with polymeric microdialysis fibers, tubing, and collection vials [53, 54, 68]. Ongoing work has employed the addition of several additives to enhance the relative recoveries of lipophilic compounds. These include the addition of albumin, different cyclodextrins and small organic molecules such as ethanol, propylene glycol, and dimethyl sulfoxide [53, 54].

1.4.4.2 Large Macromolecules

Typically, microdialysis sampling has been of small molecular weight compounds, as molecular weight cut-offs for most membranes range from 5 kDa to 30 kDa. Continued efforts have focused on expanding the use of microdialysis to include analysis of large peptides and proteins. In particular, membranes with molecular cut-offs ranging from 100 – 3000 kDa have been explored [51, 69-73]. These studies have demonstrated that slower flow rates allow for larger protein recoveries as the contact time between the protein and membrane is increased. The use of additives to the perfusate has also shown increases in protein recoveries. For example, the use of cyclodextrins, serum proteins, detergents, and antibody-coated microspheres have all demonstrated increased relative recoveries [69, 71, 73, 74].

1.4.4.3 Tissue Damage

Another concern to be addressed is the potential of tissue damage following probe insertion. Increases in blood flow, skin thickness, and histamine levels in rats have been reported during the first 30 – 60 minutes following probe implantation into the dermis [29, 30, 75, 76]. Probe design, species, and anesthesia are some of the factors that have been shown to affect the length of the trauma. An appropriate recovery period can help minimize these initial implantation effects. After approximately 6 hours of implantation, infiltration of lymphocytes begins to occur. This later evolves to extensive lymphocyte infiltration and attachment of the cells to the microdialysis probe approximately 24 hours post-implantation [14]. For longer time studies, the addition of an internal standard is helpful in evaluating the extraction efficiency of the microdialysis probe during the course of the experiment.

1.4.4.4 Analytical Considerations

One of the difficulties encountered with microdialysis sampling is the analysis of small microliter sample sizes that contain low analyte concentrations. Typical flow rates used for microdialysis sampling range between 0.1 – 5 μL/min, generating sample volumes between 1 – 50 μL. In order to analyze the compound of interest, separation techniques are normally required and are typically completed using liquid chromatography or capillary electrophoresis. Ideally, the use of on-line sampling systems is preferred as sample loss is kept to a minimum [77, 78]. Multiple detector schemes have been utilized following separation and include ultraviolet,

electrochemical, fluorescence, and mass spectrometry. As dialysis fibers with larger molecular weight cut-offs are becoming more prevalent, additional detection methods are being utilized. These include bead based immunoassays, biosensors, protein microarrays and again mass spectrometry [51, 70, 73, 79].

1.5 Focus of this Research

The goal of this research was to utilize microdialysis for the determination of drug permeability studies across biological surfaces. An application of multi-probe microdialysis for the study of drug penetration is first presented in Chapter Two. This study looked at drug flow in an incised skin region under both passive and iontophoretic conditions. The use of microdialysis was found to be critical in this study as results obtained from other traditional dermal penetration methods would have only given part of the results which could lead to false findings. Chapter Three begins to explore alternative animal models for dermal penetration studies. This involved developing dermal ultrafiltration and microdialysis sampling techniques on the Göttingen minipig. A comparison of microdialysis and ultrafiltration sampling was then completed on the Göttingen minipig and the Sprague Dawley rat. Chapter Four presents a study on the use of an alternative pumping device for microdialysis sampling. An Alzet® osmotic pump was implanted into the subcutaneous region of the Sprague Dawley rat and utilized for cutaneous microdialysis. Finally, Chapter Five explores the uses of microdialysis for drug permeability studies in cell culture.

This design required the growth of a monolayer of cells on a microdialysis fiber in order to determine permeability across the cell monolayer.

1.6 References

1. *IMS Health Reports U.S. Prescription Sales Jump 8.3 Percent in 2006, to $274.9 Billion*. 2007 March 8 [cited 2007 March 20]; Available from: http://www.imshealth.com.

2. *IMS Health Reports Global Pharmaceutical Market Grew 7.0 Percent in 2006, to $643 Billion*. 2007 March 20 [cited 2007 March 20]; Available from: http://www.imshealth.com.

3. Hillery, A.M., A.W. Lloyd, and J. Swarbrick, *Drug Delivery and Targeting*. 2001, New York: Taylor and Francis.

4. Langer, R., *Transdermal Drug Delivery: Past Progress, Current Status, and Future Prospects.* Advanced Drug Delivery Reviews, 2004. **56**: p. 557-558.

5. Prausnitz, M.R., S. Mitragotri, and R. Langer, *Current Status and Future Potential of Transdermal Drug Delivery*. Nature Reviews, 2004. **3**: p. 115-124.

6. Brown, M.B., et al., *Dermal and Transdermal Drug Delivery Systems: Current and Future Prospects.* Drug Delivery, 2006. **13**: p. 175-187.

7. Guy, R.H. and J. Hadgraft, eds. *Transdermal Drug Delivery*. Drugs and the Pharmaceutical Sciences, ed. J. Swarbrick. Vol. 123. 2003, Marcel Dekker, Inc.: New York.

8. Menon, G.K., *New Insights into Skin Structure: Scratching the Surface.* Advanced Drug Delivery Reviews, 2002. **54**: p. S3-S17.

9. Wagner, H., et al., *Human Skin and Skin Equivalents to Study Dermal Penetration and Permeation.* Cell Culture Models of Biological Barriers, 2002: p. 289-309.

10. Walters, K.A., ed. *Dermatological and Transdermal Formulations*. Drugs and the Pharmaceutical Sciences, ed. J. Swarbrick. Vol. 119. 2002, Marcel Dekkar, Inc.: New York.

11. Williams, A., *Transdermal and Topical Drug Delivery*. 2003, London: Pharmaceutical Press.

12. Bronaugh, R.L., *Determination of Percutaneous Absorption by in Vitro Techniques*, in *Percutaneous Absorption*. 1985. p. 267-279.

13. Bronaugh, R.L. and H.I. Maibach, eds. *Percutaneous Absorption*. Dermatology, ed. C.D. Calnan and H.I. Maibach. Vol. 6. 1985, Marcel Dekker, Inc.: New York.

14. Ault, J.M., et al., *Dermal Microdialysis Sampling in Vivo.* Pharmaceutical Research, 1994. **11**(11): p. 1631-1639.

15. van Ravenzwaay, B. and E. Leibold, *A Comparison between in Vitro Rat and Human in Vivo Rat Skin Absorption Studies.* Human and Experimental Toxicology, 2004. **23**: p. 421-430.

16. Pershing, L.K., G.E. Parry, and L.D. Lambert, *Disparity of in Vitro and in Vivo Oleic Acid-Enhanced Β-Estradiol Percutaneous Absorption across Human Skin.* Pharmaceutical Research, 1993. **10**(12): p. 1745-1750.

17. Silcox, G.D., et al., *Percutaneous Absorption of Benzoic Acid across Human Skin Ii. Prediction of an in Vivo, Skin-Flap System Using in Vitro Parameters.* Pharmaceutical Research, 1990. **7**: p. 352-358.

18. Wojciechowski, Z., et al., *An Experimental Skin Sandwich Flap on an Independent Vascular Supply for the Study of Percutaneous Absorption.* The Journal of Investigative Dermatology, 1987. **88**: p. 439-446.

19. Wester, R.C. and H.I. Maibach, *In Vivo Methods for Percutaneous Absorption Measurements*, in *Percutaneous Absorption*, R.L. Bronaugh and H.I. Maibach, Editors. 1999, Marcel Dekker, Inc.: New York. p. 411-422.

20. Laugel, C., et al., *Contribution of Atr/Rt-Ir Spectroscopy for Studing the in Vivo Behavior of Octylmethoxycinnamate (Omc) after Topical Application.* Applied Spectroscopy, 2001. **55**: p. 1173-1180.

21. Robertson, J.D., et al., *Noninvasive in Vivo Percutaneous Absorption Measurements Using X-Ray Fluorescence.* Pharmaceutical Research, 1992. **9**: p. 1410-1414.

22. Wester, R.C. and H.I. Maibach, *In Vivo Methods for Percutaneous Absorption Measurements*, in *Percutaneous Absorption*, R.L. Bronaugh and H.I. Maibach, Editors. 2001, Marcel Dekker, Inc.: New York. p. 411-422.

23. Bronaugh, R.L. and H.I. Maibach, eds. *Topical Absorption of Dermatological Products*. Basic and Clinical Dermatology, ed. A.R. Shalita and D.R. Norris. Vol. 21. 2002, Marcel Dekker, Inc.: New York.

24. Borg, N., et al., *Distribution to the Skin of Penciclovir after Oral Famciclovir Administration in Healthy Volunteers: Comparison of the Suction Blister Technique and Cutaneous Microdialysis.* Acta Dermato-Venereologica, 1999. **79**: p. 274-277.

25. Sasongko, L., et al., *Human Subcutaneous Tissue Distribution of Fluconazole: Comparison of Microdialysis and Suction Blister Techniques.* British Journal of Clinical Pharmacology, 2003. **56**: p. 551-561.

26. Bashir, S.J., et al., *Physical and Physiological Effects of Stratum Corneum Tape Stripping.* Skin Research and Technology, 2001. **7**: p. 40-48.

27. Jacobi, U., et al., *Estimation of the Relative Stratum Corneum Amount Removed by Tape Stripping.* Skin Research and Technology, 2005. **11**: p. 91-96.

28. Tokumura, F., et al., *Region Differences in Adhesive Tape Stripping of Human Skin.* Skin Research and Technology, 2006. **12**: p. 178-182.

29. Kreilgaard, M., *Assessment of Cutaneous Drug Delivery Using Microdialysis.* Bulletin Technique Gattefosse, 2002. **95**: p. 101-122.

30. Schnetz, E. and M. Fartasch, *Microdialysis for the Evaluation of Penetration through the Human Skin Barrier- a Promising Tool for Future Research?* European Journal of Pharmaceutical Sciences, 2001. **12**: p. 165-174.

31. Groth, L., *Cutaneous Microdialysis - a New Technique for the Assessment of Skin Penetration.* Current Problems in Dermatology, 1998. **26**: p. 90-98.

32. McCleverty, D., R. Lyons, and B. Henry, *Microdialysis Sampling and the Clinical Determination of Topical Dermal Bioequivalence.* International Journal of Pharmaceutics, 2006. **308**: p. 1-7.

33. Anderson, C.D., *Cutaneous Microdialysis: Is It Worth the Sweat?* Journal of Investigative Dermatology, 2006. **126**: p. 1207-1209.

34. Anderson, C., T. Anderson, and A. Borman, *Cutaneous Microdialysis for Human in Vivo Dermal Absorption Studies*, in *Dermal Absorption and Toxicity Assessment*. 1998, Marcel Dekker, Inc.: New York. p. 231-244.

35. Anderson, C., T. Andersson, and M. Molander, *Ethanol Absorption across Human Skin Measure by in Vivo Microdialysis Technique.* Acta Derm Venereol (Stockh), 1991. **71**: p. 389-393.

36. Ault, J.M., et al., *Microdialysis Sampling for the Investigation of Dermal Drug Transport.* Pharmaceutical Research, 1992. **9**(10): p. 1256-1261.

37. Müller, M., et al., *Diclofenac Concentrations in Defined Tissue Layers after Topical Administration.* Clinical Pharmacology and Therapeutics, 1997. **62**(3): p. 293-299.

38. Morgan, C.J., et al., *Cutaneous Microdialysis as a Novel Means of Continuously Stimulating Eccrine Sweat Glands in Vivo.* Journal of Investigative Dermatology, 2006. **126**: p. 1220-1225.

39. Davies, M.I. and C.E. Lunte, *Simultaneous Microdialysis Sampling from Multiple Sites in the Liver for the Study of Phenol Metabolism.* Life Sciences, 1996. **59**(12): p. 1003-1013.

40. Janle, E.M. and M. Cregor, *Interstitial Fluid Calcium, Magnesium and Phosphorus Concentrations in Bone, Muscle and Subcutaneous Tissue Sampled with Ultrafiltration Probes.* Current Separations, 2001. **19**(3): p. 81-85.

41. Plock, N. and C. Kloft, *Microdialysis-Theoretical Background and Recent Implementation in Applied Life-Sciences.* European Journal of Pharmaceutical Sciences, 2005. **25**: p. 1-24.

42. McDonald, S. and C.E. Lunte, *Determination of the Dermal Penetration of Esterom Components Using Microdialysis Sampling.* Pharmaceutical Research, 2003. **20**(11): p. 1827-1834.

43. Weiss, D.J., C.E. Lunte, and S.M. Lunte, *In Vivo Microdialysis as a Tool for Monitoring Pharmacokinetics.* Trends in Analytical Chemistry, 2000. **19**(10): p. 606-616.

44. Joukhadar, C. and M. Muller, *Microdialysis: Current Applications in Clinical Pharmacokinetic Studies and Its Potential Role in the Future.* Clinical Pharmacokinetics, 2005. **44**(9): p. 895-913.

45. Müller, M., *Microdialysis in Clinical Drug Delivery Studies.* Advanced Drug Delivery Reviews, 2000. **45**: p. 255-269.

46. Hansen, D.K., et al., *Pharmacokinetic and Metabolism Studies Using Microdialysis Sampling.* Journal of Pharmaceutical Sciences, 1999. **88**: p. 14-27.

47. Herrera, A.M., D.O. Scott, and C.E. Lunte, *Microdialysis Sampling for Determination of Plasma Protein Binding of Drugs.* Pharmaceutical Research, 1990. **7**(10): p. 1077-1081.

48. Torto, N., et al., *Technical Issues of in Vitro Microdialysis Sampling in Bioprocess Monitoring.* Trends in Analytical Chemistry, 1999. **18**: p. 252-260.

49. de Lange, E.C.M., A.G. de Boer, and D.D. Breimer, *Methodological Issues in Microdialysis Sampling for Pharmacokinetic Studies.* Advanced Drug Delivery Reviews, 2000. **45**: p. 125-148.

50. Janle, E.M. and P.T. Kissinger, *Implanted Membrane Fibers Get You Closer to the Action.* Today's Chemist at Work, 1996: p. 49-53.

51. Clough, G.F., *Microdialysis of Large Molecules.* The AAPS Journal, 2005. **7**(3): p. E686-E692.

52. Zhao, Y., X. Liang, and C.E. Lunte, *Comparison of Recovery and Delivery in Vitro for Calibration of Microdialysis Probes.* Analytica Chemica Acta, 1995. **316**: p. 403-410.

53. Mary, S., et al., *Assessment of the Recovery of Three Lipophilic Psoralens by Microdialysis: An in Vitro Study.* International Journal of Pharmaceutics, 1998. **161**: p. 7-13.

54. Sun, L. and J.A. Stenken, *Improving Microdialysis Extraction Efficiency of Lipophilic Eicosanoids.* Journal of Pharmaceutical and Biomedical Analysis, 2003. **33**: p. 1059-1071.

55. Song, Y. and C.E. Lunte, *Calibration Methods for Microdialysis Sampling in Vivo: Muscle and Adipose Tissue.* Analytica Chimica Acta, 1999. **400**: p. 143-152.

56. Stenken, J.A., et al., *Examination of Microdialysis Sampling in a Well-Characterized Hydrodynamic System.* Analytical Chemistry, 1993. **65**: p. 2324-2328.

57. Lee, Y.S., et al., *Cutaneous Microdialysis of Uric Acid Level in the Dermis: Modification of in Vitro Recovery.* Acta Dermato-Venereologica, 2003. **83**: p. 10-13.

58. Lee, Y.S., et al., *Age-Dependent Change of Uric Acid Level in the Dermis Using Cutaneous Microdialysis.* Gerontology, 2005. **51**: p. 231-233.

59. Lönnroth, P., et al., *Microdialysis of Intercellular Adenosine Concentration in Subcutaneous Tissue in Humans.* The American Physiological Society, 1989. **256**: p. E250-E255.

60. Lönnroth, P., P.A. Jansson, and U. Smith, *A Microdialysis Method Allowing Characterization of Intercellular Water Space in Humans.* The American Physiological Society, 1987. **253**: p. E228-231.

61. Bouw, M.R. and M. Hammarlund-Udenaes, *Methodological Aspects of the Use of a Calibrator in in Vivo Microdialysis-Further Development of the Retrodialysis Method.* Pharmaceutical Research, 1998. **15**(11): p. 1673-1679.

62. Simonsen, L., et al., *Differentiated in Vivo Skin Penetration of Salicylic Compounds in Hairless Rats Measured by Cutaneous Microdialysis.* European Journal of Pharmaceutical Sciences, 2004. **21**: p. 379-388.

63. Yokel, R.A., et al., *Antipyrine as a Dialyzable Reference to Correct Differences in Efficiency among and within Sampling Devices During in Vivo Microdialysis.* Journal of Pharmacological and Toxicological Methods, 1992. **27**: p. 135-142.

64. Kaptein, W.A., et al., *Continuous Ultraslow Microdialysis and Ultrafiltration for Subcutaneous Sampling as Demonstrated by Glucose and Lactate Measurements in Rats.* Analytical Chemistry, 1998. **70**: p. 4696-4700.

65. Hashimoto, Y., et al., *In-Vivo Calibration of Microdialysis Probe by Use of Endogenous Glucose as an Internal Recovery Marker: Measurement of Skin Distribution of Tranilast in Rats.* Journal of Pharmacy and Pharmacology, 1998. **50**: p. 621-626.

66. Brunner, M., et al., *Validation of Urea as an Endogenous Reference Compound for the in Vivo Calibration of Microdialysis Probes.* Life Sciences, 2000. **67**: p. 977-984.

67. Sorg, B.S., et al., *Method for Improved Accuracy in Endogenous Urea Recovery Marker Calibrations for Microdialysis in Tumors.* Journal of Pharmacological and Toxicological Methods, 2005. **52**: p. 341-349.

68. Groth, L. and A. Jørgensen, *In Vitro Microdialysis of Hydrophilic and Lipophilc Compounds.* Analytica Chemica Acta, 1997. **355**: p. 75-83.

69. Ao, X., et al., *Multiplexed Cytokine Detection in Microliter Microdialysis Samples Obtained from Activated Cultured Macrophages.* Journal of Pharmaceutical and Biomedical Analysis, 2006. **40**: p. 915-921.

70. Averbeck, M., et al., *In Situ Profiling and Quantification of Cytokines Released During Ultraviolet B-Induced Inflammation by Combining Dermal Microdialysis and Protein Microarrays.* Experimental Dermatology, 2006. **15**: p. 447-454.

71. Kjellström, S., et al., *Microdialysis - a Membrane Based Sampling Technique for Quantitative Determination of Proteins.* Chromatographia, 1999. **50**: p. 539-546.

72. Sjögren, F., C. Svensson, and C. Anderson, *Technical Prerequisites for in Vivo Microdialysis Determination of Interleukin-6 in Human Dermis.* British Journal of Dermatology, 2002. **146**: p. 375-382.

73. Waelgaard, L., et al., *Microdialysis for Monitoring Inflammation: Efficient Recovery of Cytokines and Anaphylotoxins Provided Optimal Catheter Pore Size and Fluid Velocity Conditions.* Scandinavian Journal of Immunology, 2006. **64**: p. 345-352.

74. Ao, X., T.J. Sellati, and J.A. Stenken, *Enhanced Microdialysis Relative Recovery of Inflammatory Cytokines Using Antibody-Coated Microspheres Analyzed by Flow Cytometry.* Analytical Chemistry, 2004. **76**: p. 3777-3784.

75. Groth, L., A. Jørgensen, and J. Serup, *Cutaneous Microdialysis in the Rat: Insertion Trauma and Effect of Anesthesia Studied by Laser Doppler Perfusion Imaging and Histamine Release.* Skin Pharmacology and Applied Skin Physiology, 1998. **11**: p. 125-132.

76. Groth, L. and J. Serup, *Cutaneous Microdialysis in Man: Effects of Needle Insertion Trauma and Anesthesia on Skin Perfusion, Erythema, and Skin Thickness.* Acta Dermato-Venereologica, 1998. **78**: p. 5-9.

77. Hogan, B.L., et al., *On-Line Coupling of in Vivo Microdialysis Sampling with Capillary Electrophoresis.* Analytical Chemistry, 1994. **66**: p. 596-602.

78. Lunte, C.E., D.O. Scott, and P.T. Kissinger, *Sampling Living Systems Using Microdialysis Probes.* Analytical Chemistry, 1991. **63**: p. 773A-780A.

79. Davies, M.I., et al., *Analytical Considerations for Microdialysis Sampling.* Advanced Drug Delivery Reviews, 2000. **45**: p. 169-188.

Chapter Two

Investigation of Drug Delivery by Iontophoresis in a Surgical Wound Utilizing Microdialysis

2.1 Purpose

The purpose of this work was to gain a better understanding of drug flow near a surgical incision under both diffusive and iontophoretic conditions. This was completed by the development of a four probe microdialysis design that allowed for sampling around a surgical incision and measurement of the free blood concentration. This work was completed in collaboration with Travanti Pharma Inc. who provided the iontophoresis patches and supplies.

2.2 Introduction

2.2.1 Postoperative Pain

Surgery is a stressful event for many and a major concern is postoperative pain. It has been reported that primary hyperalgesia, an extreme sensitivity to pain, can persist for at least 4 days following an abdominal surgery [1]. The use of anesthetics is a general practice that helps reduce or eliminate some of the pain endured. Lidocaine, a common anesthetic, has been shown to have local and general anesthetic properties. The half-life of lidocaine in humans has been reported to be 80 − 108 minutes [2]. Therefore for prolonged therapeutic effects, a continual lidocaine

dose would have to be administered. Systemic treatment using lidocaine has been shown to reduce post operative pain [1, 3]. However, several studies report systemic administration of lidocaine produced minimal effects on reducing primary hyperalgesia following injury induced by both thermal and chemical pain models [4-6]. One possible explanation for these findings is the lack of therapeutic concentrations at the site of injury. Currently, there is no direct association found between lidocaine plasma concentration and its analgesic effects [2]. There is however a relationship on lidocaine plasma levels and different stages of toxicity [2]. The onset of central nervous system toxicity occurs at concentrations above 10 μg/mL, while the onset of convulsions and seizures begin at concentrations greater than 18 μg/mL [2, 7].

Dermal application of lidocaine is another form of administration that has been shown to have great promise. As drug application directly targets the site of interest, it minimizes potential side effects and drug-drug interactions in comparison to systemic delivery routes [8]. Currently there are several commercially available patches that use lidocaine as one of its main active ingredients [8, 9]. These patches have been shown to reduce pain associated with postherpetic neuralgia, painful diabetic neuropathy, lower-back pain, HIV-related pain, and refractory pain [8, 10]. Side effects from these patches have been minimal and are generally associated with skin reactions and include redness, burning sensation, and rashes [10].

Lidopain® SP is the first sterile pharmaceutical patch designed for pain relief following the surgical closing of wounds [11]. However, recent results from Phase

III clinical trials revealed that it did not achieve a statistically significant effect in comparison to placebo results [12]. One of the major drawbacks to topical drug treatments is the poor penetration properties. In order to improve this, several chemical or physical modifications have been developed.

2.2.2 Iontophoresis in Drug Delivery

One of the main limitations to dermal penetration is the restrictive nature of the stratum corneum, the major diffusional barrier. In order to enhance dermal penetration chemical or physical modifiers are often employed. Common chemical enhancers studied include bile salts, sulfoxides, surfactants, chelating agents, alcohols and cyclodextrins. The exact mechanism of chemical enhancers is not clearly understood, although they have been shown to modify the intercellular lipid matrix [13, 14]. Alternatively, physical modifiers include such techniques as iontophoresis, ultrasound, phonophoresis, heat enhancement, and laser energy enhancement [14]. Of particular interest for this project is the use of iontophoresis.

Iontophoresis is an electrically driven technique that pushes charged and neutral compounds through the skin by the application of a current. It originated in the 1750s and later gathered increased interest in the 20th century [13, 14]. Predominantly, iontophoresis focused on the delivery of small charged molecules. Within the last 30 years, its use has expanded to macromolecular drugs [15-18]. However, delivery of macromolecules is limited because iontophoretic delivery is inversely dependent on the molecular weight [17].

An iontophoretic system consists of a power supply, a cathode compartment, and an anode compartment (Figure 2.1). The ionic drug is placed in the similarly charged compartment. For example, positively charged lidocaine would be placed in the anodal reservoir. Once current is applied, ionic flow proceeds where cations are driven towards the cathode and anions are driven towards the anode. The amount of drug delivered is dependent on the amount of current applied, the length of current treatment, and the surface area of the patch [13, 19]. The flow of ionized species in an electric field is driven by two forces: electromigration and electroosmosis. Electromigration, or electrorepulsion, is a process that occurs due to an attraction or repulsion of ions to the cathode or anode. Therefore, anions are attracted towards the anode and cations are forced away from the anode. Alternatively, electroosmosis results from the net flow of ions in an electric field. The net movement of ions creates an electroosmotic flow which results in the movement of both neutrals and cationic solutes [19, 20]. A third transport mechanism, current-induced permeability changes that result from the effects of iontophoresis, can also be considered. Studies completed *in vitro* demonstrate enhanced penetration following iontophoretic treatment in comparison to pre-treatment [19, 20].

The use of iontophoresis to enhance dermal penetration of lidocaine has been well studied in intact skin [21-28]. This study explored the use of iontophoresis as a site directed drug device in a skin region containing a sutured incision. In order to understand the drug delivery route of lidocaine in an altered system the use of microdialysis was utilized.

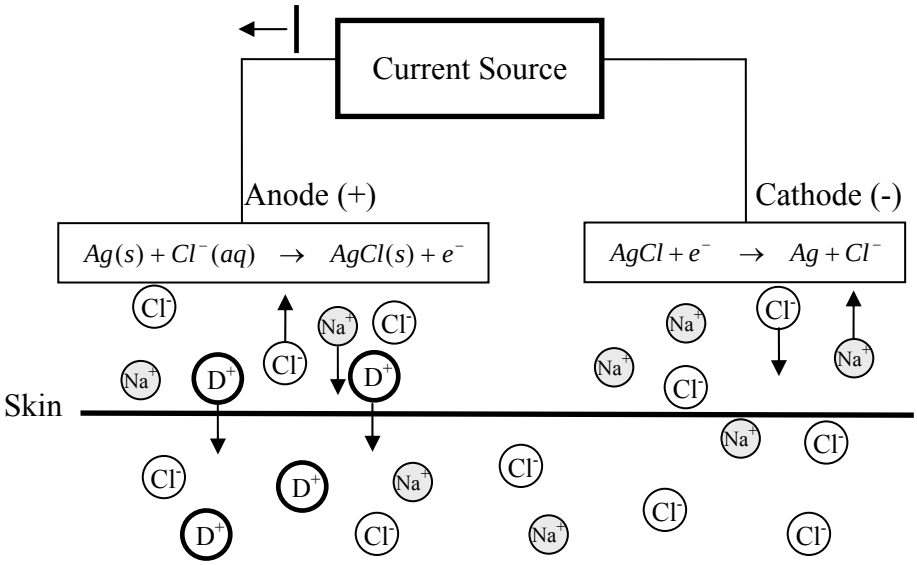

Figure 2.1. Iontophoresis using a Ag/AgCl electrode system. Adapted from Kalia, Y.N. et al., *Iontophoretic Drug Delivery*. Advanced Drug Delivery Reviews. 2004. **56**: p. 619-658.

2.2.3 Multi-Probe Microdialysis

As previously discussed, microdialysis is a sampling technique that enables the determination of analyte concentrations in site specific regions. The use of multi-probe experiments has been shown to be useful in gathering data about drug locations and drug flow throughout the body [29-31]. Due to the relatively small size of microdialysis probes, implantation of multiple probes within one organ or region is generally possible. For instance, Davies and Lunte utilized multiple linear probes in order to determine regional differences of drug and metabolite concentrations within the liver [32]. The use of multiple probe microdialysis is an ideal technique that could be used to study drug penetration around a sutured incision.

2.3 Specific Aims

The goal of this project was to utilize multiple probe microdialysis in the determination of lidocaine flow around a sutured incision in the CD hairless rat under both passive and iontophoretic conditions. This was completed by utilizing a four probe design in the vicinity of the sutured wound. In addition, lidocaine penetration in intact skin was investigated for comparison against lidocaine penetration through sutured skin.

2.4 Materials and Methods

2.4.1 Chemicals

Lidocaine HCl solution (40 mg/mL) was provided by Hospira, Inc. (Lake Forest, IL). A 4% lidocaine HCl, 2% HPMC gel and 0.9% NaCl, 2% HPMC gel was provided by Travanti Pharma Inc. (Mendota Heights, MN). Ringer's solution consisted of 145 mM NaCl, 2.8 mM KCl, 1.2 mM $CaCl_2$, and 1.2 mM $MgCl_2$ all purchased from Fisher Scientific (Fair Lawn, NJ). HPLC grade acetonitrile was purchased from Fisher Scientific. Ketamine was manufactured by Fort Dodge Animal Health (Fort Dodge, IA),xylazine was made by Ben Venue Laboratories (Bedford, OH), acepromazine was manufactured by Boehringer Ingelheim (St. Joseph, MO), and AErrane (isoflurane) was purchased from Baxter (Deerfield, IL). Microdialysis probes and surgical instruments were sterilized by ethylene oxide using an Anprolene gas sterilizer (AN 74i, Anderson Products, Inc., Haw River, NC). Water for buffer preparation was filtered through a Labconco, Water Pro Plus.

2.4.2 HPLC Instrumentation

The liquid chromatographic system consisted of a Shimadzu LC-20AD pump, Shimadzu SCL-10AVP system controller, Shimadzu SIL-20AC auto sampler, and a Shimadzu SPD-10A UV-Vis spectrophotometric detector (Shimadzu Scientific Instruments, Inc., Columbia, MD). The mobile phase consisted of 50 mM phosphate buffer (pH 6.6): acetonitrile (60:40, v/v). The flow rate was 0.20 mL/min and a detection wavelength of 210 nm. Chromatographic data were acquired using EZ Start

Software (Shimadzu Scientific Instruments, Inc., Columbia, MD). A Zorbax Eclipse XDB-C18 column (150 x 2.1 mm, 3.5 μm), purchased from Agilent (Palo Alto, CA), was used with a sample injection volume of 15 μL.

2.4.3 Statistical Analysis

Statistical analysis was completed by first testing for homogeneity using Hartley's F-max test. The non-parametric test of Mann-Whitney U test was used for all data comparisons. Results were reported at the 95% confidence limit level. All results were reported as mean +/- standard deviation

2.4.4 Iontophoretic Patch Design

The iontophoretic patches (provided by Travanti Pharma Inc., Mendota Heights, MN) were approximately 2.75 inches long and 1.25 inches wide (Figure 2.2). The patch was thin and flexible, approximately 2 mm thick, and comprised of several layers of latex-free medical tape adhesives. Active patches consisted of electrodes composed of either zinc or silver electrodes and a power supply that was either built in or independent. Each patch had an active positive electrode delivery area of 2.25 cm^2 which was positioned over the incision site. Five patch strengths were tested (Table 2.1); a zero current patch, a low current patch (operating at ~ 0.030 mA/cm^2, +/- 10%), a high current patch (operating at ~ 0.082 mA/cm^2, +/- 10%), a high 2 current patch (operating at ~ 0.15 mA/cm^2, +/- 10%), and a high 3 current patch (operating at ~ 0.30 mA/cm^2, +/- 10%).

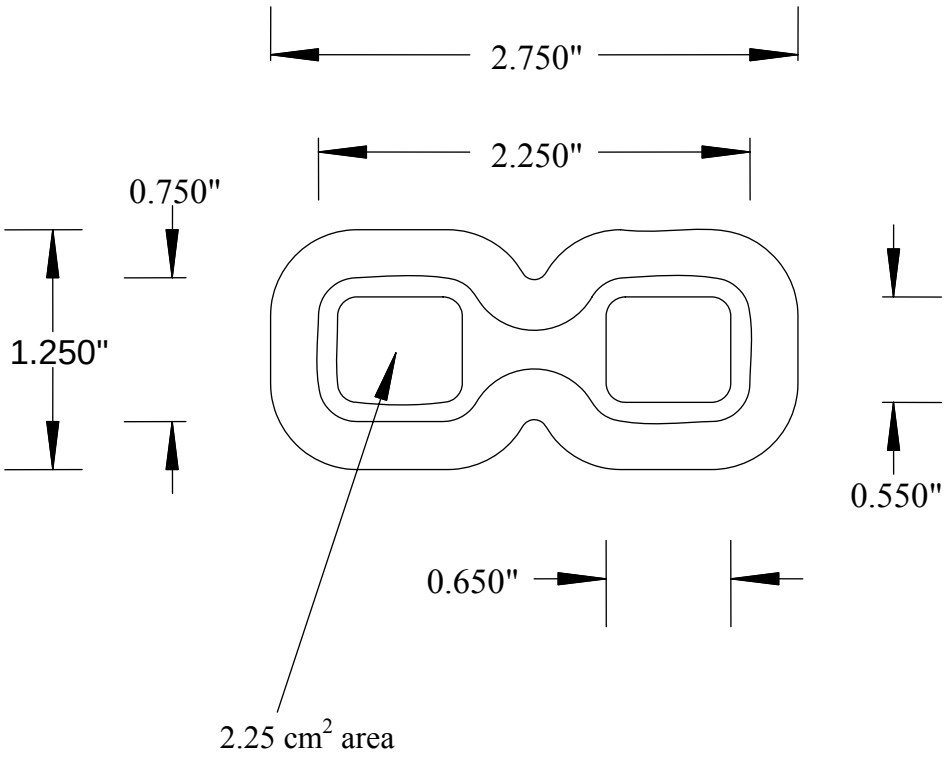

Figure 2.2. Schematic of the iontophoretic patch design.

Table 2.1. Description of the treatment groups studied using CD Hairless rats.

Group No.	Treatment	Number of Animals
1	Patch/Lidocaine solution No current	3
2	Patch/Lidocaine solution Low Current (0.030 mA/cm^2)	2
3	Patch/Lidocaine solution High Current (0.082 mA/cm^2)	7
4	Patch/Lidocaine gel High 3 Current (0.30 mA/cm^2) Zinc Electrode	3
5	Patch/Lidocaine gel No Current	4
6	Patch/Lidocaine gel High 2 Current (0.15 mA/cm^2) Zinc Electrode	5
7	Patch/Lidocaine gel High 2 Current (0.15 mA/cm^2) Silver Electrode	4

Note: Groups 1 – 4 consisted of dermal, suture, subcutaneous, and muscle probes
Groups 5 – 7 consisted of dermal, suture, subcutaneous, and vascular probes

2.4.5 Microdialysis Probe Construction

Linear microdialysis probes with a 5 mm dialysis membrane made of a polyacrylonitrile (PAN) membrane (Hospal Industrie, Meyzieu, France) were used. Probes were fabricated by placing two lengths of polyimide tubing (MicroLumen® Inc., Tampa, FL) (173 μm i.d., 216 μm o.d.) into the ends of a PAN membrane (250 μm i.d., 350 μm o.d., molecular weight cut off of 30 kDa). The connections were secured with UV glue (UVEXS, Sunnyville, CA).

Vascular probes containing a 10 mm active membrane window were constructed by first inserting a piece of polyimide (o.d 175 μm, i.d. 125 μm) into a 10 mm length of micro-renathane surgical tubing (MRE-033, Braintree Scientific, MA) so that 10 mm length of polyimide was exposed. The exposed polyimide was threaded into a piece of PAN membrane. The membrane was also threaded into the MRE-033 tubing. The end of the membrane was sealed with UV glue and glued to the MRE-033 tubing. A second piece of polyimide was inserted approximately one third into the top of the MRE-033 and secured with UV glue. The polyimide ends were protected by threading them into a piece of MRE-040 tubing. Two large beads of glue were placed at the junction of MRE-033 and MRE-040 tubing.

2.4.6 Surgical Procedure

CD Hairless male rats (Charles River Laboratories, Raleigh, NC), 6 − 7 weeks of age, were housed in cages maintained in temperature controlled rooms and were allowed free access to food and water. One day prior to patch/drug application, the

rats were anesthetized by inhalation of isofluorane followed by subcutaneous injection of a ketamine (67.5 mg/kg), acepromazine (0.67 mg/kg), and xylazine (3.4 mg/kg) mixture. A subcutaneous injection of atropine (0.05 mg/kg) was given to reduce bronchial and salivary secretions. As necessary, additional ketamine (20 mg/kg, intramuscular) was given to maintain anesthesia. The animal's body temperature was maintained until it had recovered from surgery by placing the animal on a heating pad. Strict aseptic techniques were used during the surgical procedure.

The fur from the treatment site was shaved using an Oster® Vorteq clipper. After cleaning the skin by swabbing betadiene and 70% alcohol alternating three times each, a 1 cm long full thickness skin incision was made to the left lumbar region of each rat. Three 5 mm linear microdialysis probes were implanted in-line with the surgical incision. One probe was sutured into the incision using a 4-0 Dexon II suture (Tyco Healthcare, King of Prussia, PA), one probe was implanted in the subcutaneous layer, and one probe was implanted in the underlying muscle, except as noted subsequently (Figure 2.3). One additional probe was implanted in the dermis parallel to the incision but at a distance of 5 – 10 mm medially. The probes were implanted with a 23-gauge needle by threading one end of the probe's polyimide tubing through the needle. The needle was withdrawn leaving the dialysis membrane imbedded in the surrounding tissue. The polyimide inlet and outlet were protected using MRE-040 tubing. The tubing was then held secure to the polyimide by UV glue. This tubing kept the muscle and dermal probes fixed. In order to keep the subcutaneous probe stationary, a small suture was placed in the muscle and tied to the

polyimide above and below the active membrane of the subcutaneous probe. The probes were then tunneled under the skin to the nape of the neck using a trocar. At the end of the surgical procedure, 10 mL of sterile saline solution was given subcutaneously to replace fluids that may have been lost during surgery.

The animal was placed in a harness and the probes were pulled through a small hole in the harness. Tubing connectors were UV glued to both ends of the microdialysis probes which were then connected to fluorinated ethylenepropylene (FEP) tubing. The animal was placed in a Rodent bowl and set up in the Raturn awake animal containment system. The inlet of the FEP tubing was connected to a Hamilton syringe mounted on a CMA 400 infusion pump (CMA, North Chelmsford, MA). The microdialysis probe outlet was connected to a Honeycomb Refrigerated Fraction Collector (Bioanalytical Systems (BAS), West Lafayette, IN) with FEP tubing. The microinjection pump delivered the perfusion medium at a flow rate of 1 $\mu L\ min^{-1}$.

Based on preliminary results, the muscle probe was eliminated in Groups 5 – 7 and replaced with a vascular probe. Implantation of the vascular probe into the jugular vein was completed prior to implantation of the dermal, subcutaneous, and suture probes. A small incision was made to expose the jugular vein, which was separated from the artery and nerve. A vascular microdialysis probe was inserted in the vein and advanced distally and affixed by tying two sutures around the vein and

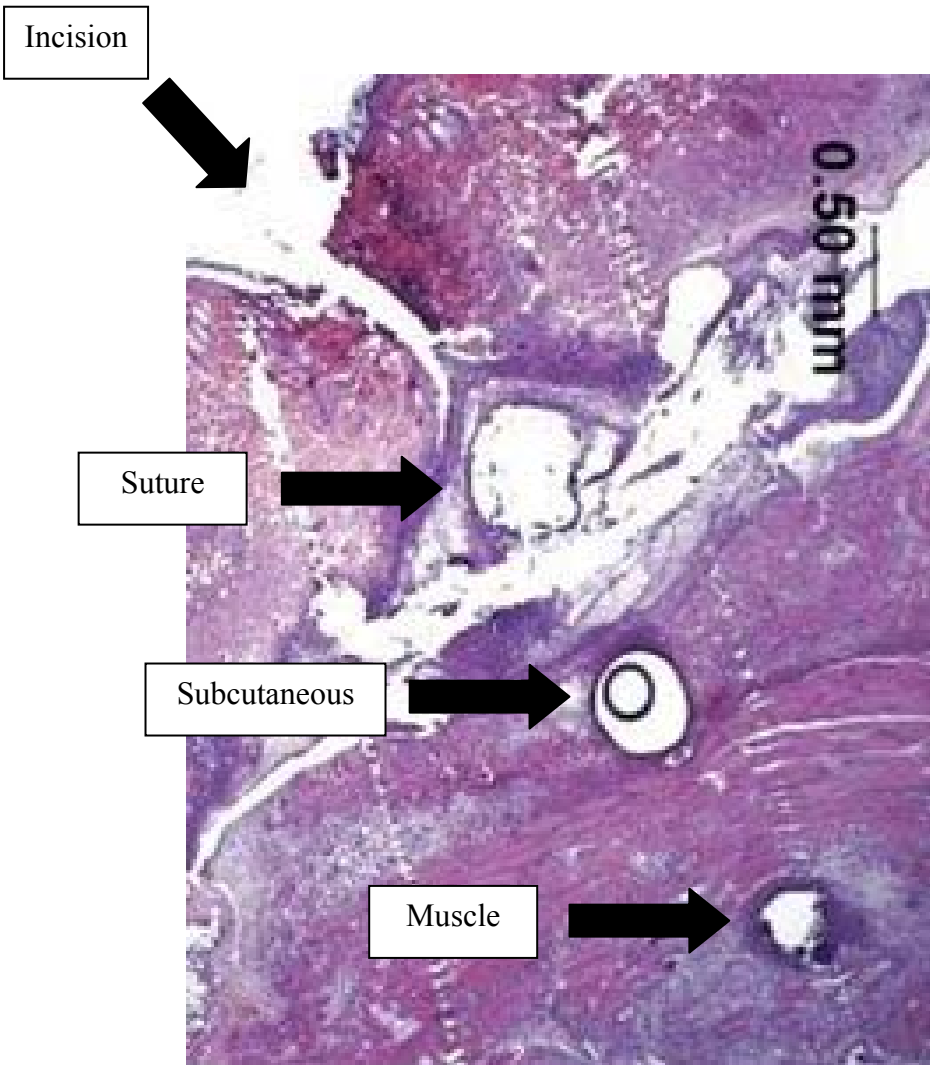

Figure 2.3. Representative histology slide of the linear microdialysis probes in-line with the sutured incision.

probe. The end of the vascular probe was tunneled using a trocar to the nape of the neck. Finally, the incision was sutured shut.

Following the course of each experiment, tissue was harvested at the site of probe implantation and fixed in 10% buffered formaldehyde solution. Histology slides were completed at Lawrence Memorial Hospital (LMH) in order to assess tissue reaction and determined membrane placement.

2.4.7 Dosing Protocol

2.4.7.1 Lidocaine Solution

Lidocaine HCl solution (0.4 mL; 40 mg/mL) was loaded onto each patch immediately prior to patch application by adding the lidocaine solution to the positive donor reservoir in a drop-wise fashion (the absorbent pad was almost completely saturated). Normal saline solution (0.4 mL) was added to the return electrode pad in the same manner.

2.4.7.2 Lidocaine Gel

Uniform layers of 0.4 mL lidocaine gel (4% Lidocaine HCL, 2% hydroxypropyl methylcellulose (HPMC)) and 0.4 mL saline gel (0.9% NaCl, 2% HPMC gel) were applied to individual absorbent pads 1.5 hours prior to application. Once imbibed, the lidocaine pad was placed onto the positive electrode and the saline pad was placed onto the negative electrode. Prior to patch application on the rat, an additional 0.4 mL of lidocaine gel was applied over the suture region and 0.4 mL of

saline gel was applied onto the contralateral (right) side of the rat back. This was completed by first dispensing the gel onto the dermis and then evenly spreading the gel over the patch site using a cotton swab.

2.4.8 Patch Application

Prior to patch application, the rat was lightly sedated using isoflurane (to effect) in order to limit movement that could hinder proper placement of the patch. The rat was removed from the bowl and placed on a short table that allowed it to remain connected to the Raturn containment system. The suture region and site for saline application were covered using strips of adhesive while the back of the rat was sprayed with Mastisol®, a liquid adhesive. The patch was applied while the back of the rat was half arched and pressed securely into place. Three strips of adhesive were wrapped around the rat to ensure good contact between the patch and the application site. The rat was returned to the bowl and allowed to recover.

2.5 Results and Discussion

2.5.1 Calibration of Microdialysis Probes

Microdialysis probe calibration was completed for each individual probe at the start of every experiment using the delivery method discussed in Section 1.4.3.3. Mean percent delivery for each probe reported with their standard deviations can be seen in Table 2.2. In general, delivery to the muscle, subcutaneous, suture, and dermal regions were determined to be approximately the same. Lidocaine delivery

Table 2.2. Mean percent delivery of microdialysis probes.

Probe	Mean % Delivery
Muscle[a]	28.5 ± 7.4
Vascular[a]	70.5 ± 14.0
Subcutaneous[b]	29.7 ± 5.5
Suture[b]	26.4 ± 7.5
Dermal[b]	22.9 ± 5.3

[a]n~15 [b]n~30

determined in the vascular probe was over two times greater than the other probe regions. This is in part due to the larger membrane size (10 mm vs 5 mm) and also related to the non-stagnant environment of the blood vessel which allows for the removal of lidocaine near the probe membrane.

Several issues in microdialysis sampling have been shown to affect the extraction efficiency during the course of an experiment. These include immunological responses around the membrane and blood flow changes [33, 34]. For example, i*n vivo* fouling which is a result of protein or macromolecule absorption to the microdialysis membrane would result in a decrease in the extraction efficiency. In addition, change in blood flow is one of the reported side effects associated with ionotophoresis. Other responses include edema, erythema, changes in pH, and increase in temperature [35]. For these studies calibration was completed at the start of the experiment by delivery of lidocaine. Therefore to assess possible changes in extraction efficiencies, control calibration studies were completed that included

continuous calibration throughout the length of an experiment with and without the addition of an iontophoretic patch.

For the initial calibration study, a solution of 1 μg/mL lidocaine was perfused through the microdialysis probes for a total of 32 hours in order to allot time for the initial calibration completed at the start of every experiment (Figure 2.4). Steady state was found to occur following the first one hour collection period. All probes, except the subcutaneous probe, were found to have approximately the same delivery during the course of the 32 hours. The subcutaneous probe was found to decrease to approximately 80% of the original steady state value determined during the first four hours of collection by the end of the sampling period.

In order to assess the effects that iontophoresis has on probe calibration, the same experiment was repeated however this time an iontophoresis patch with saline in both drug reservoirs was applied after the first eight hours. A similar experiment was completed by Stagni *et al.* who monitored microdialysis recovery over a two hour sampling period. Their results indicated no change in microdialysis recovery [35]. This experiment was repeated for this study since sampling times were much greater. Again, probe deliveries were found to be approximately the same throughout the course of the sampling period (Figure 2.5). In addition, lidocaine delivery in the subcutaneous probe was consistent the entire time and did not decrease as previously seen without the addition of an iontophoretic patch. This demonstrates that the recovery of lidocaine during the course of the 24 hour sampling period was constant and unaffected from any physiological responses caused from the iontophoretic patch.

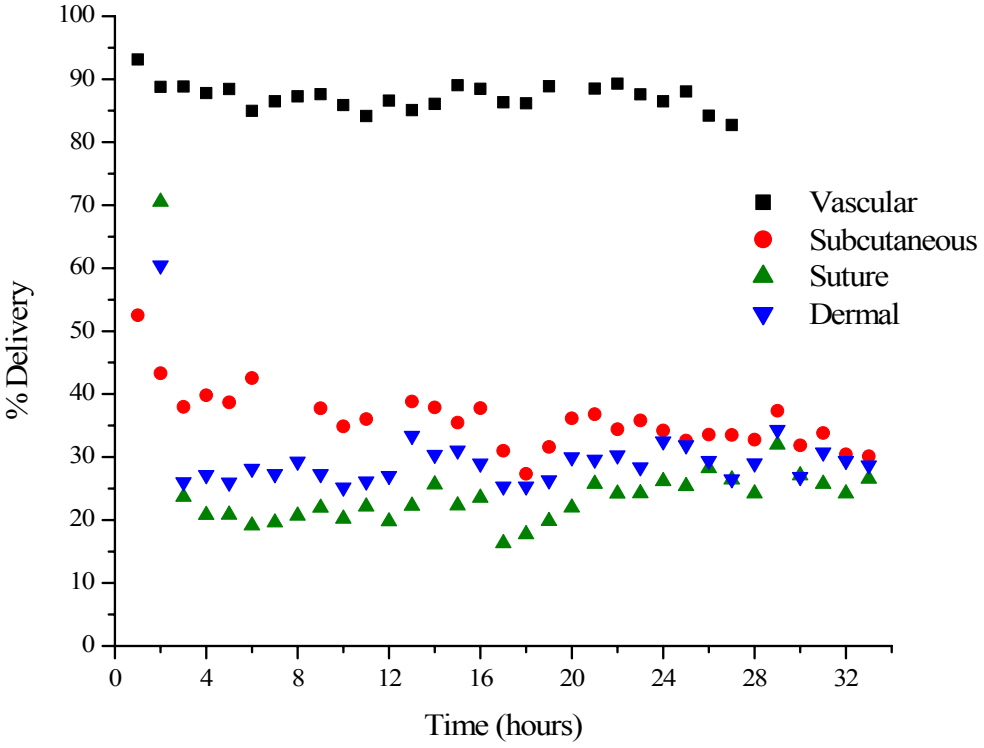

Figure 2.4. Continuous microdialysis probe calibration using 1 μg/mL lidocaine for 32 consecutive hours.

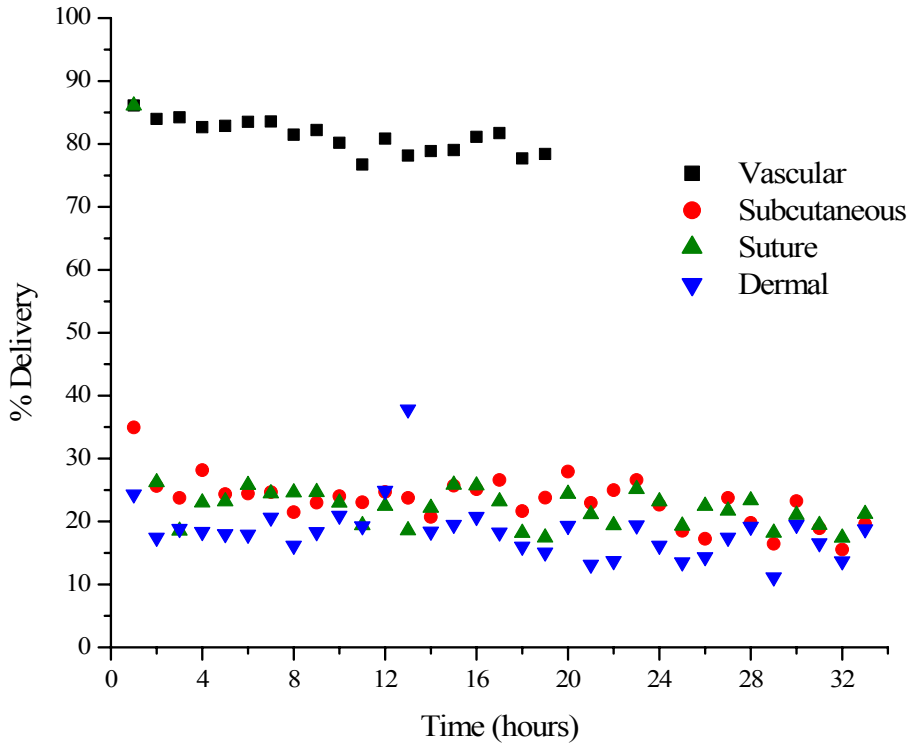

Figure 2.5. Continuous microdialysis probe calibration using 1 μg/mL lidocaine during the course of an experiment. The addition of an iontophoretic patch occurred after the first eight hours of collection.

2.5.2 Drug Formulation

Initial studies focused on determining the difference in lidocaine concentrations following the application of three patches; passive, low current (0.030 mA/cm^2), and high current (0.082 mA/cm^2). Concentration max (C_{max}) and total area under the curve (AUC_{tot}) obtained with these studies are shown in Table 2.3. Mean values for the suture and muscle probes in the low current group were not determined as only one probe was functional. Statistical analysis was conducted using the C_{max} and AUC_{tot} values of each probe location and were compared between treatment groups. It was determined that there was not a significant difference between the three treatment groups at any of the four probe locations at the 95% confidence level. In general, lidocaine concentrations in the dermal region increased as the level of current increased. This was seen in both the C_{max} and AUC_{tot} values. Lidocaine concentrations in the subcutaneous region also increased. However, this was only present in the C_{max} measurements and not the AUC_{tot}. Lidocaine concentrations (AUC_{tot} and C_{max}) in the suture and muscular regions were also less using the high current patch compared to the passive patch.

It was hypothesized that higher lidocaine concentrations would travel through the suture compared to the dermal levels as it exhibits the path of least resistance. This was previously shown in *in vitro* studies completed by the sponsor company Travanti Pharma Inc.. The results obtained in this study did not show an increase in the lidocaine concentrations in the suture region using ionotophoresis compared to the

Table 2.3. Mean data obtained following application of a self-contained iontophoretic patch containing 0.4 mL of lidocaine solution for a 24 hour application period.

Group		Units	Dermal	Suture	Subcutaneous	Muscle
1 n=3	C_{max}	μg/mL	0.64 ± 0.34	21.7 ± 23.7	0.23 ± 0.20	0.16 ± 0.22
	AUC_{tot}	hr·μg/mL	6.8 ± 3.4	257.6 ± 240.8	2.9 ± 2.3	1.4 ± 1.2
2 n=2	C_{max}	μg/mL	1.7 ± 2.3	*	0.56 ± 0.029	*
	AUC_{tot}	hr·μg/mL	28.5 ± 35.0	*	0.79 ± 0.61	*
3[a] n=7	C_{max}	μg/mL	9.06 ± 18.4	16.2 ± 13.0	7.8 ± 18.90	0.06 ± 0.03
	AUC_{tot}	hr·μg/mL	53.8 ± 105.0	131.9 ± 130.9	4.8 ± 4.2	0.41 ± 0.13

*n=1 for these groups

passive patches. One possible explanation for this is that poor contact was made with the skin, thus iontophoresis was not occurring. In order to improve skin contact, a gel solution of lidocaine, made by the addition of 2% hydroxypropyl methylcellulose (HPMC), was utilized. In addition to changing the lidocaine formulation, patches with higher currents (0.15 mA/cm^2 and 0.30 mA/cm^2) were investigated in order to detect a greater penetration difference compared to the passive patch.

Three experiments were conducted using the 0.30 mA/cm^2 self-contained patch (Group 4). Increased lidocaine concentrations in the dermis were obtained, however they were not statistically different at the 95% confidence level when the mean AUC_{tot} values for each individual probe region was tested against previous passive patch data using the liquid drug solution (Table 2.4). This difference again suggested that there may still have been a problem with skin contact to the patch.

In order to address poor patch to skin contact, it was decided that in addition to imbibing the patch with 0.4 mL of lidocaine gel, an extra 0.4 mL of gel would be applied directly to the skin. The current was also monitored throughout the course of the experiment using a multimeter. As the patch was no longer self-sufficient, it

Table 2.4. Mean data obtained for Group 4 (Lidocaine gel, High 3 current, Zinc electrode) patches (0.30 mA/cm2) imbibed with 0.4 mL lidocaine gel.

Group		Units	Dermal	Suture	Subcutaneous	Muscle
4	C_{max}	μg/mL	3.3 ± 4.8	33.8 ± 15.6	1.2 ± 0.72	0.42 ± 0.17
n=4	AUC_{tot}	hr·μg/mL	13.1 ± 17.9	109.9 ± 26.0	3.8 ± 1.4	1.3 ± 0.12

could now be split, another precautionary measure to aid in good contact. In addition, it was decided to replace the muscle probe with a vascular probe in order to monitor the free lidocaine concentration in the blood.

This new application technique was able to maintain constant current throughout the twenty-four hour sampling period (Figure 2.6). Although not determined to be significantly different, C_{max} and AUC_{tot} increased when using the High 2 patch (0.15 mA/cm^2) compared to the passive patch for all probes (Table 2.5). It was found however, that a greater amount of lidocaine penetrated the suture in comparison to the dermis when the current was applied. Under passive conditions, the C_{max} in the suture was approximately 25 times greater than the C_{max} in the adjacent dermis. However, when 0.15 mA/cm^2 of current was applied, the C_{max} in the suture was approximately 60 times greater than the C_{max} of the adjacent intact skin.

Lidocaine concentrations reached maximum levels between 2 3 hours following patch application and then leveled off to concentrations similar to the passive patch (see Figure 2.7). This was not expected as the current was maintained at 0.30 mA or 0.15 mA/cm^2 during the 24 hour sampling period. This was the first time the sponsor had conducted a study of this time length. Initial patches were designed to have the anode constructed out of zinc metal and the cathode from silver chloride. When the zinc metal in the anode compartment is oxidized it forms zinc ions which could be acting as a competing ion. This hypothesis was tested using a patch constructed with silver electrodes. When silver metal is oxidized, it forms

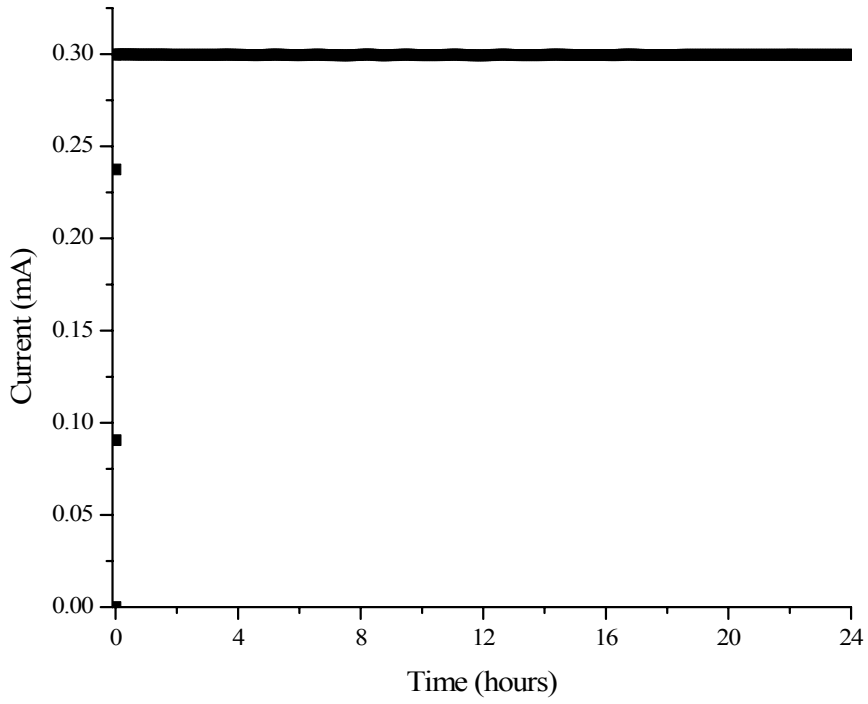

Figure 2.6. Current reading taken over 24 hour patch application.

Table 2.5. Mean data obtained for Group 5 (Lidocaine gel, No current) and Group 6 (Lidocaine gel, High 2 current, Zinc electrode).

Group		Units	Dermal	Suture	Subcutaneous	Vascular
5	C_{max}	μg/mL	0.93 ± 0.87	27.0 ± 20.0	0.67 ± 0.78	0.032 ± 0.02
n=4	AUC_{tot}	hr·μg/mL	9.6 ± 8.5	301.9 ± 208.0	5.4 ± 6.5	0.41 ± 0.19
6	C_{max}	μg/mL	2.6 ± 2.9	119.6 ± 122.8	6.3 ± 10.5	0.051 ± 0.025
n=5	AUC_{tot}	hr·μg/mL	10.2 ± 7.2	936.7 ± 1330.8	45.9 ± 90.2	0.48 ± 0.19

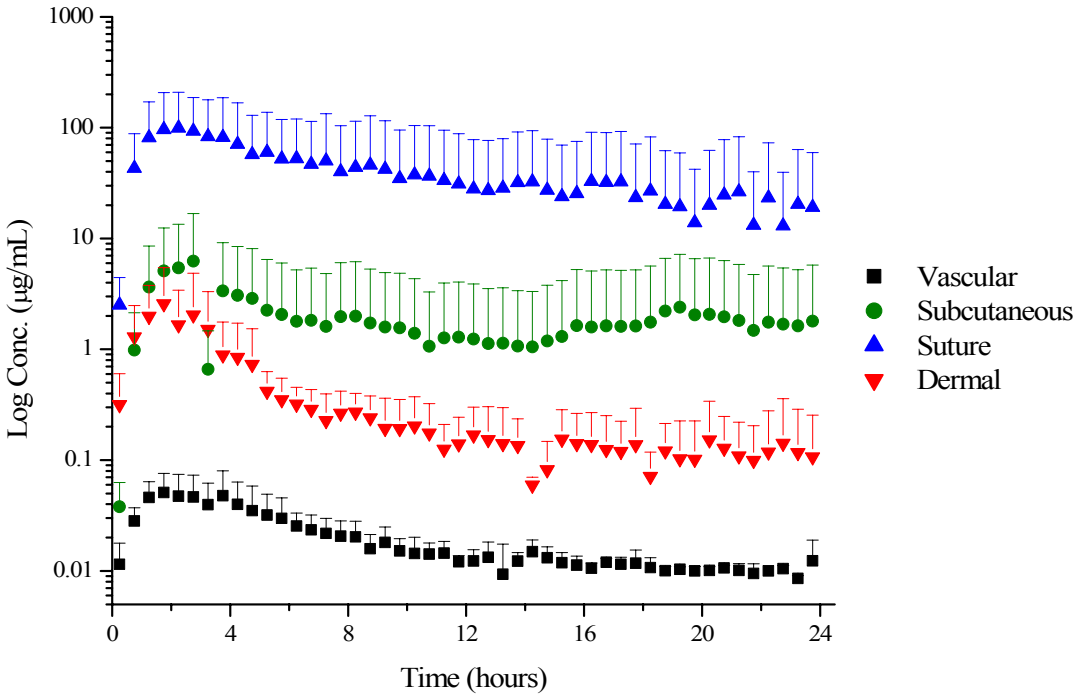

Figure 2.7. Mean data for Group 6 (Lidocaine gel, High 2 Current, Zinc electrode).

silver chloride which will precipitate out of solution, reducing the number of competing ions.

2.5.3 Silver vs. Zinc Electrodes

Lidocaine penetration using an iontophoretic patch constructed with silver electrodes established a continuous delivery of lidocaine throughout the 24 hour sampling period. This trend was found in all four probes (Figure 2.8). Lidocaine levels reached their initial elevated concentrations after approximately two hours of patch application. This demonstrated a faster delivery rate compared to passive diffusion which obtained C_{max} values approximately three hours after application. In addition, lidocaine concentrations were found to slowly increase during the course of the experiment a result that can be explained by the hydration of the skin. Previous studies have demonstrated increases in water permeation for up to 30 hours of hydration [14, 36].

A significant difference ($p < 0.05$) in the AUC_{tot} was determined in both the vascular and suture probes when using the silver electrode iontophoretic patch (0.15 mA/cm^2) in comparison to the passive patch. The subcutaneous ($p < 0.08$) and dermal ($p < 0.08$) $AUCt_{ot}$ were also found to be different compared to the passive patch values (Table 2.6). After approximately 12 hours, lidocaine concentrations obtained from passive delivery achieved an approximate steady state. At this time point, dermal lidocaine values achieved using the silver iontophoretic patch was 10 times greater than those obtained by passive diffusion. Lidocaine levels in the suture

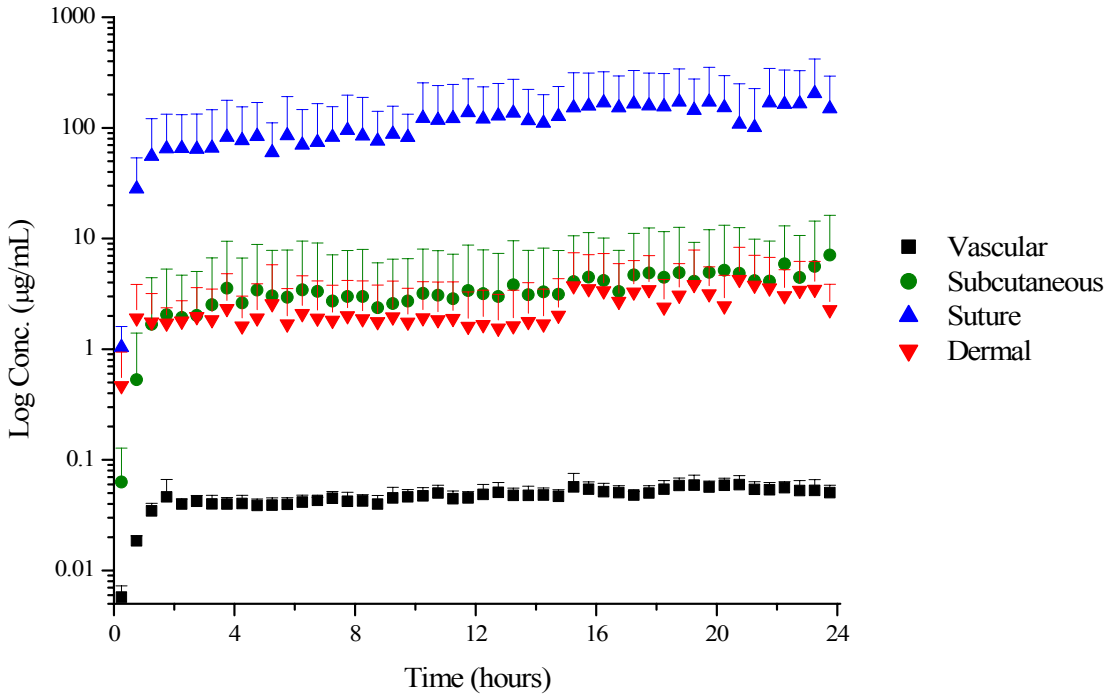

Figure 2.8. Mean data for Group 7 (Lidocaine gel, High 2 current, Silver electrode).

Table 2.6. Mean data obtained for Group 5 (Lidocaine gel, No current) and Group 7 (Lidocaine gel, High 2 current, Silver electrode).

Group		Units	Dermal	Suture	Subcutaneous	Vascular
5 n=4	AUC_{tot}	hr·μg/mL	9.6 ± 8.5	301.9 ± 208.0	5.4 ± 6.5	0.41 ± 0.19
7 n=4	AUC_{tot}	hr·μg/mL	44.3 ± 43.1	2717.7* ± 2557.6	79.9 ± 120.7	1.09* ± 0.16

*$p < 0.05$

were 15 times greater after iontophoresis. Subcutaneous amounts were nearly 15 times greater and vascular concentrations were five times the value determined when using the passive patch.

The difference in penetration between the silver and zinc electrodes can be explained by the transport properties of lidocaine. As discussed previously, two main driving forces (electromigration and electroosmosis) dictate the flow of analytes in an electric field. The predominant mode that an analyte travels under iontophoresis is important in the preparation of an effective patch. For example, drugs that are transported mainly by electromigration must have the number of competing ions minimized for optimal delivery. However, larger ions that move predominantly by electroosmosis require a different formulation as the net flow of ions is important for their movement [14, 19].

A study conducted by Marro and others analyzed the contributions of electromigration and electroosmosis in an iontophoretic drug delivery system of lidocaine [37, 38]. By using the neutral marker mannitol, they were able to determine the extent of contribution each process had on the movement of lidocaine across

excised pig ear skin. It was concluded that electromigration was the dominant mechanism in lidocaine penetration and contributed ~90% of the total flux [37, 38]. Therefore, the addition of competing ions could lead to poor transport of lidocaine.

When using patches constructed out of a zinc anode electrode an initial rise in lidocaine concentration is observed during the first three hours. As zinc continues to be oxidized at the electrode surface, the amount of Zn^{2+} accumulates. This is a small, highly charged ion that can compete with lidocaine. When a large quantity of zinc ions is generated, lidocaine penetration decreases. In order to eliminate this effect, a new patch was constructed using a silver electrode. When the silver metal is oxidized, it forms silver chloride which precipitates out of solution, eliminating the chance of a competing ion.

2.5.4 Usefulness of Microdialysis

During the course of this study, several sets of patches were received from the sponsor. One particular batch of the silver electrode patches was found to produce inconsistent results from previous studies using the same patch. Figure 2.9 displays a representative plot of the data collected from several of these patches. Lidocaine concentrations were found to peak during the first two hours and then rapidly drop to concentrations previously determined in the passive treatment group. Patches constructed with this design were previously shown to provide continual delivery of lidocaine throughout the course of the 24 hour sampling period. Current data from these experiments (Figure 2.10) also supported a continual drug delivery. An examination of the patch after the completion of the study revealed that the solder

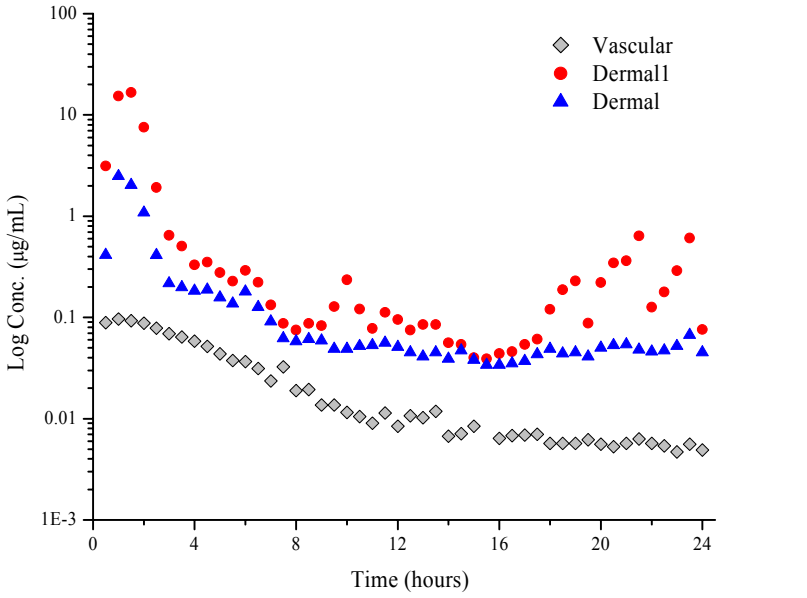

Figure 2.9. Representative plot of defective iontophoretic patches (0.15 mA/cm^2) composed of silver electrodes.

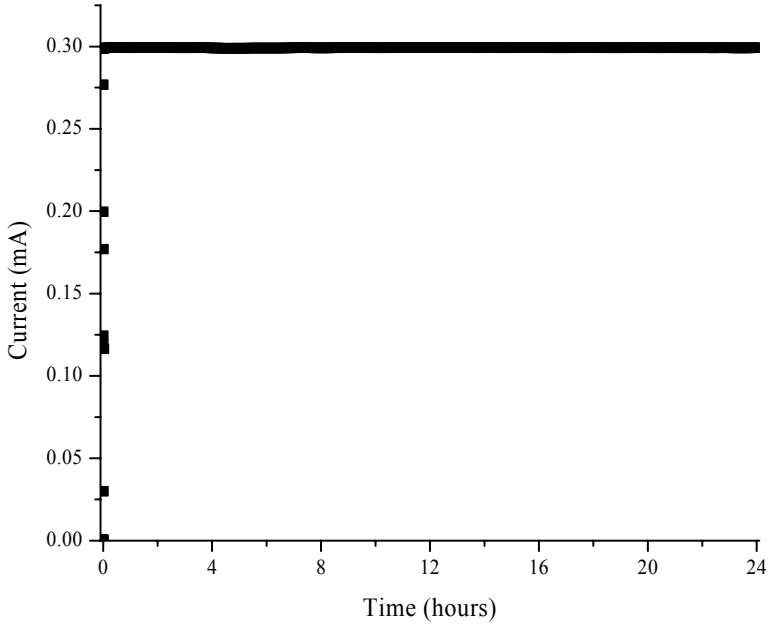

Figure 2.10. Representative current trace for batch of defective patches.

joint used to connect the anode electrode to the power supply was within the drug reservoir region. This joint was constructed out of tin metal which has a lower oxidation potential than silver. Therefore the production of tin ions would occur prior to the oxidation of silver. This particular patch would be expected to behave similar to patches constructed with zinc metal as again the production of competing ions is produced affecting the delivery of lidocaine.

2.5.5 Variability of Microdialysis Probes

2.5.5.1 Dermal Microdialysis Probes

Variations near 100 percent were determined for both the C_{max} and AUC_{tot} for the dermal probe. High inter- and intra-individual variability of exogenous species for cutaneous microdialysis has been previously reported in the literature [39]. Several factors contribute to this, including differences in skin barrier function which could affect skin absorption rates, metabolism and diffusion rate to the systematic circulation, and differences in probe implantation, mainly probe depth. The influence of probe depth has been under debate in the literature. A correlation between depth of penetration and concentration of lidocaine has been previously illustrated by Singh and Roberts when using tissue homogenates [21, 40]. Müller *et al*. reported a correlation between probe depth and the log of the area under the curve for nicotine penetration [41]. In addition, Mathy *et al.* demonstrated that probe depth and total drug penetration was independent when implanted to a depth of approximately 350 μm. Implantations below this depth, however, were found to have a significant

correlation between AUC and probe depth [42]. Conversely, several authors have reported no association of probe depth and concentration [43-47].

In order to evaluate this finding within this data set, histology slides were processed for each rat. Findings for the rats receiving the passive or no current treatment can be seen in Figure 2.11. These results show no correlation ($R^2 = 0.39$) between probe depth and log AUC_{tot}. When assessing depths greater than 350 μm as suggested by Mathy *et al.*, a stronger correlation is noted ($R^2 = 0.82$) [42]. A similar comparison was made using the C_{max} values of the no current treatment group (Figure 2.12). Again no correlation ($R^2 = 0.11$) between C_{max} and probe depth was found. When looking at probe depths greater than 350 μm, a stronger correlation was observed ($R^2 = 0.66$). It should be noted that the measurements plotted are from a single point along the membrane and some variation in depth along the length of the probe could exist.

Variation intra-animal was also examined via a control experiment that ensured an even drug penetration throughout the entire patch region. These experiments involved implanting two dermal probes parallel to one another in intact skin. Similar lidocaine penetration values were determined between probes within the same animal (Figure 2.13 and 2.14). A greater amount of inter-animal variation was observed especially in the passive delivery of lidocaine where three different penetration levels could be noted. In addition, greater variation in lidocaine concentrations was noted after longer application times of the iontophoretic patch.

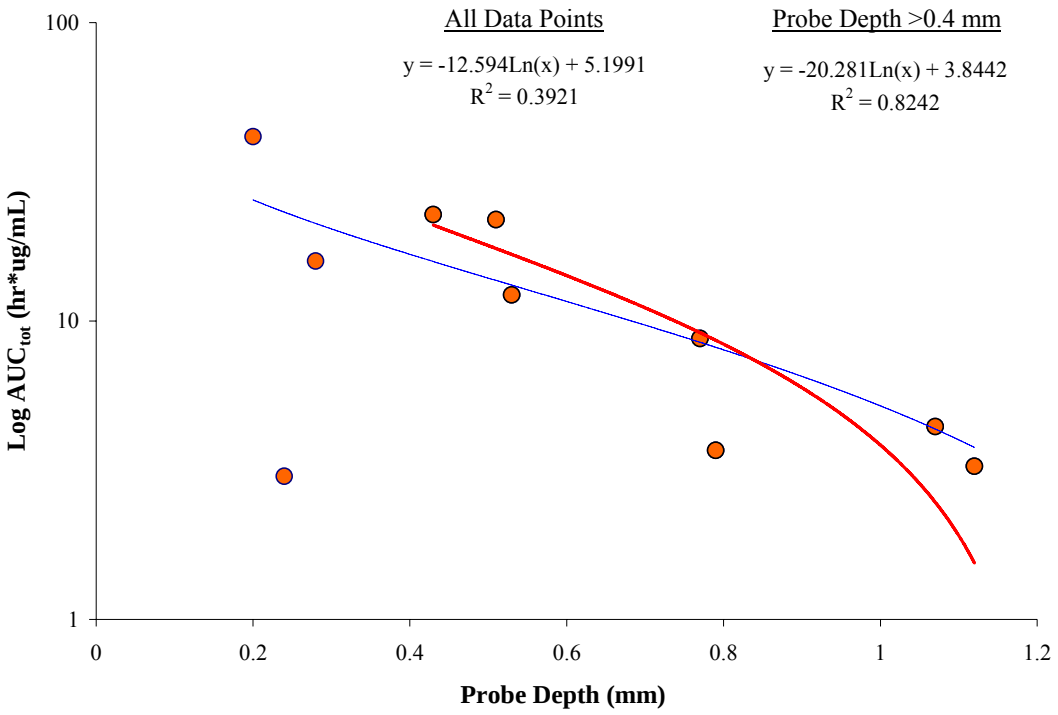

Figure 2.11. Correlation between log AUC_{tot} and dermal probe depth determined from histology slides.

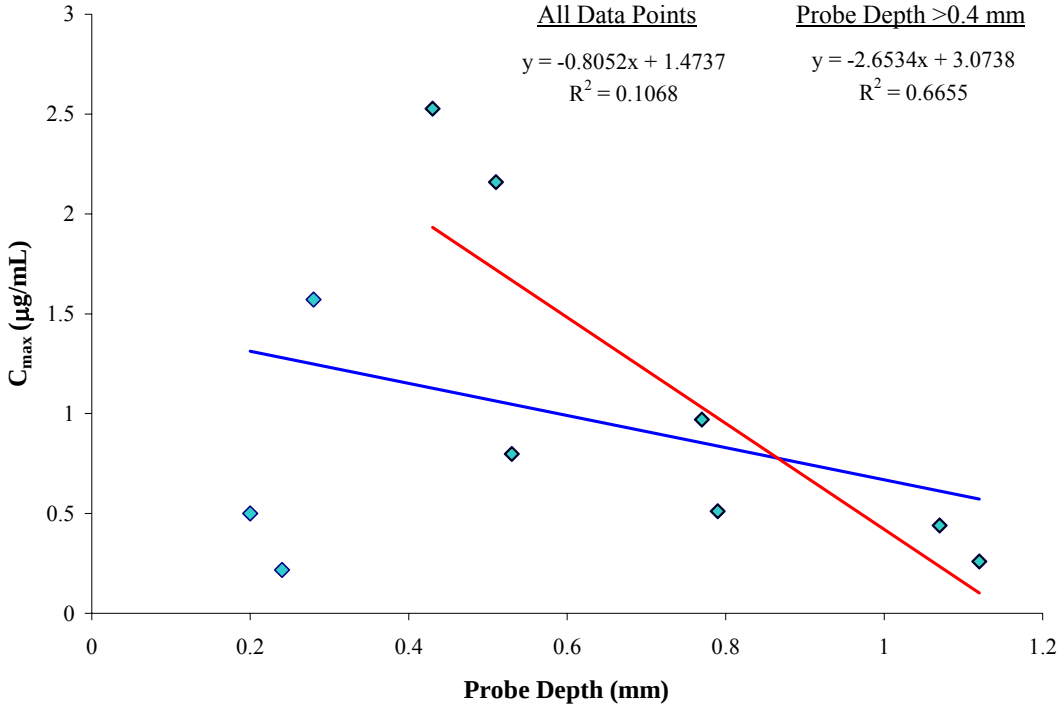

Figure 2.12. Correlation between C_{max} and probe depth determined from histology slides.

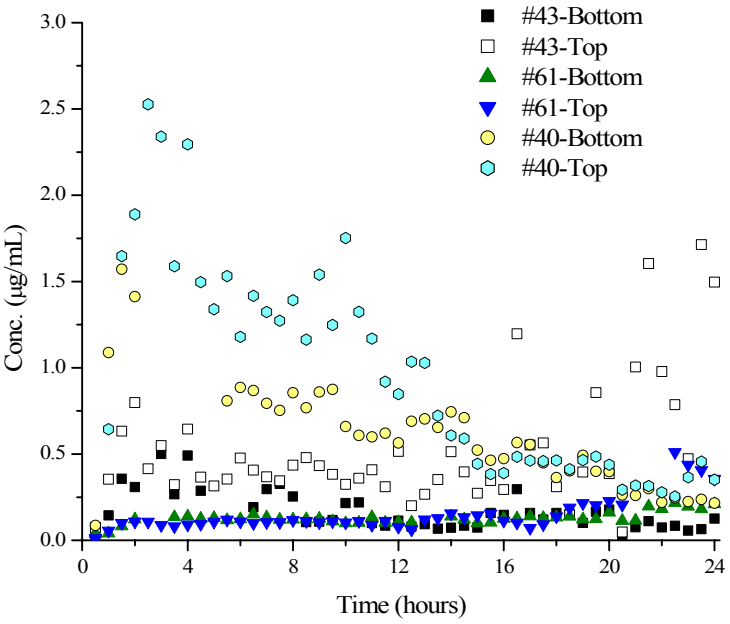

Figure 2.13. Two parallel dermal microdialysis probes experiment followed by passive diffusion of lidocaine gel.

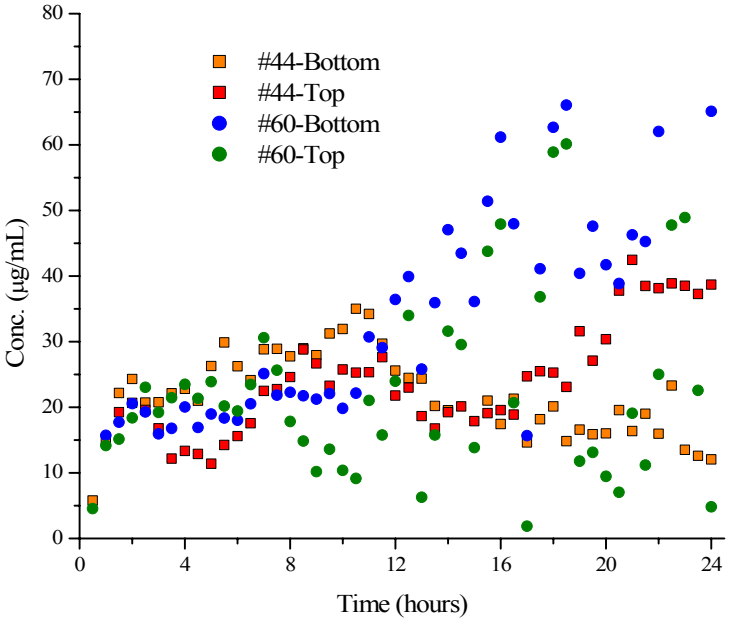

Figure 2.14. Two parallel dermal microdialysis probes followed by iontophoretic delivery of lidocaine using a silver electrode iontophoresis patch at 0.15 mA/cm^2.

2.5.5.2 Suture Microdialysis Probes

The flow of ions during iontophoresis has been shown to follow the path of least resistance [14]. In a system with intact skin, the greatest amount of ion flow has been shown to be through the sweat glands and the hair follicles [13, 17]. It is therefore believed that when the skin is damaged by an incision an increased amount of ions will flow through the incision. In order to test this theory a microdialysis probe was placed in the incision and sutured inside. After 12 hours of application, the suture lidocaine concentration was found to be 20 times greater for passive and 60 times greater for iontophoretic than the dermal concentration. Results for the total AUC showed 30 times higher levels in the suture than the dermal for passive delivery and 60 times greater values in the suture than the dermal for iontophoretic delivery.

Again, variations close to 100% were found for the C_{max} and AUC_{tot} for the suture results. As this was a new surgical technique, probe placement was evaluated for each individual rat via histological examinations. Probe placement was consistently found to be at the deeper region of the dermis. Another consideration for the large variation is differences in the rate of healing between rats. It has been shown that incisional wounds often begin epithelialization within the first 24 − 48 hours following the injury [48]. Since the patch is not applied until approximately 30 hours post-incision, differences in healing could lead to considerable changes in penetration. However, a study conducted by Spence and Pomeranz showed minimal increases in skin resistance up to five days after injury [49]. In this study they made a one centimeter incision on the dorsal region and monitored wound healing by

measuring the electrical resistance of the epidermis over the course of 20 days. Initial resistances were found to be low the first two days of healing with a marked increase in resistance beginning around day five [49]. As the flow of ions under iontophoresis is through the region of least resistance, it would seem that a large increase in penetration should be detected in the suture region for the initial five days following the incision.

Other areas that could affect drug penetration through the suture include the angle the incision is made at, the position of the incision in respect to the rat, the lay of the skin following suturing, the tightness of the suture and the positioning of the patch in respect to the rat. These particular details are defined by the surgeon and the particular procedure completed on the patient. The variation seen within this study was created by one surgeon. This is a real concern as the deviations from multiple surgeons could be much greater.

2.5.6 Effects of Suture

This project looked at the role of lidocaine penetration under passive conditions and when electrically driven. It was found that the suture plays an important role when evaluating both tissue specific concentrations and total free lidocaine concentrations. When lidocaine was allowed to penetrate due to diffusion as with the passive patch, similar dermal concentrations were found between intact skin and sutured skin (Figure 2.15). When driven by current, dermal levels were found to be different based on the presence of a suture. With a suture present, dermal

lidocaine levels approximately 0.5 cm – 1 cm medial from the suture were found to be roughly 2 − 3 μg/mL. However, when the skin was intact, dermal concentrations were approximately 20 μg/mL (Figure 2.16). The addition of an incision was found to significantly ($p < 0.05$) affect the dermal concentration when placed under iontophoresis (Table 2.7). The AUC_{tot} of lidocaine in the dermis was found to be approximately 12 times greater when the skin was intact compared to sutured skin under iontophoretic conditions. This demonstrates that without the suture lidocaine ions are forced through the dermis. When a suture is present, the ions will follow the path of least resistance and flow along the break in the dermis.

Table 2.7. Compiled parallel dermal microdialysis probe data.

Group		Units	Passive	Iontophoresis*
With Incision	AUC_{tot}	hr·μg/mL	9.6 ± 8.5	44.3 ± 43.1
Without Incision	AUC_{tot}	hr·μg/mL	10.3 ± 8.1	564.0 ± 186.6

*$p < 0.05$

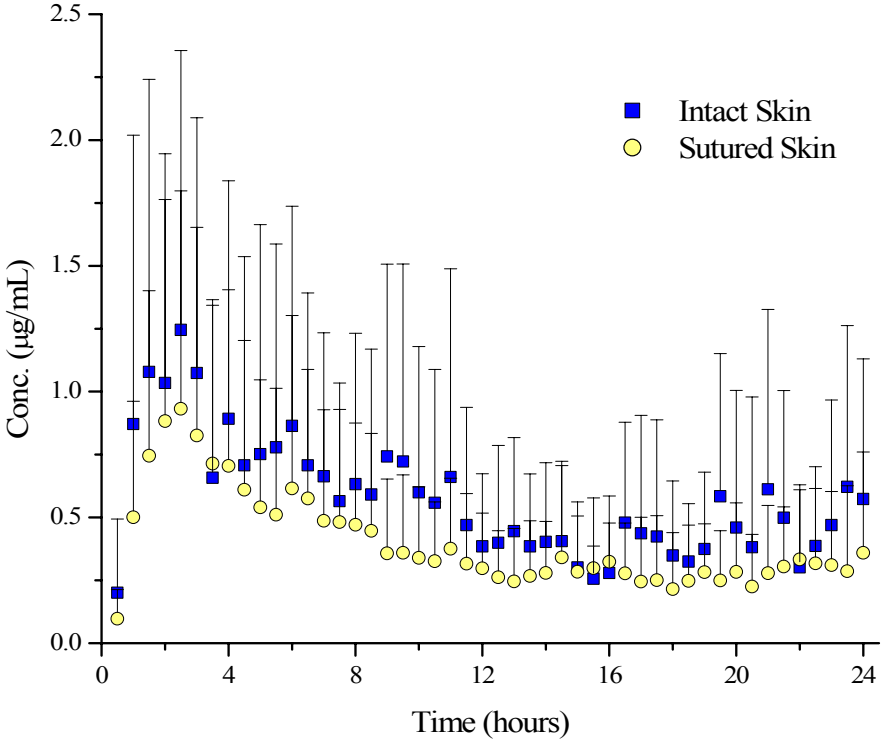

Figure 2.15. Comparison of dermal lidocaine penetration with and without incised skin following application of a passive patch.

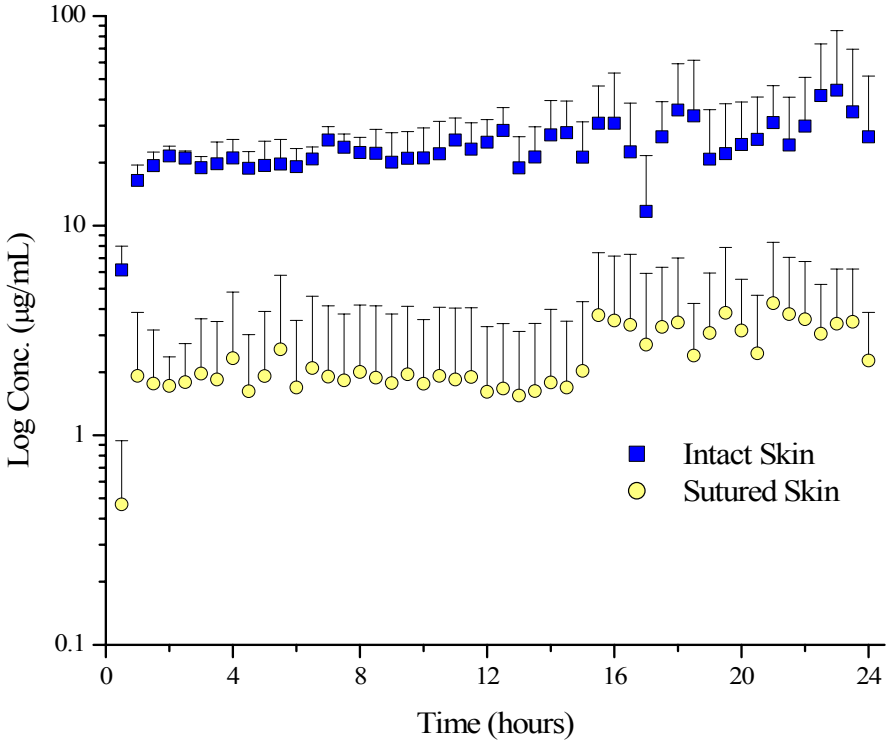

Figure 2.16. Comparison of dermal lidocaine penetration with and without incised skin following application of a silver electrode iontophoretic patch (0.15 mA/cm^2).

The addition of an incision also played an important role in the free blood concentration of lidocaine. When lidocaine penetrated the skin under passive conditions, an increased amount of free lidocaine was observed in the blood when a suture was present compared to intact skin (Figure 2.17). The AUC_{tot} was found to be five times greater when a suture was present compared to intact skin when tested using passive conditions. However, when a current was applied, the free lidocaine concentration between intact skin and sutured skin was found to be similar (Figure 2.18).

As discussed previously, the addition of an incision causes the net flow of ions to flow through the incision under both passive and iontophoretic conditions. The addition of an incision was found to significantly affect the free lidocaine concentration under passive conditions (Table 2.8). The presence of an incision did not play a role in the total concentration of lidocaine to reach the vascular system when placed under iontophoresis. These results suggest that the free blood concentration is dictated by the overall current of the iontophoretic patch and is independent to the pathway the ions travel.

Table 2.8. Compiled vascular data of both passive diffusion and iontophoretic (silver electrode patch at 0.15 mA/cm^2) diffusion of lidocaine.

Group		Units	Passive*	Iontophoresis
With Incision	AUC_{tot}	hr·μg/mL	0.41 ± 0.19	1.09 ± 0.16
Without Incision	AUC_{tot}	hr·μg/mL	0.080 ± 0.0052	1.30 ± 0.36

*$p < 0.05$

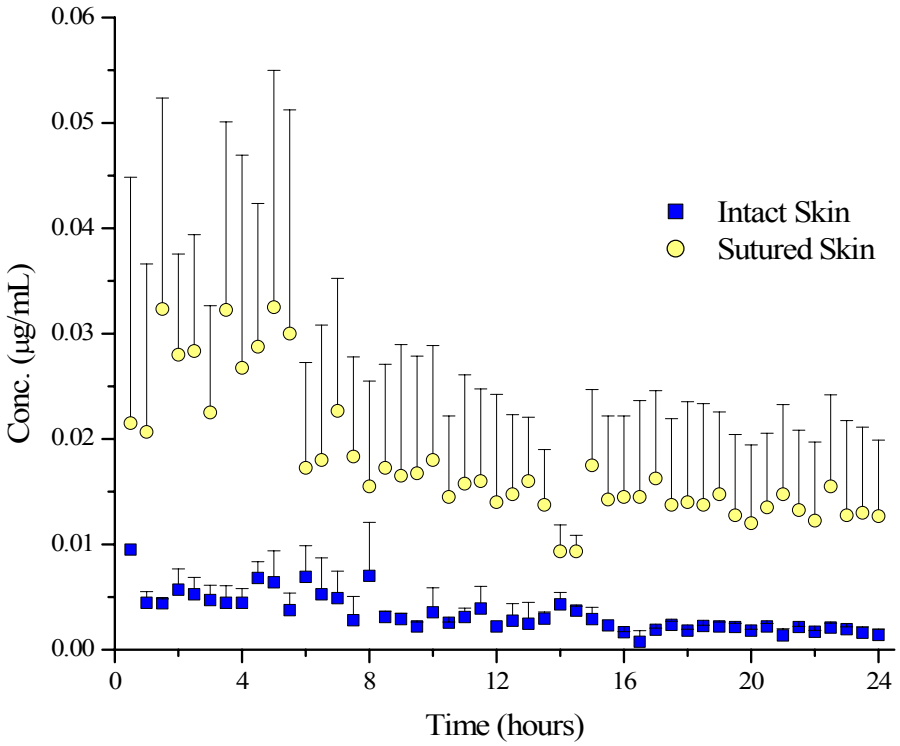

Figure 2.17. Comparison of free lidocaine concentration with and without incised skin following application of a passive patch.

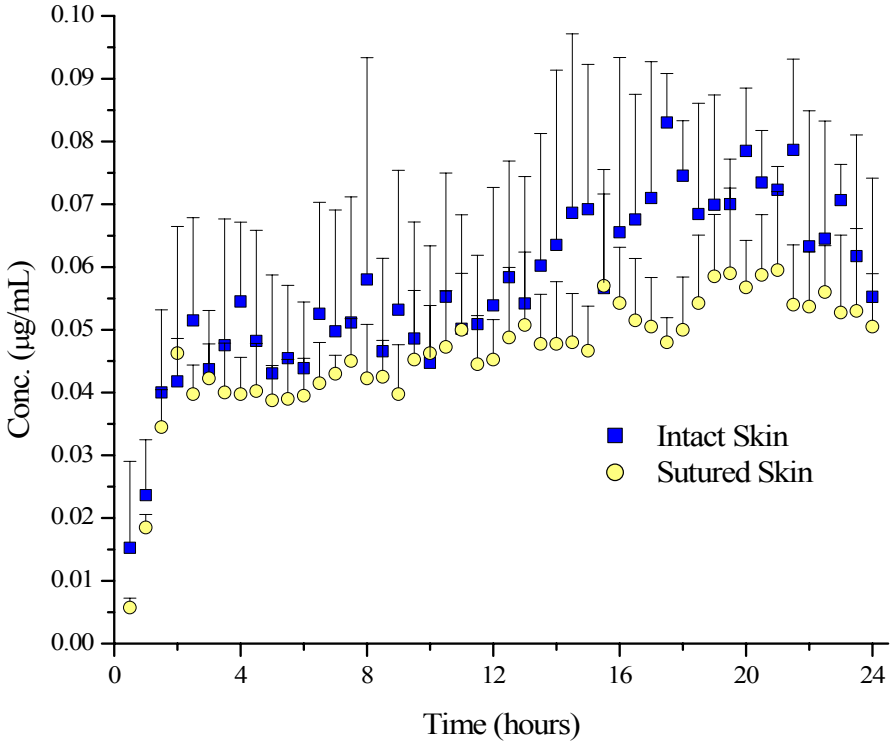

Figure 2.18. Comparison of free lidocaine concentration with and without incised skin following application of a silver electrode iontophoretic patch (0.15 mA/cm^2)

2.6 Conclusions

The presence of an incision was found to play a significant role in the path of drug flow. Overall, penetration of lidocaine was greater in the incision, when compared to adjacent intact skin, suggesting the dominant route of delivery is through the path of least resistance. This was noted under both passive and iontophoretic conditions. Under passive conditions, free lidocaine was found to be significantly greater with the existence of an incision. However, there was no change in the dermal lidocaine levels. When exposed to iontophoresis, the dermal concentration was found to be significantly less when a suture was present compared to intact skin. The total free lidocaine concentration however, was found to be unaffected by the presence of an incision. This demonstrates that total drug concentration is independent of the direction of drug flow.

Microdialysis was shown to be an important tool in the determination of drug flow. The free blood concentration data alone does not suggest the overall flow of drug. However, the addition of multi-probe microdialysis was needed in order to obtain a full understanding of drug flow.

On average, increased penetration values were determined in each of the suture, dermal, subcutaneous, and vascular probe locations when comparing an iontophoretic patch at a current of approximately 0.15 mA/cm^2 to passive patches. Patches constructed from zinc increased lidocaine penetration for approximately the first four hours proceeding patch application while the current remained constant. However, when the electrode was constructed from silver, drug penetration remained constant

or steadily increased throughout the 24 hour sampling period. Significant differences were found in the free blood concentration and the suture concentration between the passive and silver electrode iontophoretic patches.

2.7 References

1. Kawamata, M., et al., *Experimental Incision-Induced Pain in Human Skin: Effects of Systemic Lidocaine on Flare Formation and Hyperalgesia.* Pain, 2002. **100**: p. 77-89.

2. Wilson, D.V., K.S. Barnes, and J.G. Hauptman, *Pharmacokinetics of Combined Intraperitoneal and Incisional Lidocaine in the Dog Following Ovariohysterectomy.* Journal of Veterinary Pharmacological Therapy, 2004. **27**: p. 105-109.

3. Wallace, M.S., et al., *Concentration-Effect Relations for Intravenous Lidocaine Infusions in Human Volunteers: Effects on Acute Sensory Thresholds and Capsaicin-Evoked Hyperpathia.* Anesthesiology, 1997. **86**(6): p. 1262-1272.

4. Dirks, J., et al., *The Effect of Systemic Lidocaine on Pain and Secondary Hyperalgesia Associated with the Heat/Capsaicin Sensitization Model in Healthy Volunteers.* Anesth Analg, 2000. **91**: p. 967-72.

5. Gottrup, H., et al., *Differential Effects of Systemically Administered Ketamine and Lidocaine on Dynamic and Static Hyperalgesia Induced by Intradermal Capsaicin in Humans.* British Journal of Anaesthesia, 2000. **84**(2): p. 155-62.

6. Holthusen, H., S. Irsfeld, and P. Lipfert, *Effect of Pre- or Post-Traumatically Applied I.V. Lidocaine on Primary and Secondary Hyperalgesia after Experimental Heat Trauma in Humans.* Pain, 2000. **88**: p. 295-302.

7. Insler, S.R., et al., *Lidocaine and the Inhibition of Postoperative Pain in Coronary Artery Bypass Patients.* Journal of Cardiothoracic and Vascular Anesthesia, 1995. **9**(5): p. 541-546.

8. Argoff, C.E., et al., *Effectiveness of the Lidocaine Patch 5% on Pain Qualities in Three Chronic Pain States: Assessment with the Neuropathic Pain Scale.* Current Medical Research and Opinions, 2004. **20**: p. S21-S28.

9. Weiland, L., et al., *Pharmacokinetics of a Lidocaine Patch 5% in Dogs.* Journal of Veterinary Medicine, 2006. **53**: p. 34-39.

10. Pasero, C., *Lidocaine Patch 5%.* American Journal of Nursing, 2003. **103**(9): p. 75, 77-78.

11. *First Sterile Pharmaceutical Patch for Post-Surgical Incisional Pain Relief Gets Clearance*. 2003 [cited 2007 February 5th].

12. *Epicept Announce Results of European Phase III Trial for Lidopain® Sp*. 2006 [cited 2007 February 5].

13. Banga, A.K., *Electrically Assisted Transdermal and Topical Drug Delivery*. 1998: Taylor and Francis.

14. Smith, E.W. and H.I. Maibach, eds. *Percutaneous Penetration Enhancers*. 1995, CRC: New York.

15. Chaturvedula, A., et al., *In Vivo Iontophoretic Delivery and Pharmacokinetics of Salmon Calcitonin.* International Journal of Pharmaceutics, 2005. **297**: p. 190-196.

16. Tokumoto, S., N. Higo, and K. Sugibayashi, *Effect of Electroporation and Ph on the Iontophoretic Transdermal Delivery of Human Insulin.* International Journal of Pharmaceutics, 2006. **326**: p. 13-19.

17. Turner, N.G., et al., *Iontophoresis of Poly-L-Lysines: The Role of Molecular Weight?* Pharmaceutical Research, 1997. **14**(10): p. 1322-1331.

18. Merino, V., Y.N. Kalia, and R.H. Guy, *Transdermal Therapy and Diagnosis by Iontophoresis.* Trends in Biotechnology, 1997. **15**: p. 288-290.

19. Kalia, Y.N., et al., *Iontophoretic Drug Delivery.* Advanced Drug Delivery Reviews, 2004. **56**: p. 619-658.

20. Berner, B. and S.M. Dinh, eds. *Electronically Controlled Drug Delivery*. 1998, CRC Press: Boca Raton.

21. Singh, P. and M.S. Roberts, *Iontophoretic Transdermal Delivery of Salicylic Acid and Lidocaine to Local Subcutaneous Structures.* Journal of Pharmaceutical Sciences, 1993. **82**(2): p. 127-131.

22. Haga, H., T. Shibaji, and M. Umino, *Lidocaine Transport through Living Rat Skin Using Alternating Current.* Medical and Biological Engineering and Computing, 2005. **43**: p. 622-629.

23. Williams, P.L. and J.E. Riviere, *Model Describing Transdermal Iontophoretic Delivery of Lidocaine Incorporating Consideration of Cutaneous Microvascular State.* Journal of Pharmaceutical Sciences, 1993. **82**(11): p. 1080-1084.

24. Riviere, J.E., N.A. Monteiro-Riviere, and A.O. Inman, *Determination of Lidocaine Concentrations in Skin after Transdermal Iontophoresis: Effects of Vascoactive Drugs.* Pharmaceutical Research, 1992. **9**(2): p. 211-214.

25. Riviere, J.E., B. Sage, and P.L. Williams, *Effects of Vasoactive Drugs on Transdermal Lidocaine Iontophoresis.* Journal of Pharmaceutical Sciences, 1991. **80**(7): p. 615-620.

26. Karami, K., et al., *On Iontophoretic Delivery Enhancement: Ionization and Transport Properties of Lidocaine Hydrochloride in Aqueous Propylene Glycol.* International Journal of Pharmaceutics, 2000. **201**: p. 121-124.

27. Sintov, A.C. and R. SBrandys-Sitton, *Facilitated Skin Penetration of Lidocaine: Combination of a Short-Term Iontophoresis and Microemulsion Formulation.* International Journal of Pharmaceutics, 2006. **316**: p. 58-67.

28. Zempsky, W.T., et al., *Evaluation of a Low-Dose Lidocaine Iontophoresis System for Topical Anesthesia in Adults and Children: A Randomized, Controlled Trial.* Clinical Therapeutics, 2004. **26**(7): p. 1110-1119.

29. Huang, Y.-J., J.-F. Liao, and T. Tung-Hu, *Concurrent Determination of Thalidomide in Rat Blood, Brain, and Bile Using Multiple Microdialysis Coupled to Liquid Chromatography.* Biomedical Chromatography, 2005. **19**(7): p. 488-493.

30. Tung-Hu, T., *Pharmacokinetics of Pefloxacin and Its Interaction with Cyclosporin a, a P-Glycoprotein Modulator in Rat Blood, Brain, and Bile, Using Simultaneous Microdialysis.* British Journal of Pharmacology, 2001. **132**: p. 1310-1316.

31. Ting-Yu, T. and T. Tung-Hu, *Measurement of Unbound Geniposide in Blood, Liver, Brain, and Bile of Anesthetized Rats: An Application of Pharmacokinetic Study and Its Influence on Acupuncture.* Analytica Chemica Acta, 204. **517**: p. 47-52.

32. Davies, M.I. and C.E. Lunte, *Simultaneous Microdialysis Sampling from Multiple Sites in the Liver for the Study of Phenol Metabolism.* Life Sciences, 1996. **59**(12): p. 1003-1013.

33. Stenken, J.A., *Methods and Issues in Microdialysis Calibration.* Analytica Chemica Acta, 1999. **379**: p. 337-358.

34. Song, Y. and C.E. Lunte, *Calibration Methods for Microdialysis Sampling in Vivo: Muscle and Adipose Tissue.* Analytica Chimica Acta, 1999. **400**: p. 143-152.

35. Stagni, G., et al., *Iontophoretic Current and Intradermal Microdialysis Recovery in Humans.* Journal of Pharmacological Toxicology, 1999. **41**: p. 49-54.

36. Bronaugh, R.L. and H.I. Maibach, eds. *Percutaneous Absorption*. Dermatology, ed. C.D. Calnan and H.I. Maibach. Vol. 6. 1985, Marcel Dekker, Inc.: New York.

37. Marro, D., et al., *Contributions of Electromigration and Electroosmosis to Iontophoretic Drug Delivery.* Pharmaceutical Research, 2001. **18**(12): p. 170-1708.

38. Marro, D., et al., *Optimizing Iontophoretic Drug Delivery: Identification and Distribution of Charge-Carrying Species.* Pharmaceutical Research, 2001. **18**(12): p. 1709-1713.

39. Schnetz, E. and M. Fartasch, *Microdialysis for the Evaluation of Penetration through the Human Skin Barrier- a Promising Tool for Future Research?* European Journal of Pharmaceutical Sciences, 2001. **12**: p. 165-174.

40. Singh, P. and M.S. Roberts, *Dermal and Underlying Tissue Pharmacokinetics of Lidocaine after Topical Application.* Journal of Pharmaceutical Sciences, 1994. **83**(6): p. 774-782.

41. Müller, M., et al., *In Vivo Characterization of Transdermal Drug Transport by Microdialysis.* Journal of Controlled Release, 1995. **37**: p. 49-57.

42. Mathy, F.-X., et al., *Fluconazole Distribution in Rat Dermis Following Intravenous and Topical Application: A Microdialysis Study.* Journal of Pharmaceutical Sciences, 2005. **94**(4): p. 770-780.

43. Ault, J.M., et al., *Dermal Microdialysis Sampling in Vivo.* Pharmaceutical Research, 1994. **11**(11): p. 1631-1639.

44. Chaturvedula, A., et al., *Dermal, Subdermal, and Systematic Concentrations of Granisetron by Iontophoretic Delivery.* Pharmaceutical Research, 2005. **22**(8): p. 1313-1319.

45. Kreilgaard, M., *Dermal Pharmacokinetics of Microemulsion Formulations Determined by in Vivo Microdialysis.* Pharmaceutical Research, 2001. **18**(3): p. 367-373.

46. Kreilgaard, M., et al., *Influence of a Microemulsion Vehicle on Cutaneous Bioequivalence of a Lipophilic Model Drug Assessed by Microdialysis and Pharmacodynamics.* Pharmaceutical Research, 2001. **18**(5): p. 593-599.

47. Stagni, G., et al., *Intradermal Microdialysis: Kinetics of Iontophoretically Delivered Propranolol in Forearm Dermis.* Journal of Controlled Release, 2000. **63**: p. 331-339.

48. Coulombe, P.A., *Wound Epithelialization: Accelerating the Pace of Discovery.* Dermatology Foundation, 2003. **37**(1): p. 219-230.

49. Spence, D.W. and B. Pomeranz, *Surgical Wound Healing Monitored Repeatedly in Vivo Using Electrical Resistance of the Epidermis.* Physiological Measurements, 1996. **17**: p. 57-69.

Chapter Three

Ultrafiltration and Microdialysis Sampling in the Göttingen Minipig and Sprague Dawley Rat

3.1 Purpose

The purpose of this research project was to establish a cutaneous sampling technique in the Göttingen minipig. The use of microdialysis and ultrafiltration were both explored. A complete comparative analysis of these techniques was further continued for cutaneous sampling in the Sprague Dawley rat. This work was in collaboration with Pfizer, Inc.

3.2 Introduction

3.2.1 Skin Model Comparison

As transdermal drug delivery continues to gain acceptance as a viable application technique, the need for an appropriate skin model lingers. The majority of skin penetration studies are completed as *in vitro* experiments. These generally use the Franz diffusion cell which sandwiches the skin sample between the donor and acceptor compartments [1]. Several different skin types besides human skin have been studied, including rat, mouse, guinea pig, pig, reptile, miniature pig, horse, goat, rhesus monkey, and chimpanzee [2-11]. In addition, several commercially available human reconstructed skin models and artificial membranes have been evaluated [12-15]. Although important preliminary data can be collected from these *in vitro*

systems, they do not incorporate many of the body's immunological responses that include the circulatory system and enzymatic degradation. This often leads to over-estimation of drug penetration in comparison to *in vivo* systems [16-19]. This was first documented by Ault et al. who demonstrated a forty-fold increase in dermal penetration *in vitro* compared to the same system *in vivo* [16]. Therefore, *in vitro* models are generally used as an initial screening for determining approximate penetration ranks [1].

Several *in vivo* models have commonly been used for dermal penetration studies. The variety of animals used for these studies are decreased from the *in vitro* list and generally include humans, rats, mice, and guinea pigs. Due to its ease of handling and relatively low cost, the rat is typically the animal of choice for cutaneous absorption studies [20]. More specifically, the hairless rat is an appealing animal for dermal studies as it has similar hair structure as compared to humans [21]. Yet again greater penetration often occurs across animal skin in relation to human skin [4, 5, 20-22]. Using results based solely on animal experiments could result in under estimation of the proper dosing regimen to humans. In order to develop a more accurate model for human exposure, van Ravenzwaay and Leibold developed a relationship between human *in vitro* dermal penetration studies and both *in vivo* and *in vitro* rat dermal penetration studies, as seen below [20, 22].

$$\%\ human\ \ penetration = (\%\ rat\ in\ vivo\ \ penetration) \times \frac{in\ vitro\ rate\ \ penetration\ human}{in\ vitro\ rate\ \ penetration\ rat}$$

3.2.2 Minipig as a Skin Model

One of the leading animal models used for dermal penetration is the pig. It has been reported to follow similar penetration trends as compared to human skin and has more comparable penetration values than other animal skin models [11, 13, 21, 23]. Pig skin has been shown to have very similar skin qualities to human skin that include dermal and epidermal thickness, immunological cells, hair follicle structure, and cellular turn over rate (Table 3.1) [24-28]. In addition, the lipid composition of the stratum corneum has been reported to have similar content and structure [11, 23, 26, 29, 30]. The main difference between these two skin types is the sweat glands; humans have eccrine glands with watery secretions while minipigs have apocrine glands with oily secretions [23, 24].

Due to their smaller stature, fairly mild temperament, and physical cooperation in comparison to domestic swine, the minipig is beginning to be used more frequently in toxicological and pharmacokinetics studies [25]. The Göttingen minipig is genetically and environmentally controlled, as far as microbiological contamination and feeding restrictions are concerned [25, 31]. To date, dermal penetration has only been studied using *in vitro* techniques or tape stripping on the pig. This project therefore proposed to evaluate ultrafiltration as a method for dermal sampling and to compare it microdialysis, an established cutaneous sampling technique, in both the Sprague Dawley rat and the Göttingen minipig.

Table 3.1. Skin comparison between human skin and pig skin.

Characteristic	Pig skin	Human skin
Epidermal thickness	30-140 μm[11, 24, 26-28]	50-120 μm[11, 24, 26-28]
Dermal thickness	2.0 mm[25, 27]	1.2 mm[25]
Lipid composition and organization	Same[13]	Same[13]
Sweat glands	Apocrine[23, 24]	Eccrine[23, 24]
Body hair	Sparse[24, 26-28]	Sparse[24, 26-28]
Langerhan's cells	Present[24, 27, 31]	Present[24, 27, 31]
Dermal vascularization	Moderate[23]	High[23]
Dermal vasoconstriction	High[24]	Low[24]

3.2.3 Sampling Technique Comparison

As previously discussed in Chapter One, microdialysis offers several advantages over other dermal sampling techniques. One major disadvantage to microdialysis sampling is that it requires the use of an infusion pump connected to the subject. For small animals such as mice and rats, this is generally not a problem; awake animal systems have been developed that allow the animal to be freely moving while still being connected to the pumping device as seen in Chapter Two. However, for larger animals such as the minipig, confinement in movement is necessary which limits the applicability of the microdialysis technique. For this reason, ultrafiltration would provide a good alternative as a sampling method. A comparison between microdialysis sampling and ultrafiltration sampling can be seen in Table 3.2.

Ultrafiltration functions by applying a negative pressure across a membrane fiber by either a small vacutainer or peristaltic pump which allows for direct sampling of the extracellular fluid. The use of a vacutainer allows for sampling in larger animals as it can be enclosed in and protected by a lightweight jacket that is worn by the animal. Ultrafiltration has been demonstrated in several large animals including sheep, horse, dog, and human [32-36].

The use of ultrafiltration has been shown in a variety of tissues which includes subcutaneous, muscle, and bone marrow. However, as it extracts extracellular fluid directly from the tissue sampled, ultrafiltration is not suitable for all tissue. Its use in the study of brain neurochemistry is not possible as it could affect the phenomena being studied [37]. In addition, ultrafiltration is dependent on the body's ability to

Table 3.2. Comparison between microdialysis and ultrafiltration sampling.

	Microdialysis	**Ultrafiltration**
Operation	Pump	Negative Pressure
Flow rate	Precise	Dependent
Sample	Protein Free	Protein Free
Tissue	Variety	Most
Damage	Minimal	Increased
Length	Time-limited	Up to 6 months
Recovery	Calibration Required	100% Recovery
Movement	Restricted	Free Motion

replace the fluid in the tissue via the blood vessels, another reason sampling in the brain with ultrafiltration is not possible [38].

The flow rate for ultrafiltration is directly proportional to membrane surface area; therefore, general probe design is a multiple looped system (Figure 3.1). Under high negative pressure, volumes between 50 – 100 microliters can be collected. However, a 14-gauge cannula is needed for implantation which can cause tissue damage [38]. A second design has been developed that uses a single fiber, reducing the damage created during implantation. For this type of probe, a disposable syringe is used to create a vacuum, allowing for sampling at very low flow rates (50 – 150 nL/min) [38, 39]. For this project, a combination of the described designs was utilized (Figure 3.2). As the dermal thickness of a pig is approximately 1.2 mm, a single fiber design must be employed. To allow for free motion, the use of a vacutainer was utilized.

Another drawback with microdialysis sampling is the requirement of probe calibration before or during the course of the experiment. In addition, the length of an experiment is limited due to the body's immunological response which can cause cellular adhesion to the microdialysis fiber, affecting the recovery of an analyte [36, 37]. Ultrafiltration, however, has been shown to give recoveries close to 100% for low molecular weight compounds as it samples the extracellular fluid directly [38]. It can also give recoveries greater than 90% for model proteins with molecular weights up to 68,000 Da [40]. Sampling by ultrafiltration has been reported for up to six months [41]. The addition of a fibrous layer on the membrane may not affect the

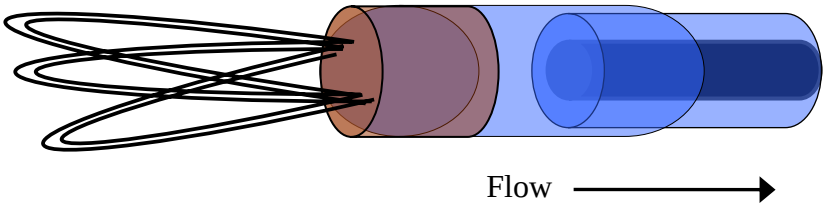

Figure 3.1. Example of the triple looped ultrafiltration probe.

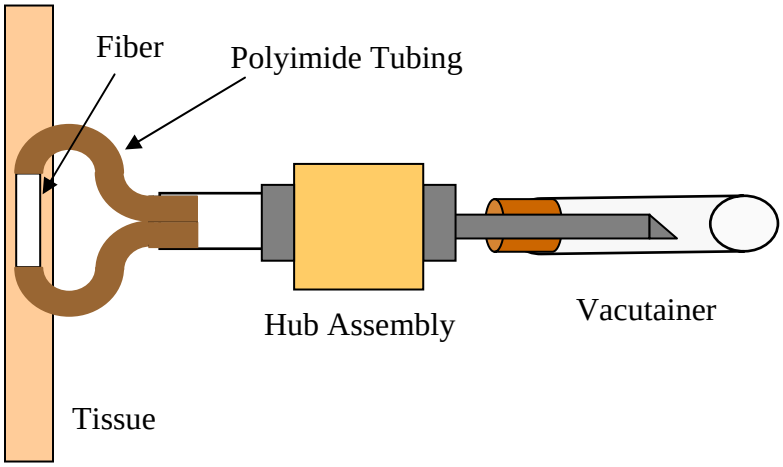

Figure 3.2. Probe schematic utilized for dermal ultrafiltration sampling.

overall recovery as the extracellular fluid is being directly sampled. The overall flow of fluid however may be affected [37].

3.3 Specific Aims

The specific aim of this project was to develop a dermal sampling protocol in the Göttingen minipig. This was completed by utilizing both ultrafiltration and microdialysis. Using these sampling techniques, a comparison between two different permeators, salicylic acid and caffeine, was completed. In addition, the Göttingen minipig was assessed as an alternative to the human model. Finally, a further look into the feasibility of ultrafiltration as a dermal sampling device was completed in the Sprague Dawley rat.

3.4 Materials and Methods

3.4.1 Chemicals

Salicylic acid, caffeine, potassium phosphate, triethanolamine, 2-aminophenol, sodium hydroxide were obtained from Sigma (St. Louis, MO). Carbopol 934 was received from Noveon, Inc. (Cleveland, OH). Ringer's solution consisted of 145 mM NaCl, 2.8 mM KCl, 1.2 mM $CaCl_2$, and 1.2 mM $MgCl_2$ all purchased from Fisher Scientific (Fair Lawn, NJ). HPLC grade acetonitrile was purchased from Fisher Scientific. Ketamine was manufactured by Fort Dodge Animal Health (Fort Dodge, IA), xylazine was made by Ben Venue Laboratories (Bedford, OH), and acepromazine was manufactured by Boehringer Ingelheim (St.

Joseph, MO). An ethylene oxide mixture called Oxyfume 2002 (Linweld, Topeka, KS) was used for sterilizing all microdialysis probes prior to insertion for survival studies. Water for buffer preparation was filtered through a Labconco, Water Pro Plus.

3.4.2 HPLC Instrumentation

Minipig data was analyzed using a Shimadzu LC-6A pump and a Shimadzu SPD-6AV UV-Vis spectrophotometric detector (Shimadzu Scientific Instruments, Inc. Columbia, MD) and acquired with a PE Nelson 900 Series Interface with programming through TurboChrom software from Perkin Elmer (San Jose, CA, USA). Sprague Dawley rat data was evaluated using a Shimadzu LC-10ADVP pump, SCL-10AVP Shimadzu system controller, Shimadzu SPD-10A UV-Vis spectrophotometric detector and Shimadzu SIL-20AC auto sampler. Chromatographic data was acquired using EZStart software (Shimadzu Scientific Instruments, Inc., Columbia, MD). Separation was achieved using a Gemini C18 column (5 μm, 150 mm x 2.0 mm). Mobile phase consisted of 30 mM phosphate buffer, pH 8.5:acetonitrile (85:15 v/v). The flow rate was set to 0.2 mL/min with the wavelength set to either 300 nm (salicylic acid only) or 285 nm (salicylic acid and caffeine).

3.4.3 Probe Construction

3.4.3.1 Microdialysis

Linear microdialysis probes with either a 5 mm (rat studies) or a 4 cm (minipig and rat studies) PAN membrane (250 μm i.d., 350 μm o.d, molecular weight cutoff of 30 kDa) were used. Probes were home-made as previously discussed in chapter two. Briefly, a piece of polyimide tubing (175 μm i.d., 215 μm o.d., MicroLumen, Tampa, FL) was threaded into a segment of PAN membrane (Hospal Industrie Meyzieu, France). UV glue (UVEX, CA) was coated on top of the connection and cured using a UV curing system (ELC-450 UV Light Spot-Cure system, Electro-Lite, Bethel, CT). A one centimeter piece of tygon tubing (Norton Performance Plastics, Akron, OH) was UV glued to the inlet of the microdialysis probe and connected to a Hamilton syringe mounted on a CMA/100 syringe pump. Ringer's solution was perfused at a flow rate of 2 μL/min.

3.4.3.2 Ultrafiltration

Ultrafiltration probes consisted of linear probes (described above). To strengthen the ultrafiltration probes and to make them visible by ultrasound, tungsten wire (California Fine Wire Company, Grover Beach, CA), 40.6 μm in size, was inserted into the probe. Following implantation, both the inlet and outlets were secured together in a piece of tygon tubing and then inserted into the hub assembly portion of the vacutainer setup (Bioanalytical Systems, West Lafayette, IN).

3.4.4 Surgical Procedure

3.4.4.1 Sprague Dawley Rat

Female Sprague Dawley rats (Charles Rivers, Raleigh, NC) weighing 200 300 g were housed in cages that were maintained in temperature-controlled rooms with animals having free access to food and water. Rats were initially sedated by inhalation with isofluorane followed by a subcutaneous. injection of the cocktail mixture: ketamine (67.5 mg/kg), xylazine (3.4 mg/kg), and acepromazine (0.67 mg/kg). The back of the rat was then shaved using an Oster Model A5 animal clipper (blade size 40, Milwaukee, WI), taking care to not damage the skin. Throughout the surgical procedure and experiment, rat body temperature was maintained by placing the animal on a heating pad. A linear probe was implanted into the dermis along the back of the rat (head to tail) using a 23-gauge needle. Once the needle was inserted into the dermis the microdialysis probe was threaded into the needle and the needle was withdrawn leaving the microdialysis probe in the dermis. The probe was then fixed into place by placing a drop of tissue glue (3M Animal Care Products, St. Paul, MN) at both the entrance and exit points of the probe. Up to five linear probes at least one centimeter apart were implanted into the back of the rat per surgery. Probe depth was determined via histological examination.

3.4.4.2 Göttingen Minipig

Castrated male Göttingen minipigs (Marshall Farms, North Rose, NY) weighing 11-24 kg were housed as a colony of four in a designated room with

temperature and humidity control. The minipigs were maintained on a restricted diet (fed twice daily) with free access to water. Animals were fasted for a minimum of two hours prior to surgical procedures. Animals were restrained in the pig sling for all surgical procedures and sampling. All drapes and instruments were autoclaved prior to use. Microdialysis probes and protective tubing were sterilized by exposure to ethylene oxide. Göttingen minipigs were lightly sedated using a combination of ketamine (20 mg/kg) and xylazine (2 mg/kg) administered i.m. in the posterior with further booster doses consisting of ketamine at ¼ to ½ of the original dose. The sides of the pig were sterilized by swabbing betadiene and 70% alcohol alternating three times each. A local anesthetic, 2% lidocaine (Abbott Laboratories, North Chicago, IL) was administered subcutaneously in a fan-like pattern at both ends of the implantation sites. Three four-centimeter linear probes were implanted on each side of the back of the minipig using a 20-gauge needle from an i.v. catheter (Terumo Medical Corporation, Somerset, NJ). Probes were secured by placing a drop of tissue glue on both the entrance and exit points. In addition, these points were covered with a piece of Ioban tape (3M, St. Paul, MN). The exposed polyimide was then protected by covering it with MRE-33 tubing (Braintree Scientific Inc., Braintree, MA). Probe area was covered with sterile pads (Telfa®) and secured by steri-drape. The minipig was then placed in a pig jacket (Lomir Biomedical, Malone, NY) and allowed to recuperate in seclusion.

3.4.5 Calibration of Microdialysis Probes

Calibration for microdialysis was completed using the method of retrodialysis described in Chapter One, Section 1.4.3.4. In short, 5 μg/mL of each drug studied was perfused at 2 μL/min until 5 consecutive samples were collected giving a relative standard deviation of less than 5%. The microdialysis probes were then perfused with just the internal standard, 2-aminophenol, until the analyte(s) of interest cleared from the surrounding tissue. Throughout the dosing period, the extraction efficiency of the analyte(s) of interest was adjusted to the changes in the extraction efficiency of the internal standard.

3.4.6 Microdialysis Probe Depth

Depth of probe placement in the Göttingen minipig was confirmed by Dr. Leon Connor, a veterinarian from Highland Park Animal Clinic, Topeka, KS. Probe depth was established by 10 MHz ultrasound scanning using a Ausonics Impact. For determination of probe depth in the Sprague Dawley rat, skin samples were initially fixed in 10% buffered formaldehyde solution and then brought to Lawrence Memorial Hospital (Lawrence, KS) for completion of histological examination.

3.4.7 Drug Application

Drug application was completed in multiple forms and indicated on each individual figure. These forms include application of cotton balls soaked in drug solution, smearing of cream, or application of hydro-alcohol gel. The hydro-alcohol

was made by mixing 30% ethanol, 67% water, 1% drug (or as indicated), and 1% carbomer (carbopol 934) [42]. Triethanolamine was added drop wise until the desired consistency was achieved.

3.5 Results and Discussion: Göttingen Minipig

3.5.1 Ultrafiltration Sampling

Using the single linear microdialysis probe design, initial investigations looked into determining the appropriate membrane length needed for 1 – 2 hour collection times. Independent of membrane length, sample volumes often varied between collection time points indicating varied flow rates. For example, using a 2 cm linear probe volumes ranged from condensation up to 20 μL collected during a three hour sampling period. To achieve even flow rates, the use of a peristaltic pump is recommended, however this would require the restraint of the animal during sampling as in microdialysis sampling. The main advantage to using ultrafiltration sampling is that it allows the animal to be freely moving as vacuum can be established using vacutainers that can be secured in a pig jacket (Figure 3.3). The LC conditions developed required the use of a 10 μL sample. Therefore, a 4 cm membrane was decided upon to ensure 1 – 2 hour sampling times and allow for an easier implantation. Figure 3.4 demonstrates the variation in the volumes collected over the course of an experiment. As seen, most samples met the minimum sample volume requirement for data analysis.

Figure 3.3. Sampling by ultrafiltration can be completed while the animal is freely moving as vacuum can be completed using vacuatiners which are placed in the pockets of the pig jacket.

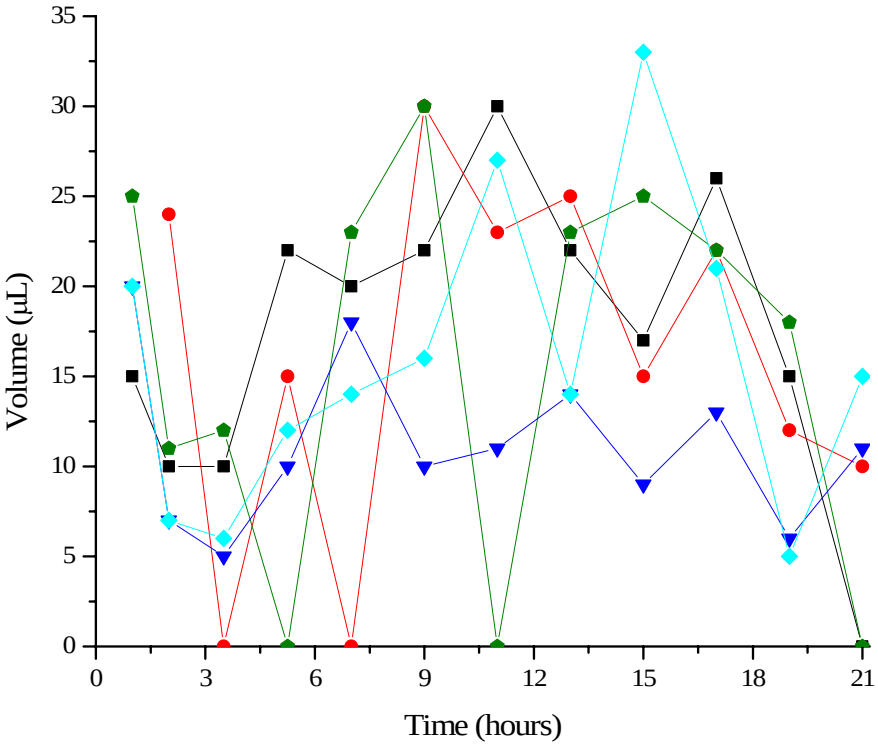

Figure 3.4. Example of volumes collected from five separate probes using dermal ultrafiltration sampling with a vacutainer.

The length of the ultrafiltration studies generally lasted for a total of three days. Over the course of the study, probe functionality decreased due to degradation of the UV glue which caused the probes to pull apart or destruction caused by the minipig. However, approximately 50% of the ultrafiltration probes were found to be functional one week post-implantation. Studies were limited to this time frame to limit the stress caused on the Göttingen minipig induced by isolation.

3.5.2 Microdialysis Sampling

As the movement of the minipig was restricted during the course of microdialysis sampling, a periodic sampling scheme was developed (Figure 3.5). Probe implantation and calibration was completed on day one. The following morning, the target drug was applied to the minipig followed by approximately six hours of sampling. At the end of the sampling, the drug was left on the minipig, microdialysis probes were secured and the minipig was re-jacketed. The following morning, the minipig was again lightly sedated for the final collection time of 3 – 4 hours. Due to the intermittent sampling scheme the use of an internal standard, 2-aminophenol, was utilized for calibration by retrodialysis as discussed in Chapter One, Section 1.4.3.4. A separation scheme (Figure 3.6) was developed for the two analytes of interest, caffeine and salicylic acid, and for the internal standard, 2-aminophenol. Delivery of the internal standard was found to be relatively constant throughout the course of the experiment, with a slight increase in delivery for the second and third day in respect to the initial delivery on day one (Figure 3.7).

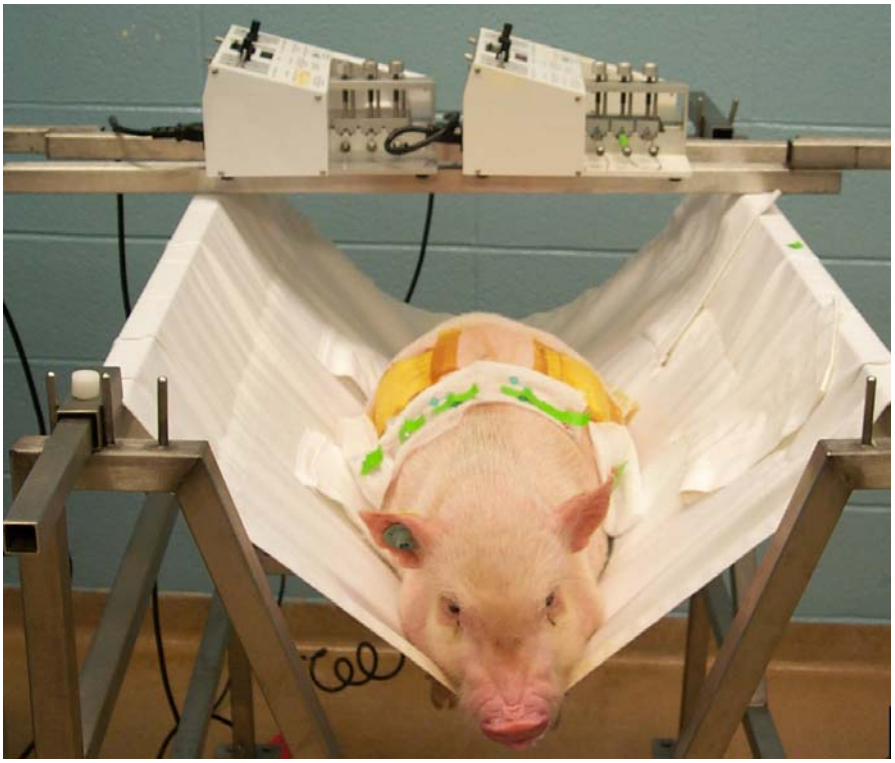

Figure 3.5. Microdialysis sampling required the minipig to be lightly sedated and restrained throughout the sampling period. Sampling was limited to approximately 6 hours as sores would develop as a result of being restrained in the pig sling.

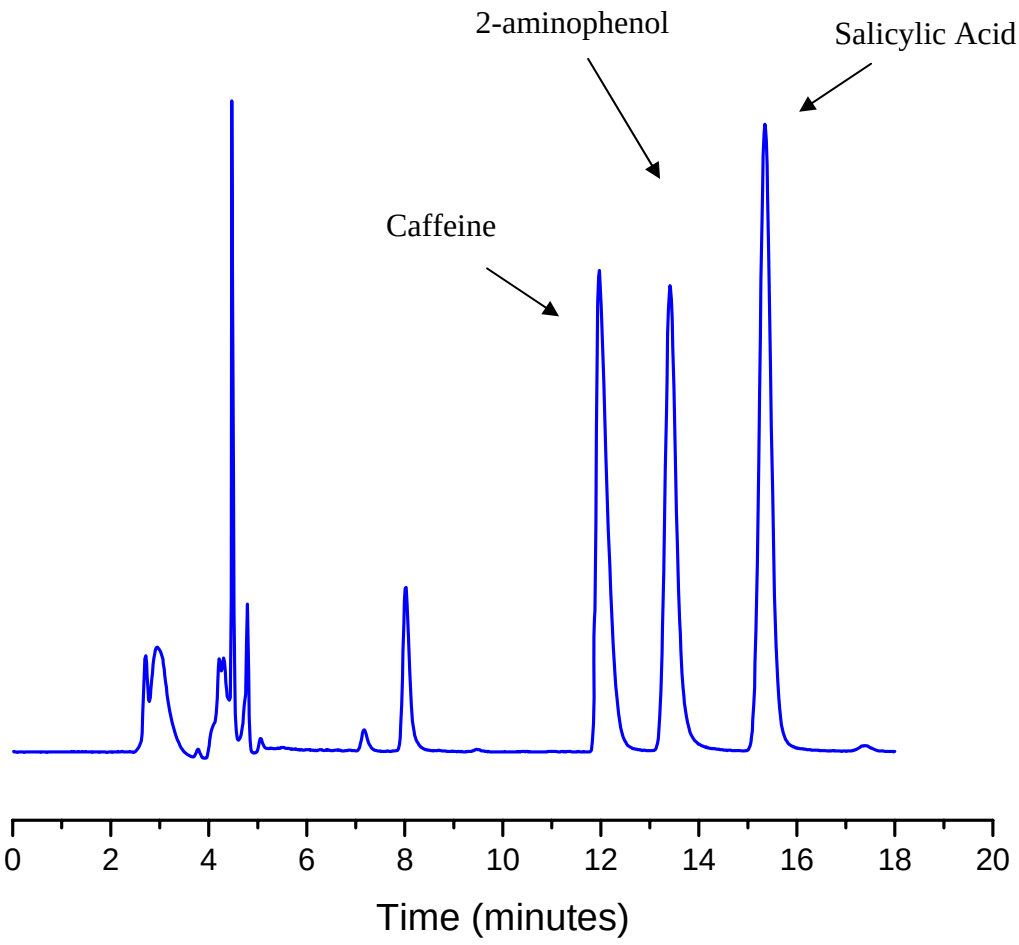

Figure 3.6. Separation of caffeine, 2-aminophenol, and salicylic acid. Mobile phase: 12:88 acetonitrile in 30 mM KH_2PO_4 (pH 8.0), flow rate: 0.2 mL/min, wavelength: 285 nm.

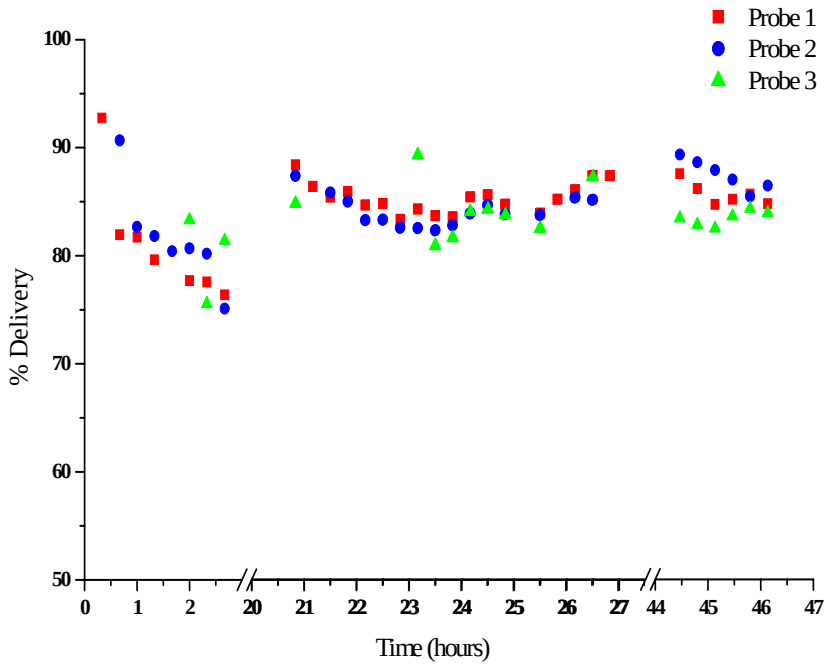

Figure 3.7. Example of the delivery of the internal standard, 2-aminophenol, during the course of three days.

3.5.3 Ultrafiltration vs. Microdialysis

The use of microdialysis and ultrafiltration sampling was assessed for both caffeine and salicylic acid (Figure 3.8 & 3.9). Ultrafiltration samples were collected every 1 – 2 hours for 18 continuous hours. Microdialysis sampling occurred every 20 minutes but was limited to a maximum of 6 hours per collection time to limit the sores endured from being restrained in the pig sling.

Detection of both salicylic acid and caffeine occurred within the first hour of sampling when utilizing microdialysis. Sampling by ultrafiltration resulted in non detectable amounts of test compound during the first five hours post-application. In addition, larger variation in the sample concentrations was found using ultrafiltration sampling.

By performing intermittent sampling with microdialysis, an understanding of localized drug concentrations at later time periods could be determined. Discontinuous microdialysis or stopped-flow microdialysis has been previously demonstrated for sampling in small volume bioreactors and for drug dissolution testing [43, 44]. The use of stopped-flow microdialysis has not been previously described in this type of experiment and its use was evaluated in this study. Of particular interest was the time required for the re-establishment of steady state upon the start of reperfusion. Figure 3.9 & 3.10 illustrate samples which were collected on day two immediately following the start of perfusion. The initial four samples collected show a steady decrease in the concentration of both salicylic acid and caffeine. This could be explained by two factors. First, when perfusion was

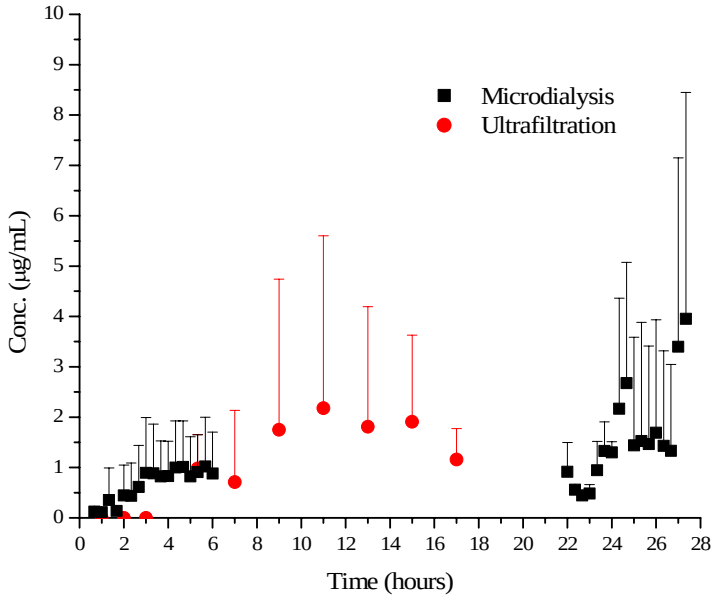

Figure 3.8. Penetration of salicylic acid in the Göttingen minipig following application of cotton balls soaked in 5 mg/mL salicylic acid in ethanol.

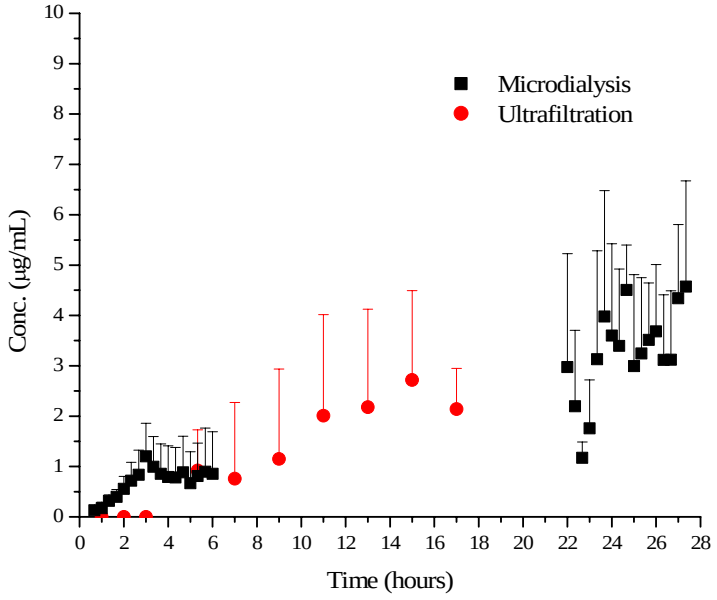

Figure 3.9. Penetration of caffeine in the Göttingen minipig following the application of soaked cotton balls in 5 mg/mL caffeine in 95% ethanol.

discontinued overnight, the concentration of both salicylic acid and caffeine were allowed to reach equilibrium between the tissue and the solution within the microdialysis probe. This would result in higher concentrations initially which would then decrease until steady state was re-established. Second, all samples were adjusted for the delivery of the internal standard. Results from prior experiments indicate that a minimum of one hour was required for steady state to be well established. Therefore, the adjustment factor from the extraction efficiency of the internal standard was inaccurate. Drug concentrations obtained after steady state was obtained were similar to maximum concentrations determined with ultrafiltration sampling. Unfortunately, sampling by ultrafiltration was not extended to this time point due to difficulties with the minipig so a direct comparison could not be made.

3.5.3 Comparison Between High and Medium Penetrator

In order to fully assess the potential of the Göttingen minipig for *in vivo* dermal studies, two model compounds with different penetration properties were selected. Initially a list of high, medium, and low penetrators was compiled. From this list, salicylic acid was selected as the high penetrator and caffeine as a moderate penetrator [10, 18, 45-47]. Results obtained from this study gave very similar penetration properties (Figure 3.10). One concern was that the cited studies were all completed *in vitro* using skin samples from either mice, rats, human, or minipig. The only direct comparison between these two compounds was an *in vitro* diffusion study using mouse skin [47]. When dissolved in methanol, the flux of salicylic acid was

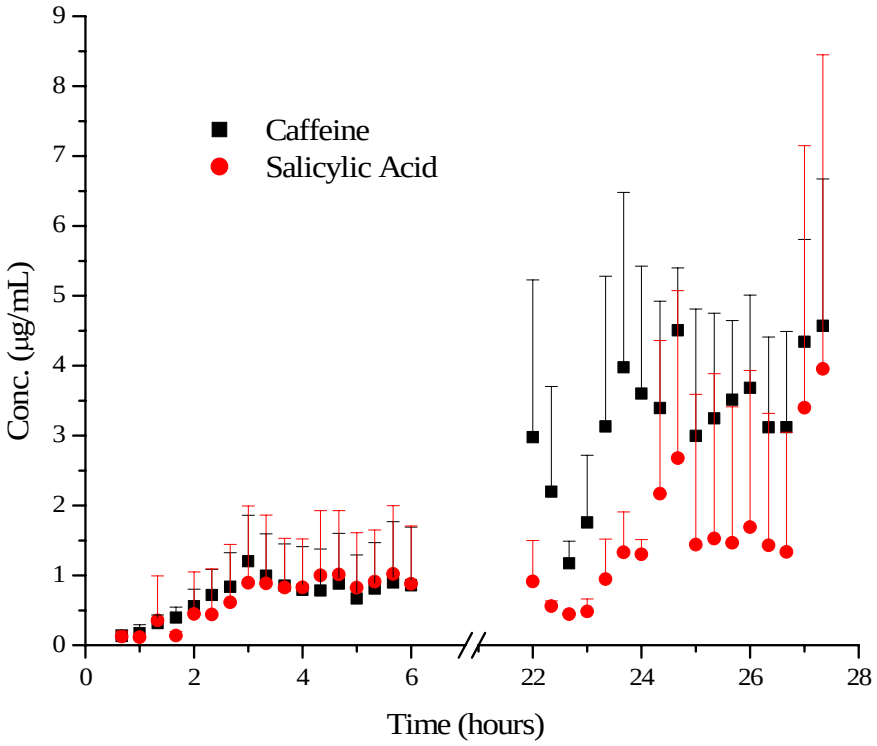

Figure 3.10. Comparison of dermal penetration of salicylic acid and caffeine.

100 times greater than the flux of caffeine. In addition, the total salicylic acid concentration in mouse skin was 16 times higher than the total caffeine concentration. This study therefore suggests that the dermal penetration of salicylic acid and caffeine is different between the Göttingen minipig and the hairless mouse.

3.5.5 Comparison to Human Skin

A study completed by Benfeldt et al. looked at the penetration of salicylic acid following different barrier perturbations utilizing microdialysis on the human forearm [48, 49]. Salicylic acid (5% in ethanol) was applied to wells on the human forearm and sampled for 4 hours. Peak concentration of salicylic acid following four hours of application to unharmed skin was approximately 0.10 μg/mL [48, 49]. This study was repeated using a similar protocol, however this time utilizing the Göttingen minipig. As seen from Figure 3.11 after three hours of collection by microdialysis, average penetration of salicylic acid in the Göttingen minipig was 2 μg/mL, 20 times the concentration previously reported by Benfeldt. These levels continued to increase for the first ten hours of application as determined from ultrafiltration sampling. Similar dermal concentrations were observed in Benfeldt's study only following skin perturbations that included tape stripping or treatment with 1% or 2% sodium lauryl sulphate pretreated skin.

One area of concern to be considered is a possible animal age dependence of dermal penetration. A study completed by Qvest et al. looked at a possible correlation between dermal penetration and age of the Göttingen minipig [25]. The

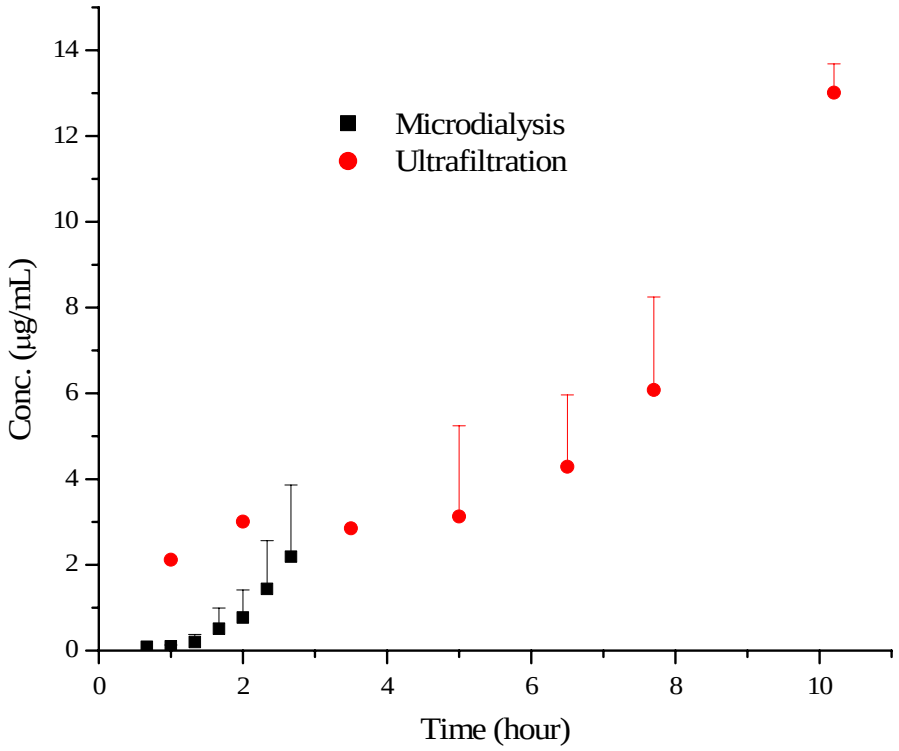

Figure 3.11. Application of 5% w/v salicylic acid in ethanol applied using soaked cotton balls. Sampling by microdialysis was stopped after three hours due to time restrictions in the pig sling.

optimal age of the Göttingen minipig for dermal studies was determined to be between 3 to 5 months. Minipigs older than 6 months had drug fluxes greater than human skin due to changes in skin structure or greater depth of the hair follicles [25]. Göttingen minipigs used for this study were between the ages of 3 to 10 months. This large age difference could account for some of the variability and discrepancy in drug penetration between human and minipig skin.

These preliminary studies indicate greater dermal penetration in the Göttingen minipig in comparison to human skin. To fully assess the usefulness of the Göttingen minipig as a model for human penetration, additional compounds will need to be tested.

3.6 Results and Discussion: Sprague Dawley Rat

Ultrafiltration enabled continual dermal sampling for extended collection times in the Göttingen minipig; however, delayed penetration was often noted and increased variation was found. In order to investigate these findings, the Sprague Dawley rat was utilized, as it was easier to handle and less expensive.

Initial investigations compared microdialysis and ultrafiltration sampling in the dermis. The average concentration of salicylic acid achieved by ultrafiltration sampling was found to be significantly lower than determined from microdialysis sampling (Figure 3.12). In fact, levels were similar to subcutaneous concentration following dermal application (Figure 3.13). These initial findings suggest that

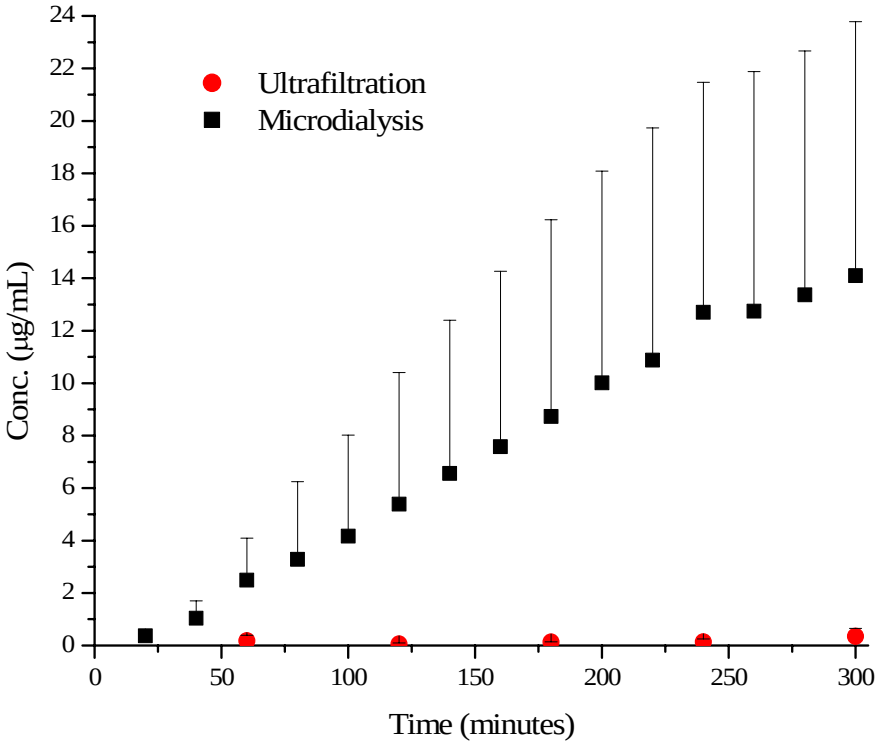

Figure 3.12. Penetration of 2% salicylic acid in carbopol gel. Microdialysis (n=10 probes, 5 rats) and ultrafiltration (n = 5 probes, 4 rats) sampling were both completed in the dermis.

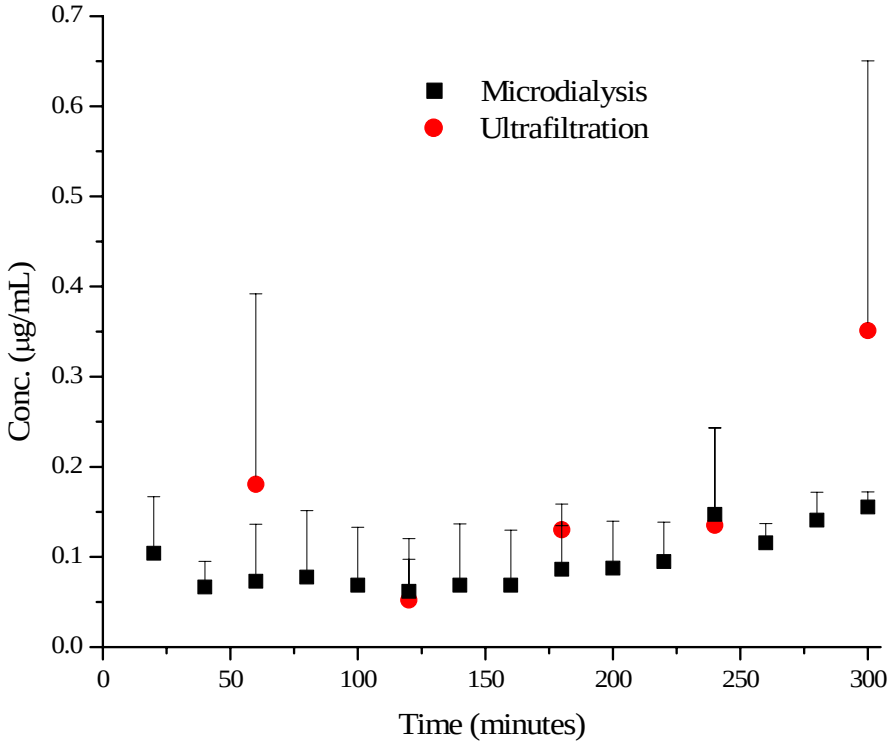

Figure 3.13. Penetration of 2% salicylic acid in carbopol gel. Microdialysis sampling (n = 4 probes, 2 rats) was completed in the subcutaneous region and ultrafiltration sampling (n = 5 probes, 4 rats) in the dermis.

extracellular fluid collected from an ultrafiltration probe in the dermis was a combination of dermal and subcutaneous extracellular fluids.

To further validate these findings, an intravenous dose of salicylic acid was administered while ultrafiltration sampling was completed in the dermis and microdialysis sampling occurred in either the dermis or subcutaneous regions. When ultrafiltration and microdialysis sampling were both in the dermis, a delayed response was noticed with ultrafiltration sampling compared to the microdialysis sampling (Figure 3.14). However after two hours, salicylic acid concentrations obtained from both sampling techniques were equivalent. When microdialysis sampling was in the subcutaneous region of the rat, salicylic acid concentrations demonstrated a slower response to the administered dose and had an overall lower concentration compared to the dermal levels (Figure 3.15). Dermal ultrafiltration samples in general had a similar initial response as the subcutaneous microdialysis sampling but then had drug concentrations comparable to dermal microdialysis sampling.

The results obtained from the intravenous dose of salicylic acid support earlier findings that extracellular fluid was being withdrawn from both the dermal regions and the subcutaneous regions. To confirm this was not analyte dependent, both salicylic acid and caffeine in a carbopol gel was applied to the back of the Sprague Dawley rat. On average, lower concentrations were again found when sampling with dermal ultrafiltration in comparison to dermal microdialysis (Figure 3.16).

A more pronounced difference in dermal ultrafiltration sampling compared to dermal microdialysis sampling was observed with the Sprague Dawley rat compared

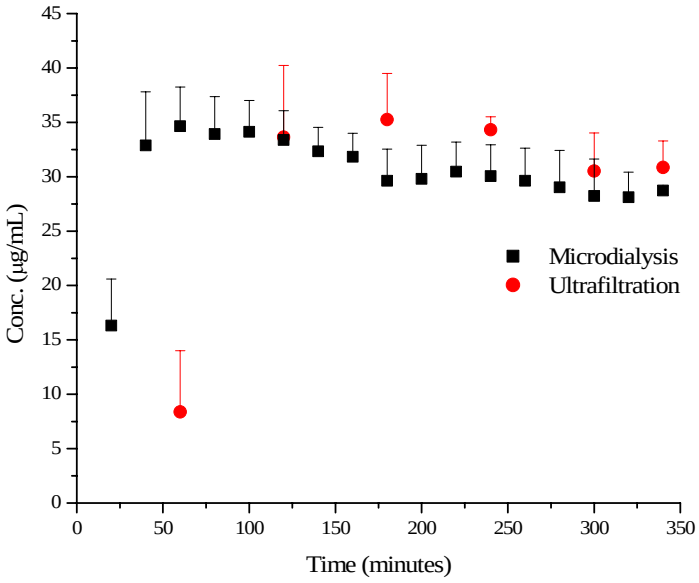

Figure 3.14. i.v. dose of 35 mg/kg salicylic acid. Ultrafiltration (n = 4 probes, 2 rats) and microdialysis (n = 7 probes, 4 rats) sampling were both completed in the dermis.

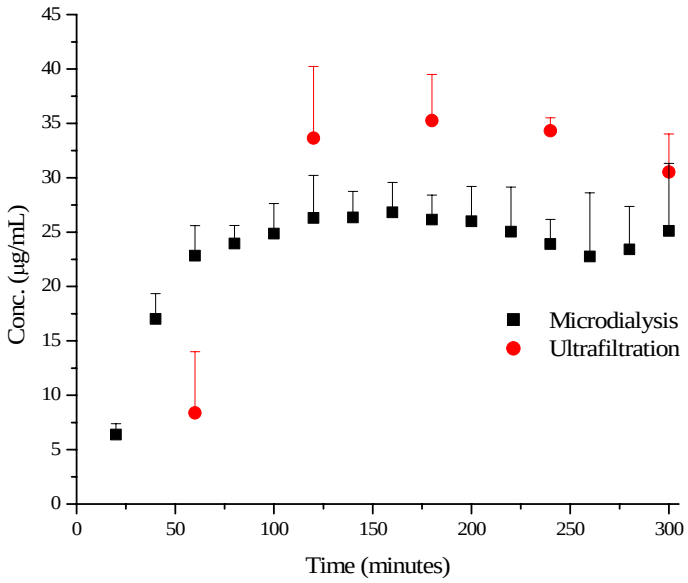

Figure 3.15. i.v. dose of 35 mg/kg salicylic acid. Dermal ultrafiltration (n = 4 probes, 2 rats), and subcutaneous microdialysis (n = 3 probes, 2 rats).

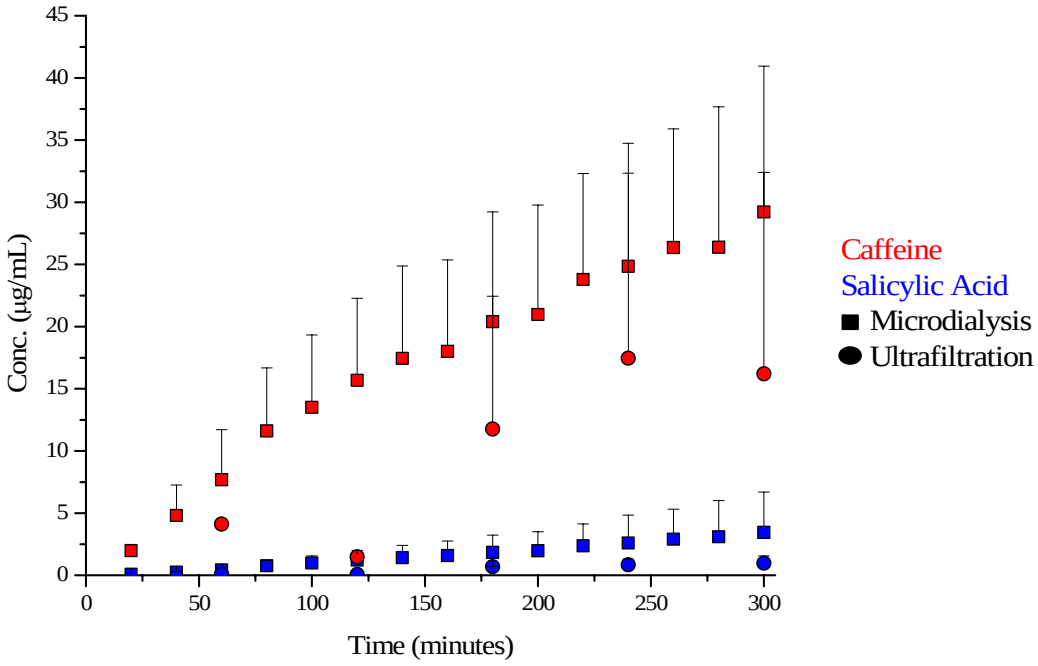

Figure 3.16. Comparison between ultrafiltration and microdialysis sampling in the dermis of a Sprague Dawley rat. Application consisted of a 2% salicylic acid and caffeine in carbopol gel. (n = 4 probes, 2 rats).

to the Göttingen minipig. A comparison between the dermal thickness of these two species show that the dermis of the Göttingen minipig is 50% to 100% thicker than the Sprague Dawley rat. The Göttingen minipig dermal thickness is age dependent with an average thickness of 1.47 mm at 3 months and 2.28 mm at 6 months of age [25]. The Sprague Dawley rat has an average dermal thickness of approximately 1 mm [50]. This means that when an ultrafiltration probe is implanted into the dermis of these two species, the Göttingen minipig would have a greater thickness of dermal tissue surrounding the ultrafiltration probe compared to the Sprague Dawley rat. Therefore, the difference between dermal ultrafiltration sampling compared to cutaneous microdialysis sampling is not as distinct in the Göttingen minipig compared to the Sprague Dawley rat.

3.7 Conclusions

Overall, methods for ultrafiltration and microdialysis dermal sampling in the Göttingen minipig were developed. For ultrafiltration, a 4 cm linear probe was needed for 1 to 2 hour sampling intervals. Continuous sampling was achieved for up to 20 hours and probes were functional up to one week post-implantation. A discontinuous microdialysis sampling scheme was developed that allowed for multi-day collections. In comparison to microdialysis, dermal ultrafiltration had a delayed penetration response and a greater variation in concentration. Salicylic acid and caffeine were found to have similar penetration properties in the Göttingen minipig.

When compared to reported human microdialysis data, a greater amount of salicylic acid penetrated through the Göttingen minipig skin than human skin.

To further investigate the usefulness of ultrafiltration sampling in the dermis, the Sprague Dawley rat was utilized. Results obtained from these experiments demonstrate that extracellular fluid collected by ultrafiltration was from both the dermal and subcutaneous region. This leads to delayed penetration responses and concentrations lower than the true value. Greater deviations in ultrafiltration data in comparison to microdialysis data was observed in the Sprague Dawley rat as a result of the small dermal layer. Dermal ultrafiltration is an alternative sampling technique to microdialysis sampling however it results in an underestimation of the true tissue concentration.

3.8 References:

1. Franz, T.J., *Percutaneous Absorption, on the Relevance of in Vitro Data.* The Journal of Investigative Dermatology, 1975. **64**: p. 190-195.

2. Conte, L., et al., *Percutaneous Absorption and Skin Distribution of [^{14}c] Flutrimazole in Minipigs.* Drug Research, 1992. **42**(6): p. 847-853.

3. Fisher, H.L., et al., *In Vivo and in Vitro Dermal Penetration of 2,4,5,2',4',5'-Hexachlorobiphenyl in Young and Adult Rats.* Environmental Research, 1989. **50**: p. 120-139.

4. Ghosh, B., et al., *Comparison of Skin Permeability of Drugs in Mice and Human Cadaver Skin.* Indian Journal of Experimental Biology, 2000. **38**: p. 42-45.

5. Lin, S.-Y., et al., *Comparisons of Different Animal Skins with Human Skin in Drug Percutaneous Penetration Studies.* Methods and Findings in Experimental Clinical Pharmacology, 1992. **14**(8): p. 645-654.

6. Machet, L., et al., *In Vitro Phonophoresis of Digoxin across Hairless Mice and Human Skin: Thermal Effect of Ultrasound.* International Journal of Pharmaceutics, 1996. **133**: p. 39-45.

7. Shah, P.V., et al., *Dermal Penetration of Carbofuran in Young and Adult Fischer 344 Rats.* Journal of Toxicology and Environmental Health, 1987. **22**: p. 207-223.

8. Valiveti, S., et al., *In Vitro/in Vivo Correlation of Transdermal Naltrexone Prodrugs in Hairless Guinea Pigs.* Pharmaceutical Research, 2005. **22**(6): p. 981-989.

9. Wagner, H., et al., *Human Skin and Skin Equivalents to Study Dermal Penetration and Permeation.* Cell Culture Models of Biological Barriers, 2002: p. 289-309.

10. Rougier, A., C. Lotte, and H.I. Maibach, *The Hairless Rat: A Relevant Animal Model to Predict in Vivo Percutaneous Absorption in Humans?* The Journal of Investigative Dermatology, 1987. **88**(5): p. 577-581.

11. Sekkat, N., Y.N. Kalia, and R.H. Guy, *Biophysical Study of Porcine Ear Skin in Vitro and Its Comparison to Human Skin in Vivo.* Journal of Pharmaceutical Sciences, 2002. **91**(11): p. 2376-2381.

12. Doucet, O., N. Garcia, and L. Zastrow, *Skin Culture Model: A Possible Alternative to the Use of Excised Human Skin for Assessing in Vitro Percutaneous Absorption.* Toxicology In Vitro, 1998. **12**: p. 423-430.

13. Schmook, F.P., J.G. Meingassner, and A. Billich, *Comparison of Human Skin or Epidermis Models with Human and Animal Skin in in Vitro Percutaneous Absorption.* International Journal of Pharmaceutics, 2001. **215**: p. 51-56.

14. Schreiber, S., et al., *Reconstructed Epidermis Versus Human and Animal Skin in Skin Absorption Studies.* Toxicology *in Vitro*, 2005. **19**: p. 813-822.

15. Ottaviani, G., S. Martel, and P.-A. Carrupt, *Parallel Artificial Membrane Permeability Assay: A New Membrane for the Fast Prediction of Passive Human Skin Permeability.* Journal of Medicinal Chemistry, 2006. **49**: p. 3948-3954.

16. Ault, J.M., et al., *Dermal Microdialysis Sampling in Vivo.* Pharmaceutical Research, 1994. **11**(11): p. 1631-1639.

17. Kreilgaard, M., *Assessment of Cutaneous Drug Delivery Using Microdialysis.* Bulletin Technique Gattefosse, 2002. **95**: p. 101-122.

18. Leveque, N., et al., *Comparison of Franz Cells and Microdialysis for Assessing Salicylic Acid Penetration through Human Skin.* International Journal of Pharmaceutics, 2004. **269**: p. 323-328.

19. Boelsma, E., et al., *Microdialysis Technique as a Method to Study the Percutaneous Penetration of Methyl Nicotinate through Excised Human Skin, Reconstructed Epidermis, and Human Skin in Vivo.* Pharmaceutical Research, 2000. **17**(2): p. 141-147.

20. van Ravenzwaay, B. and E. Leibold, *A Comparison between in Vitro Rat and Human in Vivo Rat Skin Absorption Studies.* Human and Experimental Toxicology, 2004. **23**: p. 421-430.

21. Shah, V.P. and H.I. Maibach, eds. *Topical Drug Bioavailability, Bioequivalence, and Penetration.* 1993, Plenum Press: New York.

22. van Ravenzwaay, B. and E. Leibold, *The Significance of in Vitro Rat Skin Absorption Studies to Human Risk Assessment.* Toxicology In Vitro, 2004. **18**: p. 219-225.

23. Andega, S., N. Kanikkannan, and M. Singh, *Comparison of the Effect of Fatty Alcohols on the Permeation of Melatonin between Porcine and Human Skin.* Journal of Controlled Release, 2001. **77**: p. 17-25.

24. Mortensen, J.T., P. Brinck, and J. Lichtenberg, *The Minipig in Dermal Toxicology. A Literature Review.* Scandinavian Journal of Laboratory Animal Science, 1998. **25**(1): p. 77-83.

25. Qvist, M.H., et al., *Evaluation of Göttingen Minipig Skin for Transdermal in Vitro Permeation Studies.* European Journal of Pharmaceutical Sciences, 2000. **11**: p. 59-68.

26. Sullivan, T.P., et al., *The Pig as a Model for Human Wound Healing.* Wound Repair and Regeneration, 2001. **9**(2): p. 66-76.

27. Vardaxis, N.J., et al., *Confocal Laser Scanning Microscopy of Porcine Skin: Implications for Human Wound Healing Studies.* Journal of Anatatomy, 1997. **190**: p. 601-611.

28. Vogel, B.E., et al., *Dermal Toxicity Testing in Minipigs: Assessment of Skin Reactions by Noninvasive Examination Techniques.* Scandinavian Journal of Laboratory Animal Science, 1998. **25**(1): p. 117-120.

29. Gray, G.M. and H.J. Yardley, *Lipid Compositions of Cells Isolated from Pig, Human, and Rat Epidermis.* Journal of Lipid Research, 1975. **16**: p. 434-440.

30. Songkro, S., et al., *Investigation of Newborn Pig Skin as an in Vitro Animal Model for Transdermal Drug Delivery.* S.T.P. Pharma Sciences, 2003. **13**(2): p. 133-139.

31. McAnulty, P.A., *The Value of the Minipig in Toxicity and Other Studies Supporting the Development of New Pharmaceuticals.* European Pharmaceutical Contractor, 1999: p. 82-86.

32. Janle, E.M. and S.R. Ash, *Comparison of Urea Nitrogen and Creatinine Concentrations in Dog Plasma and Subcutaneous Ultrafiltrate Samples.* Current Separations, 1994. **12**(4): p. 169-171.

33. Janle, E.M. and M. Cregor, *Interstitial Fluid Calcium, Magnesium and Phosphorus Concentrations in Bone, Muscle and Subcutaneous Tissue Sampled with Ultrafiltration Probes.* Current Separations, 2001. **19**(3): p. 81-85.

34. Janle, E.M. and J.E. Sojka, *Use of Ultrafiltration Probes in Sheep to Collect Interstitial Fluid for Measurement of Calcium and Magnesium.* Contemporary Topics, 2000. **39**(6): p. 47-50.

35. Spehar, A.M., et al., *Recovery of Endogenous Ions from Subcutaneous and Intramuscular Spaces in Horses Using Ultrafiltrate Probes.* Current Separations, 1998. **17**(2): p. 47-51.

36. Tiessen, R.G., et al., *Slow Ultrafiltration for Continuous in Vivo Sampling: Application for Glucose and Lactate in Man.* Analytica Chimica Acta, 1999. **379**: p. 327-335.

37. Janle, E.M. and P.T. Kissinger, *Microdialysis and Ultrafiltration Sampling of Small Molecules and Ions from in Vivo Dialysis Fibers.* American Association for Clinical Chemistry, 1993. **14**(7): p. 159-165.

38. Leegsma-Vogt, G., et al., *Utilization of in Vivo Ultrafiltration in Biomedical Research and Clinical Applications.* Life Sciences, 2003. **73**: p. 2005-2018.

39. Moscone, D., K. Venema, and J. Korf, *Ultrafiltrate Sampling Device for Continuous Monitoring.* Medical and Biological Engineering and Computing, 1996: p. 290-294.

40. Schneiderheinze, J.M. and B.L. Hogan, *Selective in Vivo and in Vitro Sampling of Proteins Using Miniature Ultrafiltration Sampling Probes.* Analytical Chemistry, 1996. **68**: p. 3758-3762.

41. Linhares, M.C. and P.T. Kissinger, *Capillary Ultrafiltration: In Vivo Sampling Probes for Small Molecules.* Analytical Chemistry, 1992. **64**: p. 2831-2835.

42. Puglia, C., et al., *Evaluation of in Vitro Percutaneous Absorption of Lorazepam and Clonazepam from Hydro-Alcoholic Gel Formulations.* International Journal of Pharmaceutics, 2001. **228**: p. 79-87.

43. Fang, Q., et al., *A Stopped-Flow Microdialysis Sampling-Flow Injection System for Automated Multivessel High Resolution Drug Dissolution Testing.* Talanta, 1999. **49**: p. 403-414.

44. Torto, N., et al., *On-Line Quantitation of Enzymatic Mannan Hydrolysates in Small-Volume Bioreactors by Microdialysis Sampling and Column Liquid Chromatography-Integrated Pulsed Electrochemical Detection.* Journal of Chromatography A, 1996. **725**: p. 165-175.

45. van de Sandt, J.J.M., et al., *In Vitro Predictions of Skin Absorption of Caffeine, Testosterone, and Benzoic Acid: A Multi-Centre Comparison Study.* Regulatory Toxicology and Pharmacology, 2004. **39**: p. 271-281.

46. Simonsen, L., et al., *Differentiated in Vivo Skin Penetration of Salicylic Compounds in Hairless Rats Measured by Cutaneous Microdialysis.* European Journal of Pharmaceutical Sciences, 2004. **21**: p. 379-388.

47. Phillips, C.A. and B.B. Michniak, *Transdermal Delivery of Drugs with Differing Lipophilicities Using Azone Analogs as Dermal Penetration Enhancers.* Journal of Pharmaceutical Sciences, 1995. **84**(12): p. 1427-1433.

48. Benfeldt, E. and J. Serup, *Effect of Barrier Perturbation on Cutaneous Salicylic Acid Penetration in Human Skin: In Vivo Pharmacokinetics Using Microdialysis and Non-Invasive Quantification of Barrier Function.* Arch Dermatology Research, 1999. **291**: p. 517-526.

49. Benfeldt, E., J. Serup, and T. Menné, *Effect of Barrier Perturbation on Cutaneous Salicylic Acid Penetration in Human Skin: In Vivo Pharmacokinetics Using Microdialysis and Non-Invasive Quantification of Barrier Function.* British Journal of Dermatology, 1999. **140**: p. 739-748.

50. Matsui, R., et al., *Histological Evaluation of Skin Reconstruction Using Artificial Dermis.* Biomaterials, 1996. **17**: p. 995-1000.

Chapter Four

Osmotic Pump as the Pumping Device for Microdialysis Sampling

4.1 Purpose

The purpose of this research project was to explore an alternative pumping device for cutaneous microdialysis sampling. This entailed the investigation of an Alzet® osmotic pump implanted into the subcutaneous region of the rat with attachment to a linear microdialysis probe for cutaneous sampling. A comparison of the osmotic pump and an infusion pump as pumping devices for microdialysis sampling was completed.

4.2 Introduction

4.2.1 Microdialysis Sampling

Microdialysis is a well studied sampling technique that has been evaluated and utilized in multiple regions of the body. One of the limitations of microdialysis is that it requires the use of an infusion pump connected to the test subject. For small animals such as mice and rats this is generally not a problem; awake animal systems have been developed that allow the animal to freely move while still being connected to the infusion pump. However larger animals must be confined within the laboratory during the testing period.

Ultrafiltration is one alternative to microdialysis sampling that can be used on unrestrained large animals. However, as shown in Chapter Three, the use of ultrafiltration is limited to certain regions of the body. As an alternative, the osmotic pump is an implantable pumping device that has been illustrated as a continual drug delivery device. Therefore, the use of an osmotic pump will be evaluated as a pumping device for cutaneous microdialysis.

4.2.2 Previous Uses of the Osmotic Pump

The development of the miniaturized osmotic pump was first described in 1976 by Theeuwes and Yum [1]. This design, which is similar to the design used today for the Alzet® osmotic pumps (Figure 4.1), consisted of an internal drug reservoir, an osmotic driving agent, and a semi-permeable membrane [2]. As its name suggests, the osmotic pump is driven by osmotic pressure. When water flows across the outer semipermeable membrane, pressure is exerted onto the surface of the drug reservoir, driving the drug through the flow moderator. Therefore, the amount of water that diffuses past the semipermeable membrane is equal to the amount of drug delivered.

The osmotic pump has been utilized primarily as a drug delivery device, to provide insight into several functions including therapeutic relief, information on disease states, and in the aid of imaging techniques [3-6]. The drug reservoir consists of a thermoplastic hydrocarbon elastomer and is compatible with variety of drugs, including poorly water soluble compounds that require the use of co-solvents in order

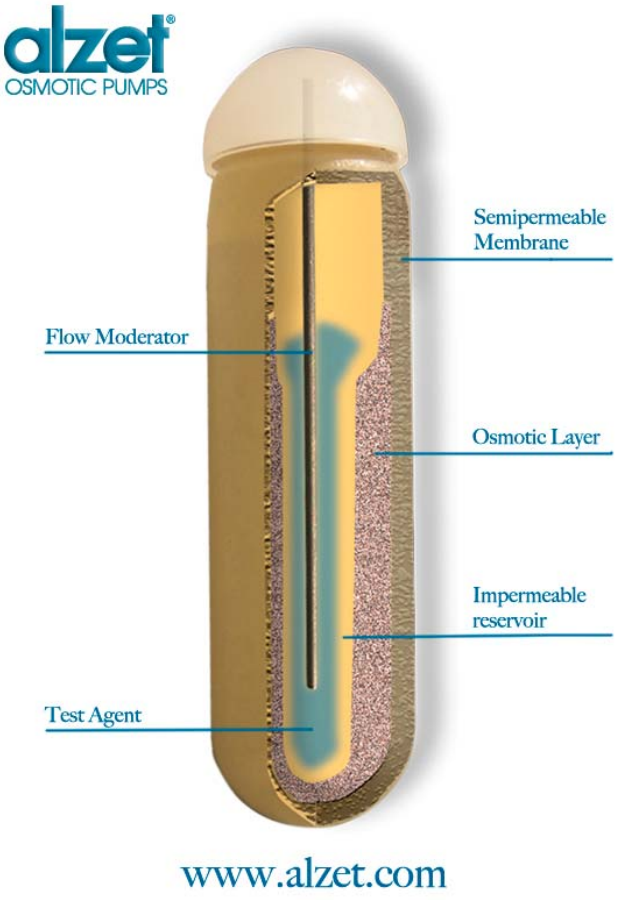

Figure 4.1. Schematic of the Alzet® osmotic pump.

to solubilize [2, 7]. The osmotic pump has also been used in conjunction with a microdialysis probe. In 1991, Bazzett first described the use of the osmotic pump with a brain microdialysis probe as a site specific drug delivery device for quinolinic acid [8]. More recently, Cooper et al. described the first use of the osmotic pump inline with a brain microdialysis probe for the recovery of neurotransmitters [9].

The Alzet® osmotic pump is a relatively inexpensive pumping device compared to mechanical devices. It comes in three different sizes that contain either 100 μL, 200 μL, or 2 mL of drug solution. Flow volumes range from 0.25 μL/hr to up to 10 μL/hr with lifespans of 1 day to four weeks. The osmotic pump is not reusable and a new pump is required at the start of every experiment or at the completion of its lifetime. In addition, the use of a catheter allows for the direct delivery of substances into the venous or arterial circulation. For these experiments the use of the catheter will allow for the direct connection of the linear microdialysis probe.

4.3 Specific Aims

The specific aim of this study was to examine the viability of the osmotic pump as a pumping device for cutaneous microdialysis. The addition of a microdialysis probe to the flow moderator of the osmotic pump was first evaluated *in vitro*. Next, a comparison between the recovery of salicylic acid and the delivery of antipyrine was obtained *in vitro* using the osmotic pump and an infusion pump was completed. Similar experiments were then completed with the osmotic pump

implanted into the subcutaneous region of the Sprague Dawley rat. Finally, the use of an osmotic pump was demonstrated following a topical application of Clearasil®.

4.4 Materials and Methods

4.4.1 Chemicals

Salicylic acid and antipyrine were both purchased from Sigma (St. Louis, MO). Alzet® osmotic pumps (2ML) were obtained from Braintree Scientific (Braintree, MA). HPLC grade acetonitrile was acquired from Fisher Scientific (Fair Lawn, NJ). Ketamine was manufactured by Fort Dodge Animal Health (Fort Dodge, IA), xylazine was made by Ben Venue Laboratories (St. Joseph, MO), acepromazine was manufactured by Boehringer Ingelheim (St. Joesph, MO), and AErrane (isoflurane) was purchased from Baxter (Deerfield, IL). Microdialysis probes and surgical instruments were sterilized by ethylene oxide using an Anprolene gas sterilizer (AN 74i, Anderson Products, Inc., Haw River, NC). Water for buffer preparation was filtered through a Labconco, Water Pro Plus.

4.4.2 HPLC Instrumentation

Data was analyzed using a Shimadzu LC-20AD pump, SCL-10AVP Shimadzu system controller, Shimadzu SPD-10A UV-Vis spectrophotometric detector. Chromatographic data was acquired using EZStart software (Shimadzu Scientific Instruments, Inc. Columbia, MD). Separation was achieved using a Gemini C18 column (Phenomenex, Torrance, CA, 5 μm, 150 mm x 2.0 mm). Mobile phase

consisted of 30 mM phosphate buffer, pH 3.0:acetonitrile (82:18 v/v). The flow rate was set to 0.3 mL/min with dual wavelength detection set to 300 nm for salicylic acid and 270 nm for antipyrine.

4.4.3 Microdialysis Probe Construction

Linear microdialysis probes were constructed with an active 5 mm PAN membrane window (250 μm i.d., 350 μm o.d, molecular weight cutoff of 30 kDa). Probes were constructed in house as previously discussed in Chapter Two, Section 2.4.5. Briefly, a piece of polyimide tubing (175 μm i.d., 215 μm o.d., MicroLumen, Tampa, Florida) was threaded into a segment of PAN membrane (Hospal Industrie, Mayzieu, France). UV glue (UVEXS, Sunnyville, California) was coated on top of the connection and cured using a UV curing system (ELC-450 UV Light Spot-Cure system, Electro-Lite, Bethel, Connecticut).

For sampling using the osmotic pump, the inlet of the linear microdialysis probe was constructed as seen in Figure 4.2. First, a 1.2 cm piece of PE-60 (0.76 mm i.d., 1.22 mm o.d., Braintree Scientific Inc., Braintree, MA), was used to connect to the flow moderator of the osmotic pump. A 4 cm piece of FEP tubing (0.12 mm i.d., 0.65 mm o.d., Bioanalytical Systems, West Lafayette, IN) was threaded into the piece of PE-60 and UV glued together. For added support of this union, the FEP and PE-60 tubing was threaded through a 1.5 cm piece of silicone tubing (0.76 mm i.d., 1.65 mm o.d., Baxter, Deerfield, IL) and secured using UV glue. Next, the end of the FEP tubing was linked with a tubing connector (Bioanalytical Systems, West Lafayette,

A: 1.2 cm PE-60
B: 1.5 cm silicone tubing
C: 4 cm FEP
D: Tubing connector
E: 2.5 cm MRE-033
F: 5 mm PAN membrane
G: MRE-040

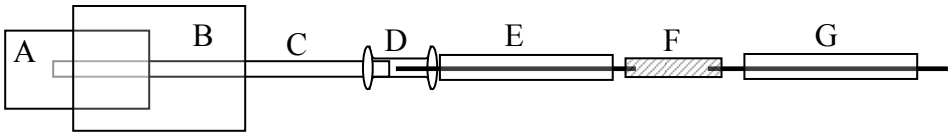

Figure 4.2. The linear microdialysis probe schematic. The probe inlet consisted of a series of connects used to prevent kinking when implanted in the rat.

IN). Polyimide tubing, protected with a 2.5 cm piece of MRE-033 tubing (0.36 mm i.d., 0.84 mm o.d., Braintree Scientific Inc., Braintree, MA), was glued into the tubing connector. The polyimide outlet of the microdialysis probe was further protected using MRE-040 tubing. This design was successful in limiting kinks in the tubing and allowed for the proper spacing of the osmotic pump to the cutaneous microdialysis probe.

4.4.4 *In Vitro* Evaluation of the Osmotic Pump

4.4.4.1 Flow Rate Evaluation

In vitro osmotic pump experiments were performed to evaluate the average flow rates and effects of the addition of a linear microdialysis probe inline with the osmotic pump. Using a four plate hot plate, two osmotic pumps were placed in separate compartments of warmed (37 ˚C) 0.9% NaCl solutions. One osmotic pump was inline with the following sequence of tubing: 3 cm piece of PE-60 tubing, 4 cm piece of MRE-33, and 30 cm of FEP tubing. The second osmotic pump was inline with the same tubing and in addition a linear microdialysis probe was placed between the MRE-33 and FEP tubing. Samples were collected every 60 minutes using a Honeycomb fraction collector (BAS) and flow rate was monitored using gravimetric analysis.

4.4.4.2 *In Vitro* Delivery and Recovery Experiments

In vitro delivery experiments of antipyrine and recovery experiments of salicylic acid were completed simultaneously. The osmotic pump was filled with a Ringer's solution containing 40 μg/mL antipyrine. The osmotic pump was then connected to a 2 cm piece of PE-60 tubing, 20 cm of FEP tubing, and connected to a linear microdialysis probe using a tubing connector. The pump was placed in a warmed water bath (37 ˚C) and allowed to prime overnight. The following morning the membrane of the microdialysis probe was placed in a Ringer's solution containing 4 μg/mL salicylic acid. The solution was warmed to 37 ˚C using a Dri-bath and kept under constant stirring conditions. Samples were collected every 60 minutes using a Honeycomb fraction collector (BAS) and the flow rate was monitored using gravimetric analysis. Samples were analyzed using dual wavelength LC-UV.

Similar studies were completed using an infusion pump. For these studies, the perfusate consisted of either 2 μg/mL antipyrine when delivered at 1 μL/min flow rates or 20 μg/mL antipyrine when delivered at 10 μL/hr. Again the microdialysis probe was placed in a Ringer's solution containing 4 μg/mL salicylic acid. The solution was warmed to 37 ˚C using a Dri-bath and kept under constant stirring conditions. Samples were collected every 15 minutes for the 1 μL/min flow rates and every 60 minutes for the 10 μL/hr flow rates using a Honeycomb fraction collector (BAS). Flow rates were monitored using gravimetric analysis and samples were analyzed using dual wavelength LC-UV.

4.4.5 Surgical Procedures on the Sprague Dawley Rat

4.4.5.1 Alzet® Osmotic Pump

The Alzet® osmotic pump was primed one day prior to insertion into the rat. This was completed by sterilely filling the pump with a Ringer's solution and then placing the pump into sterile 0.9% saline solution maintained at 37˚ C. A 1.5 cm piece of PE-60 tubing inline with 30 cm of FEP tubing was attached to the pump and the flow performance was monitored prior to implantation into the rat.

Female Sprague Dawley rats (Charles Rivers, Raleigh, NC) weighing 230 – 280 g were housed in cages that were maintained in temperature-controlled rooms and allowed free access to food and water. Rats were initially sedated by inhalation with isofluorane followed by a subcutaneous (s.c.) injection of the cocktail mixture: ketamine (67.5 mg/kg), xylazine (3.4 mg/kg), and acepromazine (0.67 mg/kg). The back of the rat was then shaved using an Oster Model A5 animal clipper (blade size 40, Milwaukee, WI), taking care to not damage the skin. The shaved regions were cleaned by swabbing betadiene and 70% isopropyl alcohol alternating three times each. Throughout the surgical procedure and experiment, rat body temperature was maintained by placing the rat on a heating pad.

For a greater success rate; the entire length of the microdialysis probes needed to be kept internally in the rat. Therefore, to insert the linear microdialysis probe, two small slits were made on the right dorsal of the rat approximately 2 centimeters apart. A 23-gauge needle (1.5 inches long) was inserted into the posterior slit and then angled up towards the skin. The needle was guided into the dermis for at least 5 mm

and then exited out of the anterior slit. One end of the polyimide tubing was threaded through the needle. The needle was withdrawn leaving the dialysis membrane imbedded in the surrounding tissue. The polyimide outlet was protected using MRE-040 tubing and the inlet was protected using MRE-033 tubing. The tubing was then held secured to the polyimide by UV glue. This tubing kept the linear microdialysis probe situated in the dermis. The outlet end of the microdialysis probe was tunneled to the nape of the neck. The fascia at the posterior of the rat was slightly cleared to allow the inlet of the microdialysis probe to curve around to the osmotic pump. Next, a larger slit was made on the left dorsal of the rat. Fascia was cleared using a hemostat and the osmotic pump was inserted. The inlet of the microdialysis probe was connected to the flow moderator of the osmotic pump. The large slit was sutured shut using 4-0 Dexon II suture (Tyco Healthcare, King of Prussia, PA). The smaller slits were glued together using tissue glue (3M Animal Care Products, St. Paul, MN). The end of a 10 mL syringe was clipped off and secured to the skin using tissue glue. This prevented drug from seeping into the small slits and also contained the drug during the course of the study. At the end of the surgical procedure, 10-mL sterile saline solution was given to the rat subcutaneously to replace fluids that may have been lost during surgery.

4.4.5.2. Infusion Pump

The linear microdialysis probe was inserted by first creating two small slits on the right dorsal of the rat approximately 2 centimeters apart. A 23-gauge needle (1.5

inches long) was inserted into the posterior slit and then angled up towards the skin. The needle was guided into the dermis for at least 5 mm and then exited out of the anterior slit. One end of the polyimide tubing was threaded through the needle. The needle was withdrawn leaving the dialysis membrane imbedded in the surrounding tissue. Both inlet and outlets were then protected using MRE-040 tubing and held secured to the polyimide tubing by UV glue. In addition, both ends were tunneled to the nape of the neck. Tubing connectors were UV glued to both ends of the microdialysis probe which were then connected to FEP tubing. The animal was placed in a Rodent bowl and set up in the Raturn awake animal containment system.

The inlet of the microdialysis probe was connected with fluorinated ethylenepropylene (FEP) tubing to a Hamilton syringe mounted on a CMA 400-microinjection pump (BAS, West Lafayette, IN). The microdialysis probe outlet was connected to a Honeycomb Refrigerated Fraction Collector (BAS, West Lafayette, IN) with FEP tubing. The infusion pump delivered the Ringer's perfusate at a flow rate of either 1 μL min^{-1} or 10 μL/hr. At the slower flow rates, samples were manually collected from the outlet of the microdialysis probe.

4.5 Results and Discussion

4.5.1 *In Vitro* Performance of the Osmotic Pump and Infusion Pump

The feasibility of using the osmotic pump inline with a linear microdialysis probe was first evaluated in a series of *in vitro* experiments. Initial work was completed to ensure that a linear microdialysis probe inline with an osmotic pump

had negligible effects on flow rate. Average flow rates for the PE-60 tubing inline with the osmotic pump was found to be 9.14 ± 1.80 μL/hr while the average flow rate for a linear microdialysis probe inline with the osmotic pump was 9.01 ± 2.16 μL/hr (Figure 4.3). The addition of a linear microdialysis probe to the osmotic pump had no significant effect on the average flow rate when tested at the 99% confidence level. The reported value for this particular batch of osmotic pumps was 9.8 ± 0.5 μL/hr. The experimental flow rates for both setups were approximately 8% lower than reported and were also found to have a much greater variation in flow rate.

Results reported from Cooper et al. observed a pulsing effect of the flow rates when collection times were 40 minutes or less [9]. This cyclic behavior was also observed for the sixty minute sampling times collected during these experiments. However, it is believed that this behavior could be a result of the cycling of the heating source and not a function of the osmotic pump. For the previous study a four plate heating source was utilized. An expanded view of the data from Figure 4.3, can be seen in Figure 4.4. This plot illustrates the similar flow trends of two discrete osmotic pumps. The similar flow trends can be further explained by examination of the effects of temperature on the flow rate. The overall flow rate can be predicted using the following equation:

$$Q_T = Q_o\left[0.141e^{0.051T} - 0.007n + 0.12\right]$$

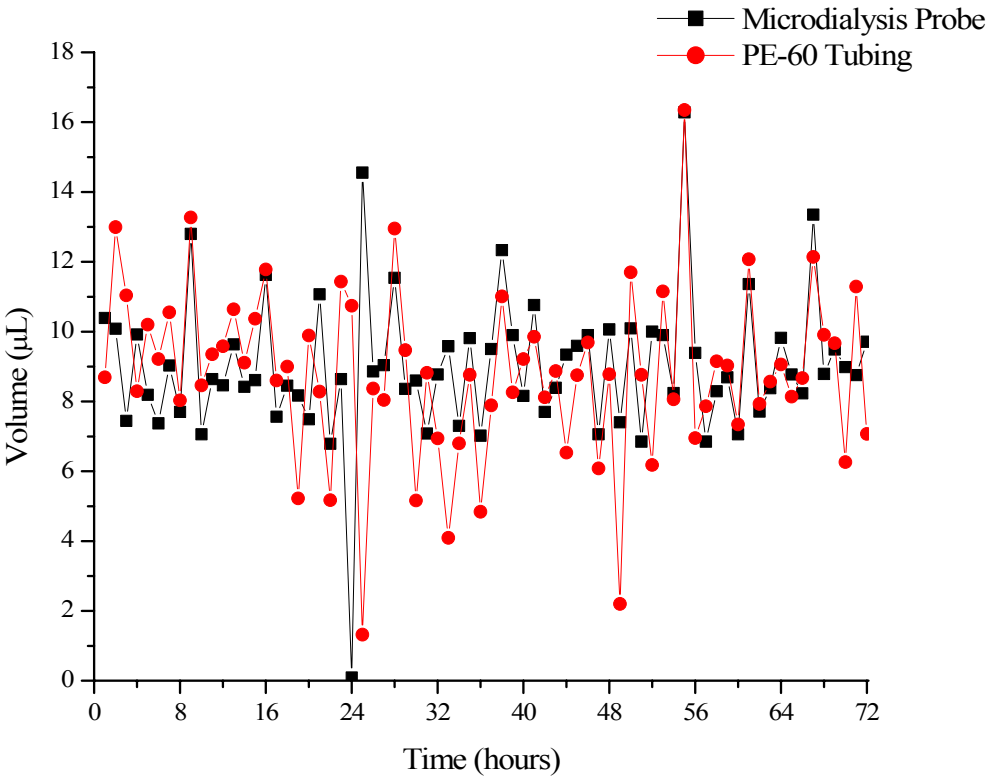

Figure 4.3. Evaluation of the effects of a linear microdialysis probe inline with an osmotic pump compared to the suggested PE-60 tubing. The 0.9% NaCl water baths were replaced every 24 hours resulting in the drop in flow rate for that collection time period.

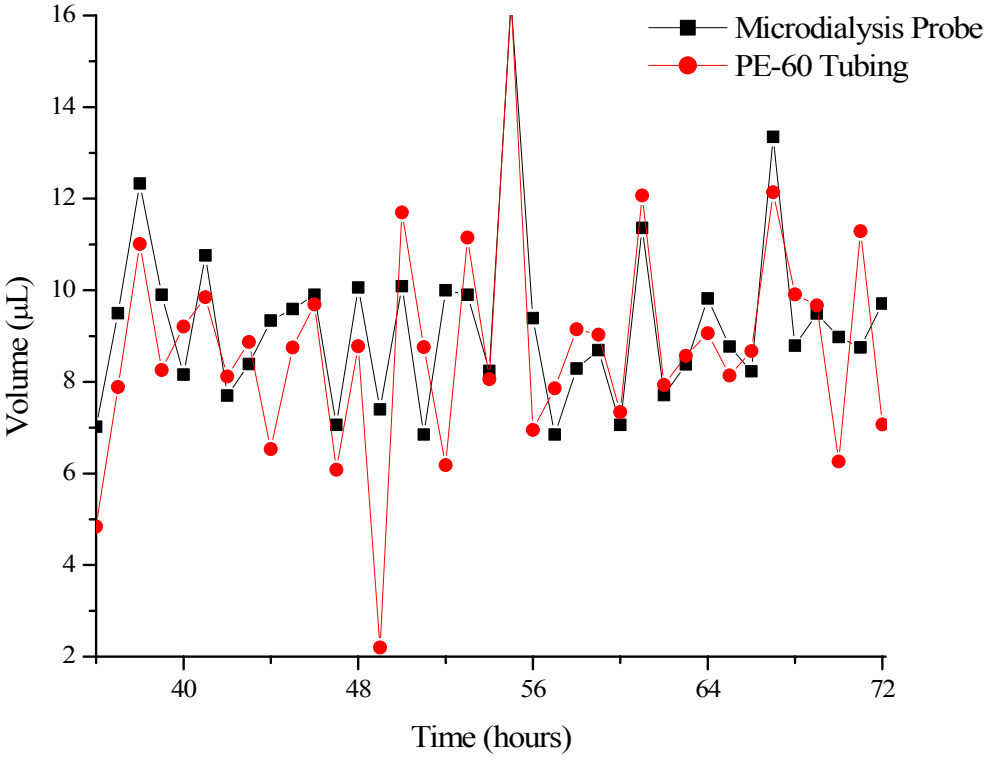

Figure 4.4. The flow rates of two independent osmotic pumps warmed in 0.9% NaCl water baths using the same heating mantle.

where Q_T is the pumping rate at temperature T, Q_o is the specified flow rate at 37 ˚C, n is the osmolality of the pumping solution outside of the pump, and T is the temperature in Celsius. Using the osmotic pressure of a normal mammalian (7.5 atm) the calculated change in flow rates at varying temperatures can be seen in Table 4.1. A change of 4 ˚C can result in a change of approximately 2 μL/hr which is a deviation of approximately 20% of the normal flow.

Similar experiments were completed using an infusion pump. Average flow rates obtained when inline with PE-60 tubing, FEP combination was 9.34 ± 0.21μL/hr. Again, the addition of a linear microdialysis probe had no significant affect on the flow rate as the average flow rate was 9.35 ± 0.52 μL/hr. The flow rate using an infusion pump was more consistent and possessed less variability compared to an osmotic pump.

Finally, both delivery and recovery values of the osmotic pump was compared to values of the infusion pump. For these experiments, a solution of antipyrine was delivered through the probe while salicylic acid was recovered from a warmed Ringer's bath. Delivery extraction efficiencies of antipyrine near 100% were

Temp. (˚C)	Q_T (μL/hr)
33	8.1
35	8.9
37	9.8
39	10.8
41	11.8

Table 4.1. Calculated effects of temperature on the over all flow rate.

obtained for both the osmotic pump and the infusion pump. The recovery of salicylic acid was significantly ($p < 0.5$) higher using the osmotic pump 98.2 ± 4.65 compared to the infusion pump 91.5 ± 1.38. Larger variation in the recovery extraction efficiencies was also noted for the osmotic pump.

4.5.2 *In Vivo* Flow Rate Performance

The performance of the osmotic pump was also monitored *in vivo* following placement into the subcutaneous region of the Sprague Dawley rat and attachment to a linear microdialysis probe implanted in the dermis. On average the flow rate was decreased to approximately 7.6 μL/hr. Variations in the flow rate were at least 20% of the total flow (Table 4.2), an unacceptable amount of variation. When using an infusion pump the average flow rate was found to be approximately 8.2 μL/hr with only a 5% variation (Table 4.3), a more acceptable amount of variation for animal studies. Both pumping devices resulted in a decreased flow rate compared to previous *in vitro* studies. This suggests that the perfusate had a greater concentration of water compared to the extracelluar fluid of the dermis, resulting in a net movement of water from the dialysis probe.

As extraction efficiency is highly dependent on flow rate in microdialysis, variations in flow rate result in unreliable determination of the true concentration. In order to minimize these variations, the use of an internal standard was explored. To assess the potential of using the internal standard antipyrine, the delivery of both the internal standard and the analyte of interest, salicylic acid, were completed *in vitro*

Table 4.2. In vivo flow rate performance of the Alzet® osmotic pump inline with a cutaneous microdialysis probe.

Osmotic Pump	Flow rate (μL/hr)	Std. Dev. (μL/hr)	% RSD
One	7.53	1.26	16.69
Two	7.42	2.42	32.63
Three	7.78	1.87	23.96
Reported	9.8	0.3	3.06

Table 4.3. *In vivo* flow rate performance of the CMA 400 infusion pump inline with a cutaneous microdialysis probe.

Infusion Pump	Flow rate (μL/hr)	Std. Dev. (μL/hr)	% RSD
One	8.05	0.44	5.5
Two	8.12	0.46	5.67
Three	8.73	0.35	3.95
Four	8.04	0.40	4.97
Reported	10.0	0.1	1.00

and *in vivo*. Prior to implantation into the subcutaneous region of the rat, the osmotic pump was allowed to prime overnight. During this time samples were collected, and the flow rate and concentration of the drug exiting the reservoir were monitored. The concentration of antipyrine was unaffected in the drug reservoir of the osmotic pump. Salicylic acid, however, was approximately 40% of the original concentration following approximately 15 hours of priming. The drug solution within the osmotic pump was checked at the completion of the experiment and compared to the final concentration exiting the reservoir at the end of the priming period. These two concentrations were found to be in agreement. It was hypothesized that salicylic acid was either adhering to the drug reservoir membrane or leaking out of the pump into the saline bath. Analysis of the saline bath at the completion of the priming period resulted in non-detectable amounts of salicylic acid present. Since the concentration of salicylic acid dispensed from the osmotic pump stabilized after approximately 12 hours, the end of the priming period, the final concentration of the drug solution within the osmotic pump was used for delivery calculations.

As shown in Figure 4.5, similar trends in percent delivery of antipyrine and salicylic acid were found *in vivo*. When the salicylic acid percent delivery was low, near 55%, antipyrine was also low. The same was found with high percent delivery, near 95%, for both compounds. This was further verified when analyzing the ratio of antipyrine to salicylic acid (Figure 4.6). An approximate ratio of 0.97 was consistent for three individual rats and gave a relative standard deviation of five percent, an allowable amount of variation (Table 4.4). Therefore for subsequent application

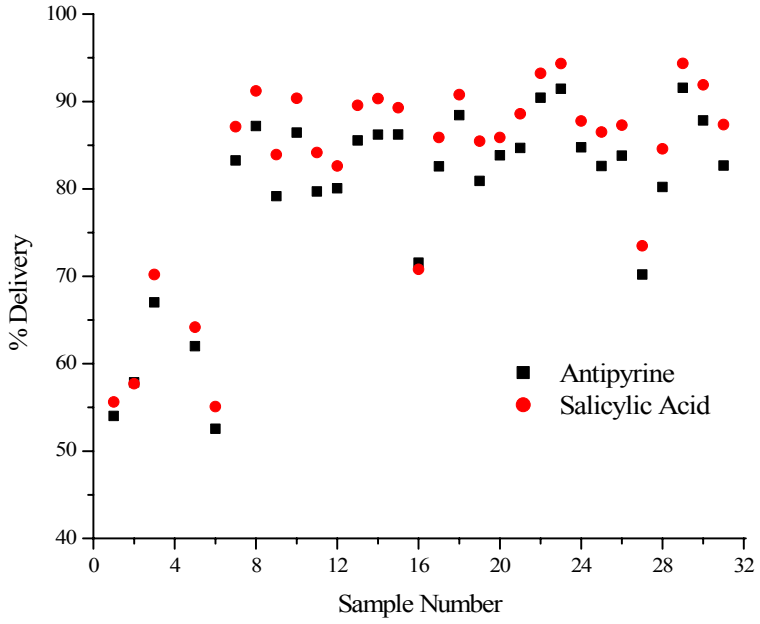

Figure.4.5. Delivery of 40 μg/mL antipyrine and salicylic acid using an osmotic pump.

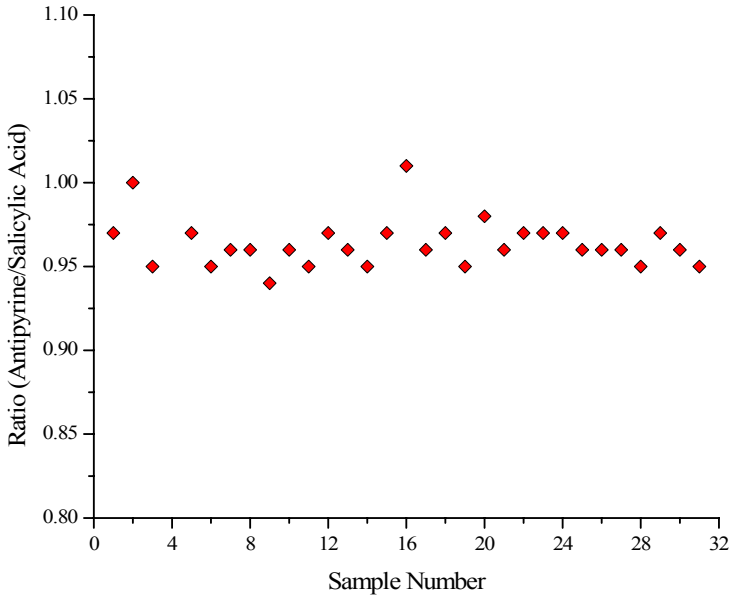

Figure 4.6. Ratio of the deliveries of antipyrine and salicylic acid using an osmotic pump.

Table 4.4. Ratio of internal standard, antipyrine, and analyte of interest, salicylic acid determined using an osmotic pump as the pumping device.

Pump	Ratio	Std. Dev.	% RSD
One	0.989	0.025	2.55
Two	0.949	0.043	4.50
Three	0.963	0.015	1.55
Average	0.967	0.052	5.36

studies, the internal standard was delivered throughout the course of the experiment. The percent delivery of antipyrine was adjusted by the predetermined ratio of 0.97 in order to give the estimated percent delivery of salicylic acid.

Similarly, the delivery of both salicylic acid and antipyrine was completed using an infusion pump. When using an infusion pump for the delivery of antipyrine and salicylic acid the percent delivery changed only 4 – 5% (Figure 4.7) compared to the 40% change observed with the osmotic pump. This was accredited to the fact that the infusion pump had more consistent and less variable flow rates compared to the osmotic pump. In addition, the ratio of antipyrine to salicylic acid was similar to that obtained using the osmotic pump (Figure 4.8). Therefore, the diffusion behavior of salicylic acid and antipyrine is independent of the pumping device.

4.5.3 Application of Clearasil®

The use of the osmotic pump as a pumping device for cutaneous microdialysis sampling of an exogenous analyte was further verified by the topical application of the 2% salicylic acid cream, Clearasil®, on the right dorsal of the Sprague Dawley rat. Results obtained using an osmotic pump as the pumping device can be seen in Figure 4.9. The determined concentrations are adjusted using the delivery values obtained for the internal standard antipyrine. The maximum concentration was approximately 10 μg/mL obtained between the 7 and 8 hour sampling interval.

For comparison a similar experiment was conducted using an infusion pump at the flow rate of 1 μL/min which allowed for 15 minute sampling intervals.

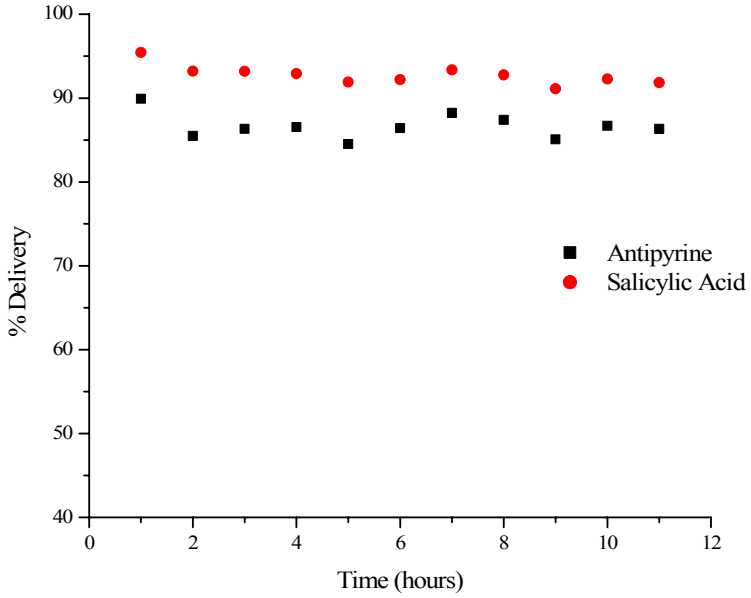

Figure. 4.7. Delivery of 20 μg/mL antipyrine and salicylic acid using an infusion pump.

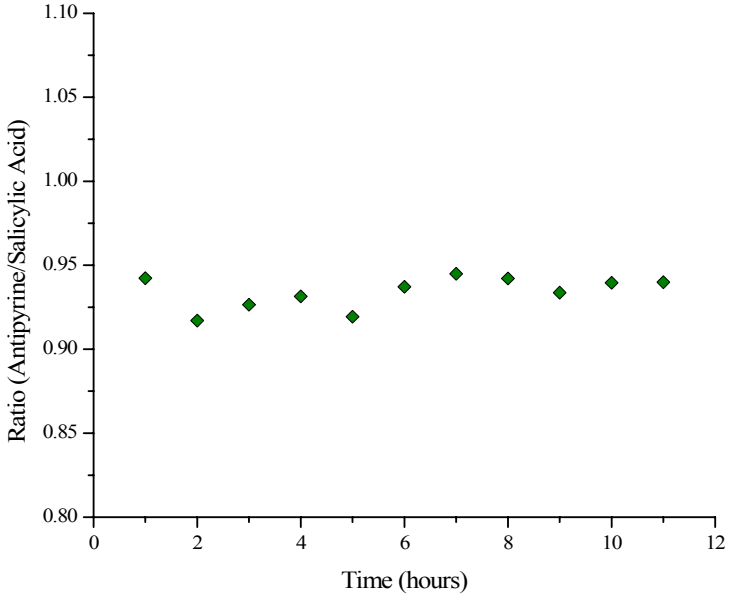

Figure. 4.8. Ratio of the deliveries of antipyrine and salicylic acid using an infusion pump.

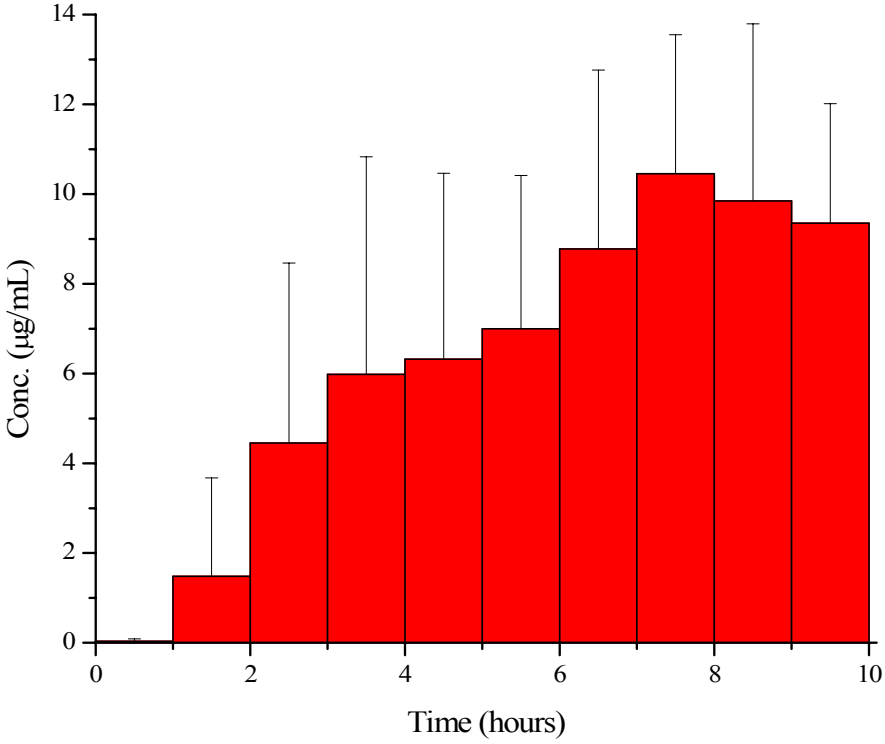

Figure. 4.9. Average penetration of salicylic acid following application of a 2% solution determined using an osmotic pump as the pumping device.

Salicylic acid concentrations measured using the infusion pump at this particular flow rate were significantly lower than the concentrations found using an osmotic pump (Figure 4.10). One possible explanation for this phenomenon is that at the reduced flow rates of the osmotic pump, the solution within the probe had a longer interaction time with the surrounding tissue. At these flow rates, equilibrium was nearly achieved between the two solutions. At higher flow rates, equilibrium is not achieved therefore proper calibration is needed in order to accurately determine the concentration of the analyte in the tissue. Calibration was completed prior to the start of the experiment using the delivery method previously described in Chapter One, Section 1.4.3.3. Using this method, it is assumed that the extraction efficiency of delivery is equal to the extraction efficiency of recovery. However, an overestimation of the percent delivery would result in an underestimation of the true tissue concentration. Another possible cause for this deviation would be due to the nature of the osmotic pump.

In order to verify which of these two outcomes was contributing to the concentration deviation, the same experiment was completed using an infusion pump set to pump at similar flow rates as the osmotic pump. Results from this particular study verified a higher concentration was obtained when using an osmotic pump as the pumping device compared to an infusion pump set at similar flow rates (Figure 4.11). Prior *in vitro* data had indicated a greater recovery was obtained using the osmotic pump compared to the infusion pump. This could indicate a possible

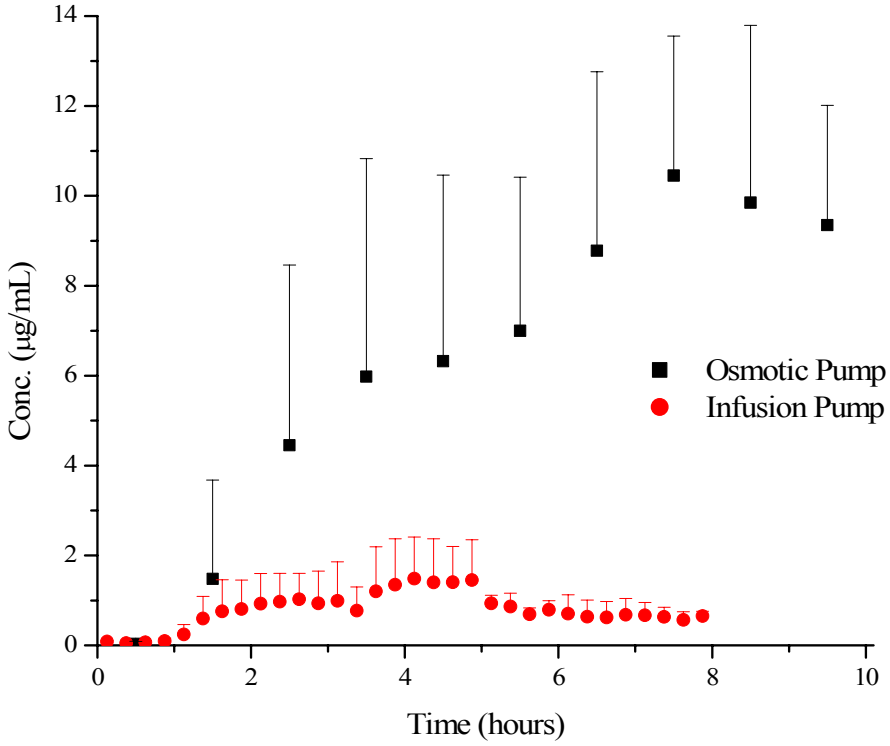

Figure. 4.10. Comparison between an osmotic pump and an infusion pump as the pumping device following the application of 2% salicylic acid cream. Osmotic pump flow rate averaged 7.6 µL/hr and the infusion pump was set to 1 µL/min.

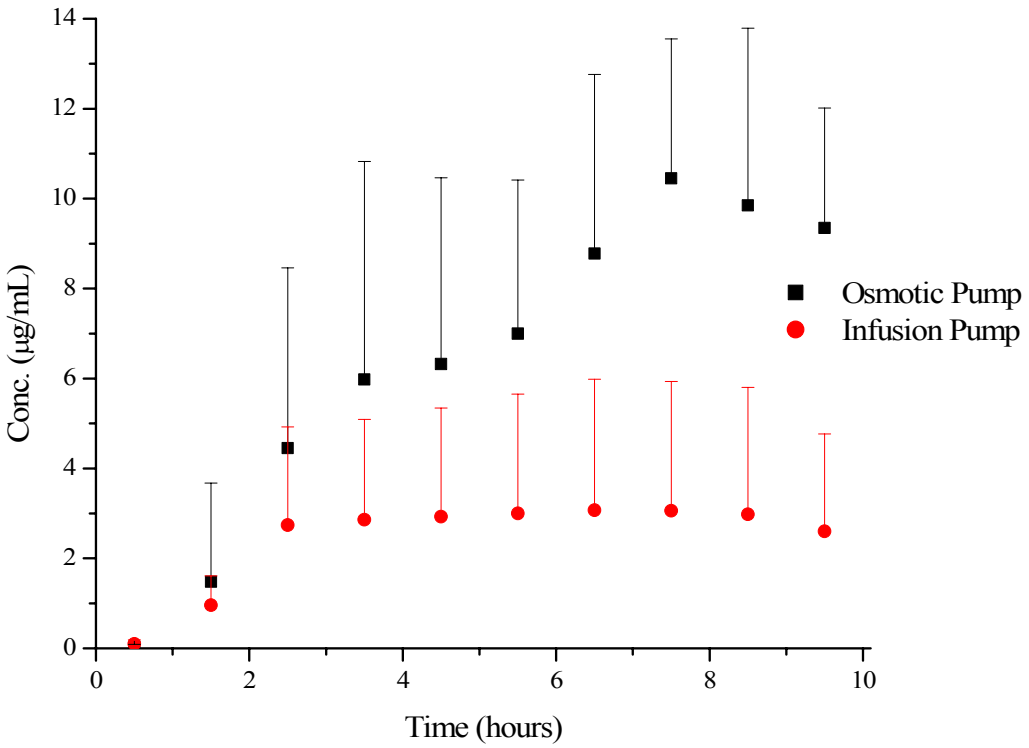

Figure. 4.11. Dermal concentration profile following application of a 2% salicylic acid cream. Flow rates for both the osmotic pump and the infusion pump were designed to flow at 10 µL/hr.

suctioning of the fluid surrounding the membrane. This was further tested by a recovery experiment using the anionic species vanillic acid which has poor recovery properties with PAN dialysis membrane due to charge repulsions [10]. If suctioning occurred when using an osmotic pump, it would be expected that a higher recovery value would be observed. However, similar recovery results were obtained for osmotic pump and an infusion pump (95.7% vs. 95.0%).

Finally, re-evaluation of the individual osmotic pump data again showed higher variable delivery of the internal standard compared to the infusion data. As samples were collected hourly, the percent delivery was the average amount of antipyrine delivered during the hour. A more frequent sampling period would discriminate flow rate changes more effectively.

4.5.4 Shorter Time Increments

Shorter collection times were also explored using the osmotic pump. On average, 3 μL was collected every 30 minutes. The compilation of osmotic pump data and infusion pump data can be found in Figure 4.12. Data obtained for the osmotic pump at shorter time increments was in good agreement with the infusion data set at slower flow rates. The shorter time increments monitored fluctuations in flow rate more frequently, resulting in a more effective use of the internal standard. Data collected when the infusion pump was set at 1 μL/min was slightly lower compared to the 10 μL/hr flow rate. This indicated that the determined delivery value was slightly over estimated.

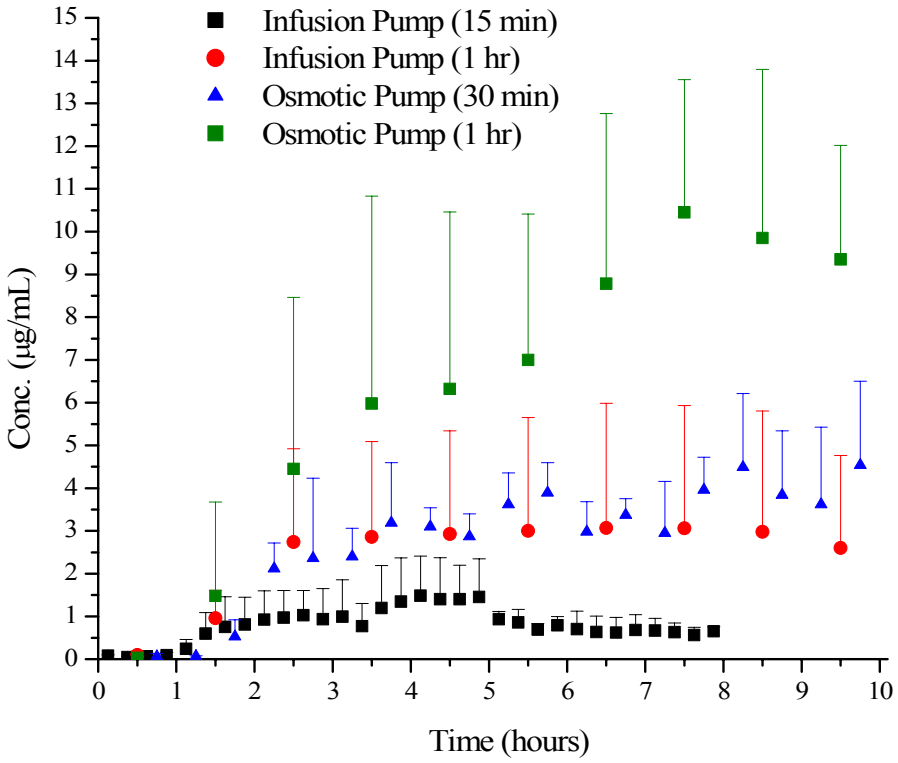

Figure. 4.12. Dermal concentration profiles following application of a 2% salicylic acid cream. Results were obtained using either an osmotic pump or an infusion pump as the pumping device.

4.6 Conclusions

The Alzet® osmotic pump was a successful alternative pumping device for cutaneous microdialysis sampling. The addition of a linear microdialysis probe had no effect on the average flow rate of the osmotic pump. Using the osmotic pump, the average flow rates were determined to be less and with a greater amount of variation than reported. In order to account for the large variations in flow rates, the use of an internal standard was evaluated. Similar trends in delivery were observed for both the analyte of interest and the internal standard. The average percent delivery ratio of antipyrine and salicylic acid was determined to be 0.97 which was used for determination of the true dermal concentration. Application of a 2% salicylic acid cream resulted in higher dermal concentrations when taking one hour samples with the osmotic pump compared to data collected using an infusion pump. However, when sampling was conducted more frequently, dermal concentrations were similar to the infusion pump data. The use of the internal standard was more effective at the shorter time increments.

4.7 References

1. Theeuwes, F. and S.I. Yum, *Principles of the Design and Operation of Generic Osmotic Pumps for the Delivery of Semisolid or Liquid Drug Formulations.* Annals of Biomedical Engineering, 1976. **4**(4): p. 343-353.

2. *Alzet Web Site*. [cited 2006 February 20]; Available from: http://www.alzet.com/.

3. Tjomsland, V. and E.-S. Magdy, *Anti-Tumour Effects of Triple Therapy with Octreotide, Galanin, and Serotonin in Comparison with Those of 5-Fluorouracil/Leukovorin on Human Colon Cancer.* International Journal of Oncology, 2005. **27**(2): p. 427-432.

4. Perez-Asensio, F.J., et al., *Inhibition of Inos Activity by 1400w Decreases Glutamate Release and Ameliorates Stroke Outcome after Experimental Ischemia.* Neurobiology of Disease, 2005. **18**: p. 375-384.

5. Turegano, L., et al., *Histochemical Study of Acute and Chronic Intraperitoneal Nicotine Effects on Several Glycolytic and Krebs Cycle Dehydrgenase Activities in the Frontoparietal Cortex and Subcortical Nuclei of the Rat Brain.* Journal of Neuroscience Research, 2001. **64**: p. 626-635.

6. Gross, S. and D. Piwnica-Worms, *Real-Time Imagining of Ligand-Induced Ikk Activation in Intact Cells and in Living Mice.* Nature Methods, 2005. **2**: p. 607-614.

7. Bittner, B., et al., *The Impact of Co-Solvents and the Composition of Experimental Formulations on the Pump Rate of the Alzet® Osmotic Pump.* International Journal of Pharmaceutics, 2000. **205**: p. 195-198.

8. Bazzett, T.J., J.B. Becker, and R.L. Albin, *A Novel Device for Chronic Intracranial Drug Delivery Via Microdialysis.* Journal of Neuroscience Methods, 1991. **40**: p. 1-8.

9. Cooper, J.D., et al., *Evaluation of an Osmotic Pump for Microdialysis Sampling in an Awake and Untethered Rat.* Journal of Neuroscience Methods, 2007. **160**: p. 269-275.

10. Zhao, Y., X. Liang, and C.E. Lunte, *Comparison of Recovery and Delivery in Vitro for Calibration of Microdialysis Probes.* Analytica Chemica Acta, 1995. **316**: p. 403-410.

Chapter Five

Investigation of the Optimization of Cell-Coated Linear Microdialysis Probes for *In Vitro* Drug Penetration Studies

5.1 Purpose

The purpose of this research was to investigate drug penetration using a new *in vitro* drug transport design. This employed using a cell-coated linear microdialysis probe instead of the typical flat membrane inserts generally used in diffusion cell experiments. Several cell culture parameters including sterilization parameters, substrate coating, and seeding densities were also explored.

5.2 Introduction

5.2.1 *In Vitro* Permeability Studies

With the onset of new synthetic processes that allows for rapid production of potential new drug entities (combinatorial chemistry), comparable high throughput analytical techniques are required to assess a compound's effectiveness. Initially a compiled drug library is screened for potential pharmacologically active compounds. Additional screening methods such as the ability of the drug to reach its desired site of action are then assessed. Many times this involves the measurement of drug transport across various biological barriers with additional focus on drug permeability and stability [1]. To improve high throughput analysis and decrease cost *in vitro*

techniques are preferred over *in vivo* techniques. A common *in vitro* technique used to study drug transport utilizes a cell culture model in a diffusion cell experiment. This cell culture model necessitates large volumes of test solution, which results in both large amounts of test compound needed and slow equilibration times, increasing analysis times and cost. As a consequence, not enough test compounds can be made available or extensive analysis times are needed. A novel approach to measure drug transport *in vitro* is to adhere live cells to a linear microdialysis probe, eliminating the need of large volume of compounds.

5.2.2 Epithelial Cell Lining

One of the main protective mechanisms of the human body is the epithelial tissue which lines all cavities and surfaces of the body. Epithelial tissue possess many functions that include secretion, absorption, selective permeability and drug transport, and protection. The general structure of the epithelial lining consists of tight junctions which form cell-cell and cell-matrix contact points. These junctions are important for the protective nature of the membrane, communication between cells, and anchoring cells in place [2].

Drug transport across epithelial lining can be divided into two main mechanisms: paracellular and transcellular (Figure 5.1). Paracellular transport occurs when a drug travels between epithelial cells and is controlled by passive diffusion. Small, hydrophilic compounds generally move by paracellular transport.

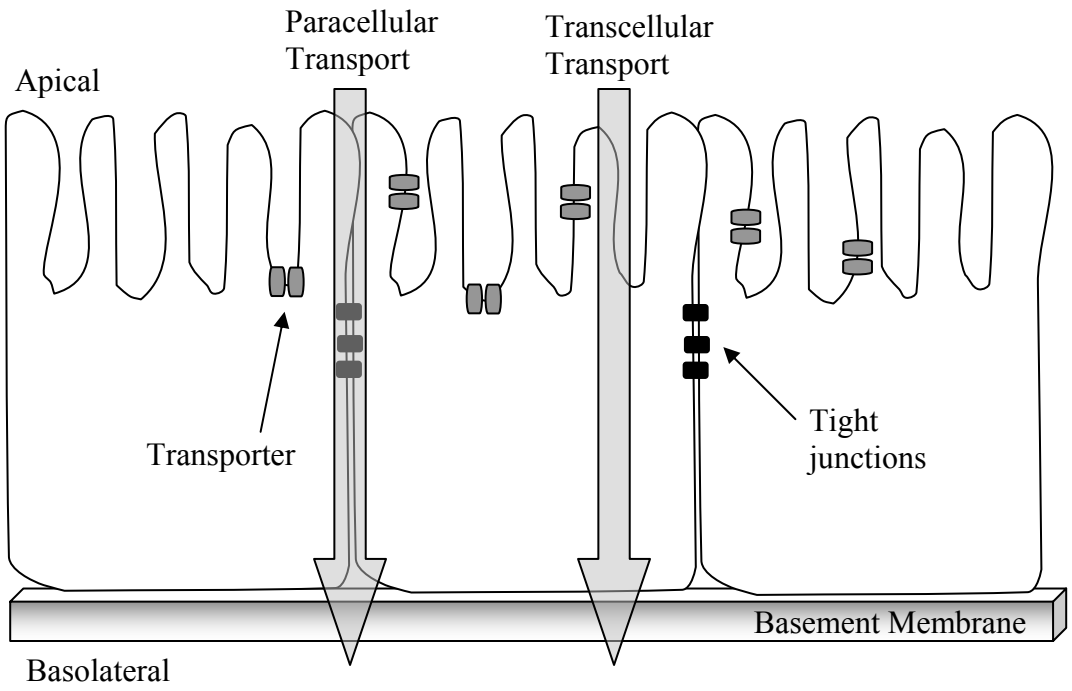

Figure 5.1. Basic schematic of drug transport across epithelial cells.

Alternatively, transcellular transport is the permeation of drugs through epithelial cells. This route can be further divided into passive and active transport. Drugs undergoing passive transcelluar transport are generally small lipophilic molecules which travel through the epithelial cell, controlled by a concentration gradient. Active transcellular transport again travel through the cell and occurs due to both carrier-mediated and endocytic process [1, 3]. Epithelial cells were chosen to line the microdialysis probe for drug penetration studies because of their role in drug transport in the body

5.2.3 Substrate Adhesion

The nature of the substrate surface is a key factor in the proliferation of cell growth. Initially, the majority of *in vitro* studies was conducted on glass surfaces as they provide the correct charge for cells to attach and grow and are reusable [14]. Disposable plastic flasks that include polystyrene, polyvinylchloride (PVC), polycarbonate, polytetrafluorethylene (PTFE), and thermanox (TPX), are an alternative substrate that can be used. However, surfaces of specific plastic flasks are not always suitable for cell growth. For example, the hydrophobic nature of polystyrene requires pretreatment by either γ-irradiation, chemical, or by an electric ion discharge to create a charged surface that can promote cell growth. Other plastics, such as PTFE, are available in a charged form and can be used for the growth of cells [14].

Additional treatment methods can also be used to improve cell attachment. The addition of minute amounts of cell residue to the substrate has been shown to promote better cell growth and attachment [14]. Several biologically significant compounds including laminin and fibronectin have also been shown to enhance adherence [14, 15]. A coating that is commonly used to improve attachment of epithelial cells is collagen, which can be obtained from rat-tail collagen (RTC) or is commercially available [14, 16, 17].

5.2.4 Cell Lines

This study focused on the use of two different cell lines: the BeWo cell line as a model of human trophoblast and the Caco-2 cell line for intestinal permeability studies.

5.2.4.1 Placental Lining: BeWo Cells

Nutrient exchange between mother and fetus is primarily controlled by passive diffusion across a single layer of trophoblasts [4]. In addition, there are several active transporters that have been identified including members of the ATP binding cassette (ABC) superfamily [5-7]. An understanding of drug permeability across the placenta lining is highly important as it can reduce complications with pregnancy and drug related birth defects.

The study of drug penetration across the placenta is primarily limited to *in vitro* studies since the unique anatomical structure of the human placenta makes it

difficult to find an animal model that can predict drug transfer accurately [8]. *In vitro* studies use either the primary cultures of human cytotrophoblasts or trophoblast-like cell lines such as BeWo, Jar, and HRP-1 [5]. The use of primary cultures of human cytotrophoblasts for transport studies is problematic because they can differentiate into syncytiotrophoblasts which do not form confluent monolayers [4]. Therefore, this study focused on the BeWo cell line.

The BeWo cell line was originally derived from a malignant gestational choriocarcinoma of the fetal placenta and characterized in 1968 [7, 9]. This particular cell line is ideal for *in vitro* transport studies because it is a relatively stable and easy cell line to maintain. A confluent monolayer can be achieved in a moderately short time frame (4-6 days) allowing for quick turnaround times which is ideal for method development [4].

5.2.4.2 Intestinal Lining: CaCo-2 Cells

Oral drug delivery is the leading drug administration route for systemic drug administration. High patient compliance is due to ease of administration and a relatively low cost compared to parenteral administration [2, 10]. Drug absorption for oral administration is predominantly absorbed within the small intestine [1, 2]. As a result, knowledge about the absorption of prospective drugs across the intestinal cell barrier is important for drug design and determination of dosing regiments.

The Caco-2 cell line is one of the most commonly used cell lines for *in vitro* oral absorption drug screening among the pharmaceutical companies [1, 10]. This

cell line was derived from human colon adenocarcinoma in 1974. Caco-2 cells form columnar absorptive cells with similar tight junctions compared to human small intestinal epithelium [11]. Growth time of 20-24 days is recommended to allow for complete monolayer formation and differentiation in order to establish appropriate transport characteristics [11]. Since Caco-2 cells take five times longer to establish a monolayer, BeWo cells were investigated initially in the cell coated microdialysis probe design.

5.3 Specific Aims

The specific aim of this study was to develop a novel device for the measurement of drug transport *in vitro* that uses smaller amounts of test compounds and provides higher throughput than previous designs. The proposed design consists of culturing cells onto the membrane of a linear microdialysis probe. This particular design yields microliter sample volumes, allows penetration determination from both directions (basal to apical and apical to basal), and enables complete pharmacokinetics data.

5.4 Materials and Methods

5.4.1 Chemicals

Acetaminophen, carbamezapine, cimetidine, antipyrine, caffeine, and diclofenac were purchased from Sigma (St. Louis, MO). Dulbecco's modified Eagle's medium (DMEM), Hanks' balanced salt solution (HBSS), L-glutamate (200

μM), and porcine trypsin in 0.2% EDTA were obtained from Sigma (St. Louis, MO). Non-essential amino acids and penicillin-streptomycin were purchased from Invitogen-Gibco (Carlsbad, CA). Fetal bovine serum heat inactivated (FBS/HI) was from Atlanta Biologicals (Lawrenceville, GA). Phosphate buffered saline (PBS) consisted of 129 mM NaCl, 2.5 mM KCl, 7.4 mM Na_2HPO_4, and 1.3 mM KH_2PO_4, all purchased from Fisher Scientific (Fairlawn, NJ). Hanks balance salt solution (HBSS) consisted of HBSS (9.7g/1 L) 4.4 mM sodium bicarbonate, 19.4 mM D-(+)-Glucose, and 12 mM N-2-hydroxyethylpiperazine-N'-2-ethanesulfonic acid (HEPES), all acquired from Sigma. HPLC grade acetonitrile and o-phosphoric acid were obtained from Fisher Scientific. Rat tail collagen (RTC) was made in house and provided by Dr. Kenneth Audus' lab (The University of Kansas, Lawrence, KS). Commercially available rat tail collagen type I was purchased from Collaborative Research (Lexington, MA). Fibronectin and poly-d-lysine were obtained from Sigma.

5.4.2 HPLC Instrumentation

Data was analyzed using a Shimadzu LC-6A pump and a Shimadzu SPD-6AV UV-Vis spectrophotometric detector (Shimadzu Scientific Instruments, Inc., Columbia, MD). Chromatographic data was acquired using Labview software (Austin, TX). Separation was completed on a Phenomenex Prodigy C18 column (3 μm, 100 x 2.0 mm). Mobile phase consisted of a mixture of 50 mM sodium

phosphate, adjusted to pH 3.8 using 10% o-phosphoric acid and acetonitrile. Table 5.1 lists the specific run conditions for the analytes of interest.

5.4.3 Cell Culture

5.4.3.1 BeWo Cell Culture

The BeWo clone (b32) was obtained from Dr. Kenneth Audus (The University of Kansas, Lawrence, KS). Cells used in this study were from passages 34 45. Cells were grown in DMEM media adjusted to pH 7.4 and supplemented with 10% heat-inactivated FBS, 0.37% sodium bicarbonate, 1% antibiotics (10,000 U/mL penicillin and 10 mg/mL streptomycin), 1% 200 mM $_L$-glutamine, and 10 mM minimal essential medium nonessential amino acids solution. Cells were maintained in 175-cm^2 Falcon flasks (Fisher Scientific) at pH 7.4 under 5% CO_2 and 95% humidity at 37 ˚C. The medium was changed the day following passage and then every other day. Cells were passed when they reached 70-90% confluency, approximately 4-6 days from the last passage.

Cells were harvested by first removing the media and then exposing the cells for 3 5 minutes to a trypsin-EDTA solution (0.25% trypsin and 0.02% EDTA in PBS). They were then transferred from the flask to a centrifuge tube and spun down for 8 minutes at 1.5 x 10^3 rpm. Cells were reconstituted in 10 mL of the previously described DMEM media. One tenth of the original cells were used for continuation of the cell line while the remainder of the cells was used for coating the microdialysis probes.

Table 5.1. LC run conditions for compounds of interest. Mobile phase consisted of acetonitrile:50 mM sodium phosphate buffered saline (pH 3.8).

Drug	Mobile Phase (v:v)	UV Absorbance (nm)	% Recovery (untreated fiber)
Acetaminophen	15:85	214	87.27 ± 1.51
Carbamezapine	55:45	214	82.74 ± 1.62
Cimetidine	12:88	214	81.35 ± 4.51
Antipyrine	40:60	244	
Caffeine	18:82	214	87.83 ± 2.53
Diclofenac	55:45	214	71.53 ± 3.11

5.4.3.2 Caco-2 Cell Culture

The Caco-2 cell line was obtained from Dr. Ronald Borchardt (The University of Kansas, Lawrence, KS). Cells used in this study were from passages 45 75. Cells were grown in DMEM media supplemented with 10% heat-inactivated FBS, 0.37% sodium bicarbonate, 1% antibiotics (10,000 U/mL penicillin and 10 mg/mL streptomycin), 1% 200 mM L-glutamine, 10 mM minimal essential medium nonessential amino acids solution, and 6 mM HEPES. Cells were maintained in 175-cm^2 Falcon flasks under 5% CO_2 and 95% humidity at 37 ˚C. The medium was changed the day following passage and then every other day. Cells were passed when they reached 70-90% confluency, approximately 12-15 days from the last passage.

Cells were harvested by first removing the media and replacing it with 20 mL of PBS. Cells were exposed to this solution for five minutes, the solution was removed and the cells were then exposed to a trypsin-EDTA solution (0.25% trypsin and 0.02% EDTA in PBS) which was run over the top of the cells and immediately removed. The flask was then allowed to sit until the cells began to detach from the sides of the flask. Next, 12 mL of the DMEM was added to the flask to re-suspend the cells. Approximately, one tenth of the original cells were used for continuation of the cell line while the remainder of the cells was used for coating the microdialysis probes.

5.4.3.3 Cell Counting and Seeding of Linear Microdialysis Probe

For cell counting, 150 μL of the cell suspension was added to 100 μL of trypan blue. The cell suspension was mixed and then counted using a hemocytometer which gave an average number of cells per milliliter. For seeding of the linear microdialysis probes, a Petri dish probe assembly was constructed as described in Section 5.2.6. The surface area of the bottom of the Petri dish was calculated and used to determine the seeding densities which were reported as cells/cm^2. The bottom of the Petri dish was filled with 25 mL of the DMEM media plus the cited cell density.

5.4.4 Microdialysis Probe Construction

Linear microdialysis probes were constructed as previously described in earlier chapters. Briefly, probes were made by threading a piece of polyimide tubing (175 μm i.d., 215 μm o.d.) into a segment of dialysis membrane creating a 1.5 cm active membrane length. The dialysis fiber consisted of either AN69 HF (PAN) or Diacepal (Hospal Industrie, Mayzieu, France). UV glue was coated on the connections and cured using a UV curing system. A 1 cm piece of tygon tubing was UV glued to the inlet of the microdialysis probe.

5.4.5 Transepithelial Resistance (TEER)

In order to assess the integrity of a cell monolayer *in vitro*, the electrical resistance across the monolayer or the transepithelial electrical resistance (TEER) was

measured. This value represents the tightness of the cell-junction structure or the integrity of the cell monolayer [12]. A well developed monolayer induces an electrolyte barrier resulting in an increase in the electrical resistance across the monolayer compared to non cell coated membranes [13].

Figure 5.2 represents the setup employed for the TEER measurements. In short, the fiber was immersed in a warm PBS solution (37 ˚C) and the microdialysis inlet and outlet were placed in a second warm PBS solution. A voltmeter was used to measure the resistance between the two solutions. Prior to resistance measurements, the microdialysis probe was perfused with the phosphate buffered saline.

5.4.6 Design of Microdialysis Probe Setup

In order to keep the probe stationary during the course of an experiment a Petri dish holder was designed (Figure 5.3). Two fittings were fixed into previously drilled holes on the Petri dish cover and held secure with UV glue. In addition, a larger hole was created at the top of the dish and covered with a teflon membrane, 0.20 μm pore size (Fisher Scientific), to allow for ventilation in the incubator and access to the probe when taking the resistance measurements. The microdialysis membrane of the probe was suspended between the two fittings to ensure that the dialysis membrane was elevated above the Petri dish bottom.

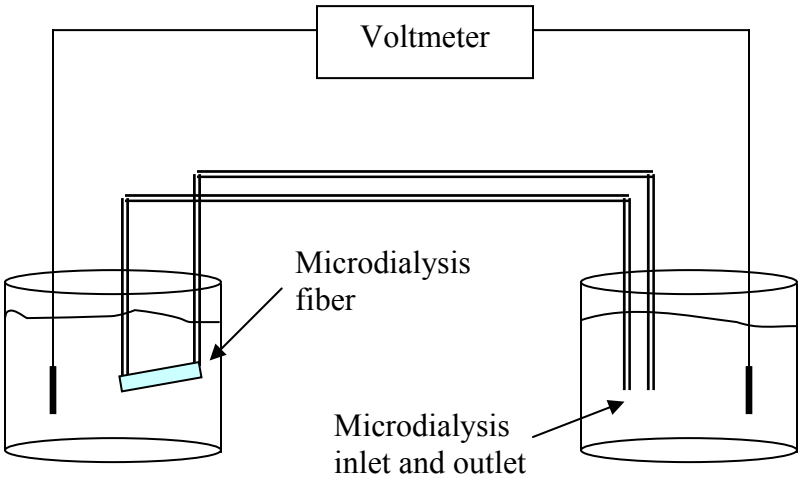

Figure 5.2. Schematic of the TEER setup. Beakers contained 0.01 M PBS solution. Probe was flushed with 0.01 M PBS prior to measurements.

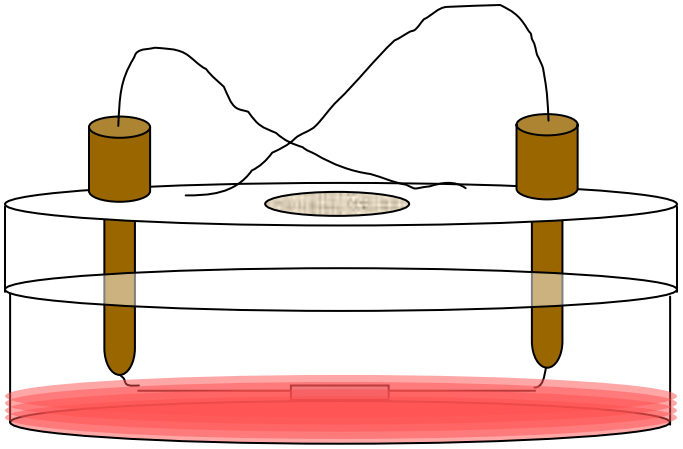

Figure 5.3. Schematic of the cell culture setup. Microdialysis fiber was held secure during cell culture and transport studies.

Table 5.2. List of analytes of interest. Log p values were obtained from the Environmental Science Center Database.

Compound	Molecular Weight	Log P
Diclofenac	318.13	4.51
Antipyrine	188.23	0.38
Cimetidine	252.34	0.40
Carbamezapine	236.27	2.45
Acetaminophen	151.16	0.46
Caffeine	194.19	-0.07

5.4.7 Analytes of Interest

In order to gain a better understanding of the permeability properties of the BeWo and Caco-2 cell lines, a list of analytes of interest was developed that included acidic, basic, and neutral compounds. Analyte selections was based on molecular weight and partition coefficients (log p) (Table 5.2).

5.5 Results and Discussion

5.5.1 Sterilization Techniques of Microdialysis Probes

Commercially available Transwell® plates and side-by-side diffusion cell membranes can be purchased sterile or can be easily sterilized either by immersion into 70% alcohol, extended exposure to UV light or autoclaved at elevated temperature (120 ˚C). The linear microdialysis probes were constructed in house and developing an appropriate method for sterilization was necessary. One difficulty with

sterilization of these probes was that the dialysis fiber is very sensitive. Once the fiber was wetted, it needed to be kept in solution to prevent the fiber from drying out, causing it to shrink in size and become extremely brittle. In addition, any extended exposure to air also removed the natural moisture of the fiber and caused the fiber to shrink and increased inconsistent results.

Initial focus of this study examined sterilization techniques of a microdialysis probe prior to exposure to cell culture conditions. Initially, the microdialysis probes were sprayed with a 70% ethanol solution and then exposed to UV light for two hours. During this process membrane fibers typically decreased from 1.5 cm to between 1.0 – 1.2 cm, an unwanted result. Next, the probes were immersed in a solution of 70% ethanol for twenty minutes and then rinsed with sterile water prior to culturing with BeWo cells. This seemed to maintain the integrity of the dialysis fiber as it was kept moist throughout the sterilization process; however, a dramatic decrease in probe success rate was noted. The use of ethanol weakened the connection of the UV glue to the polyimide tubing causing the probes to pull apart. Microdialysis probes soaked longer than five minutes in 70% ethanol resulted in a success rate below 50%. Finally, sterilization by exposure to UV light was evaluated. The microdialysis fiber was allowed to sterilize under UV light for a minimum of two hours prior to further treatments. In order to sterilize the interior of the microdialysis probe, sterile water was flushed through microdialysis probe at a flow rate of 2 μl/min throughout sterilization and any remaining treatments until the probe was ready to be seeded and placed into the DMEM media. This sterilization method provided

adequate sterilization and maintained the integrity of the microdialysis fiber. All microdialysis fibers were sterilized with this technique prior to further treatments and seeding.

5.5.2 Attachment of Cells to the Dialysis Fiber

An investigation of different coating treatments was then explored to find the most reproducible, efficient way to coat the dialysis fiber with cells. First, cell attachment to untreated dialysis fiber was evaluated. Since PAN membrane was constructed from an acrylonitrile and sodium methallyl sulfonate copolymer, it possessed both hydrophilic and hydrophobic functional groups. Linear microdialysis probes with untreated dialysis fibers were seeded with BeWo cells at a density of 100,000 cells/cm^2 on the first day. The media was maintained as previously described in section 5.2.3.1. The probe was visualized using an inverted microscope on day 5 and 6 post seeding and had minimal cell adhesion.

Second, the use of rat tail collagen (RTC) provided by Dr. Kenneth Audus was examined as a substrate coating. Generally collagen is applied by dispensing a collagen solution over the surface of the fiber, removing the excess, and then allowing the residue to air dry. As the microdialysis fiber is tubular, several different application procedures were investigated. Initially, the microdialysis fiber was immersed into the RTC solution and allowed to dry for two hours (while being perfused with sterile water as previously described). Measurement of the electrical resistance of a RTC coated dialysis fiber was 9.01 ± 1.65 MΩ or 1.49 MΩ·cm^2, a

slight increase to plain PAN membrane which had an average resistance value of 7.63 ± 1.60 MΩ or 1.26 MΩ·cm^2. This corresponds with previously reported data that found a low electrical resistance caused from the collagen layer [14]. Probes were then seeded with either 100,000 or 200,000 cells/cm^2 on day one and maintained until days five and six. Using this method, an increased amount of BeWo cells adhered to the surface of the dialysis fiber compared to the untreated fiber. However following minimal agitation of the probe setup (moving of the Petri dish), cells were visually seen with a microscope to be pulling away in clusters from the membrane (Figure 5.4). Cell interaction with the RTC was maintained but the adhesion of the RTC to the dialysis fiber was not sufficient. The electrical resistance measurement following the coating of BeWo cells was found to be approximately 8.21 ± 0.67 MΩ or 1.35 MΩ·cm^2, similar to no cells present. This supports the visual finding of cells flaking off the dialysis fiber. The permeability of a 1 mM acetaminophen solution on a non-treated microdialysis probe was 87.27 ± 1.51%. A cell coated microdialysis probe with a RTC substrate using the same conditions as described produced an average permeability of 84.62 ± 6.42%. Little change in permeability was seen as a result of the poor cell adhesion.

To try to improve the RTC and dialysis fiber interaction, the fiber was placed in an ammonia chamber after collagen application to instigate cross-linking of the collagen strands. The dialysis fiber was then rinsed in sterile water until it was seeded. Again, a similar seeding protocol was followed. This additional cross-linking step did not improve collagen linking to the fiber.

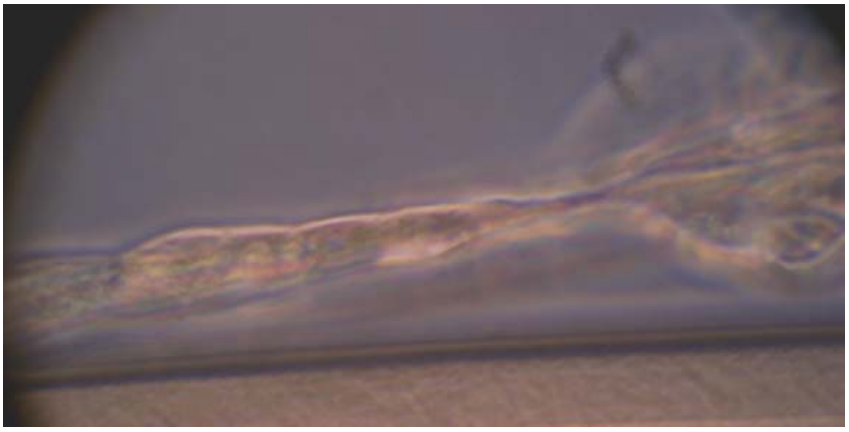

Figure 5.4. PAN dialysis fiber coated with RTC and seeded at 200,000 cells/cm^2. Cells were found in clusters indicating poor adhesion of the RTC to the PAN fiber.

Both of the previously described collagen coating methods have been reported to produce irregular and weakly bound collagen coatings [15]. Macklis et al. investigated the use of the derivatizing agent 1-cyclohexyl-3-(2-morpholinoethyl)-carbodiimide-metho-*p*-toluenesulfonate (carbodiimide) to aid in the strength and durability of the collagen coating. Their results showed an increased amount of collagen deposited on the substrate surface and less collagen degradation in comparison to the conventional methods [15]. Two different coating mixtures were tested using this carbodiimide derivatizing agent. The first one used a 50% RTC:50% water with 130 μg/mL carbodiimide and the second mixture consisted of 25% RTC:75% water with 130 μg/mL carbodiimide. Probes were dried under UV light and then seeded on days one and three with 100,000 cells/cm^2. The addition of the derivatizing agent carbodiimide did not improve the adhesion the RTC to the PAN dialysis membrane, since the cells were seen coming off in clusters (Figure 5.5).

Initial investigations looked into the use of the PAN membrane as a microdialysis fiber. However, it was determined that the RTC coating did not form a very adhesive bond with the PAN membrane. Another membrane, Diacepal, was examined as an alternative to PAN. Diacepal is a thin-walled (15 μm) cellulose diacetate-based membrane that required a support in order to maintain the stability of the membrane. Therefore, a 7/0 piece of black monofilament nylon (Ashaway Line and Twine, Ashaway, RI) was threaded through the entire linear microdialysis probe and held into place. Cell adhesion investigations were first conducted using microdialysis probes with untreated diacepal membrane and a seeding density of

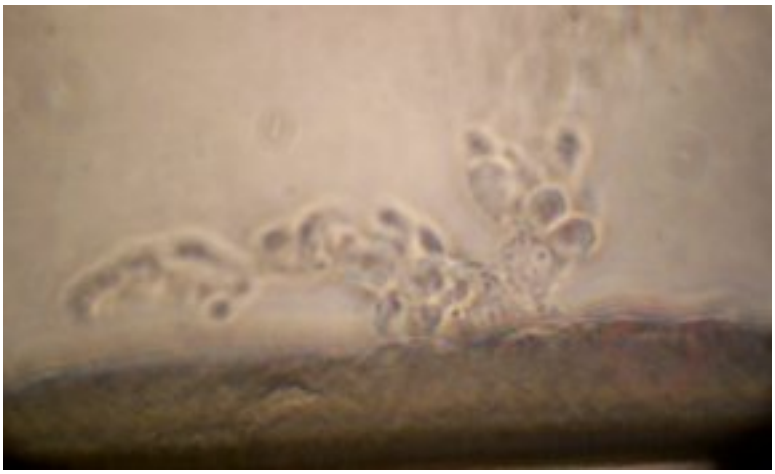

Figure 5.5. PAN dialysis fiber coated with RTC derivatized with carbodiimide and seeded at 200,000 cells/cm^2. Cells were found to come in clusters indicating a poor adhesion of the RTC to the PAN fiber.

100,000 cells/cm^2. As previously seen with the PAN membrane, very minimal amounts of cells were found to adhere to the membrane following 4 – 6 days of culture. Next a coating of RTC was applied as previously described. Additional cell adhesion was noted with this coating, however similar results to the PAN membrane were achieved as small agitations disrupted cell adhesion to the diacepal fiber.

Finally, the combination of fibronectin and poly-d-lysine was explored as a coating method. As previously mentioned, fibronectin is thought to improve adhesion as it binds to integrins which mediate cell substrate interactions [16]. In addition, poly-d-lysine creates an overall net positive charge on the substrate which promotes cell adhesion [17]. When applied separately, fibronectin induced a greater attachment of cells to the dialysis membrane than poly-d-lysine. However, neither treatment method promoted a complete monolayer of BeWo cells to the membrane. When fibronectin and poly-d-lysine were used in combination a uniform monolayer of BeWo cells were found to proliferate on the microdialysis fiber. The microdialysis fiber was dipped in a poly-d-lysine solution (25 mL of 1 μg/μL poly-d-lysine to 5 mL of 30% ethanol solution), allowed to air dry for five minutes, re-dipped in the same solution and again allowed to dry for 3 hours under fluorescent lighting while perfusing water through the microdialysis probe as previously described. The probe was sterilized for the final 45 minutes under UV lighting. Next the probe was dipped twice into a fibronectin solution (50 μg/mL), allowing 10 minutes drying time between applications. Cell adhesion was found to withstand normal agitations and transportation across campus (Figure 5.6).

5.5.3 Examination of Seeding Density and Frequency

Liu et al. determined a direct relationship exists between seeding density and BeWo monolayer permeability [4]. Higher seeding densities resulted in multiple cell layers on transwell plates. Optimal seeding densities for cells seeded on a Transwell insert were determined to be 100,000 cells/cm^2 [4]. A look into multiple seeding densities for a suspended microdialysis probe was next explored to determine optimal seeding density for a PAN dialysis fiber.

Initially, a one-time seeding density of 100,000 cells/cm^2 was used to coat a PAN microdialysis fiber. Minimal cell attachment to the microdialysis fiber was evident following 6 days of growth, and an insufficient layer of cells was observed (Figure 5.7). This was not unexpected since the microdialysis fiber was suspended in the media and had a round surface compared to Transwell® inserts, which are flat and stationary surfaces. Next seeding densities including 200,000, 300,000, 500,000, 600,000, or 1,000,000 cells/cm^2 were examined on the fibers. When seeding large densities of cells, multiple cell layers were often observed (Figure 5.8). This was not desired so multiple seedings at a lower seeding density was investigated. For a suspended microdialysis probe, the ideal seeding density and frequency was determined to be 150,000 cells/cm^2 for two days. This resulted in a confluent monolayer of cells around the entire microdialysis fiber (Figure 5.9). Average TEER

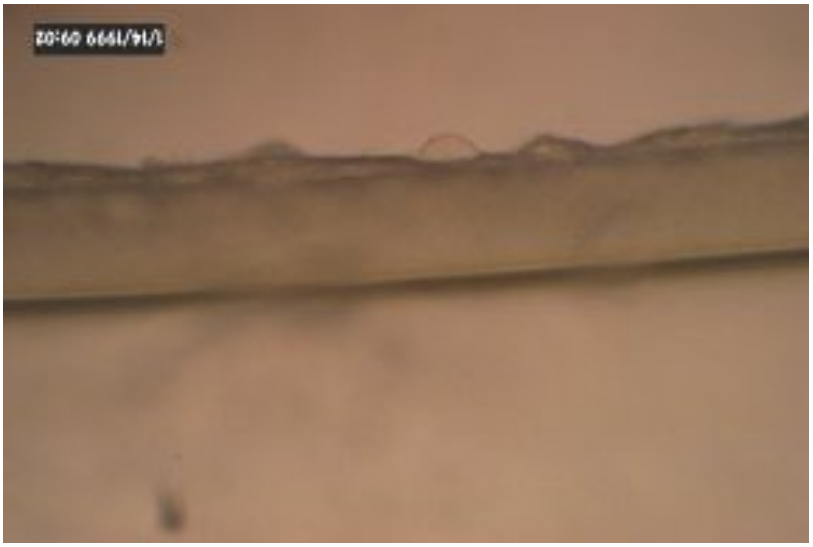

Figure 5.6. PAN membrane coated with two coatings of poly-d-lysine, allowed to dry and then coated with fibronectin. Fiber was seeded with 150,000 cells/cm^2 on day one and day two.

Figure 5.7. PAN membrane coated with the combination of fibronectin and poly-d-lysine. Seeding with cells at a density of 100,000 cells/cm^2.

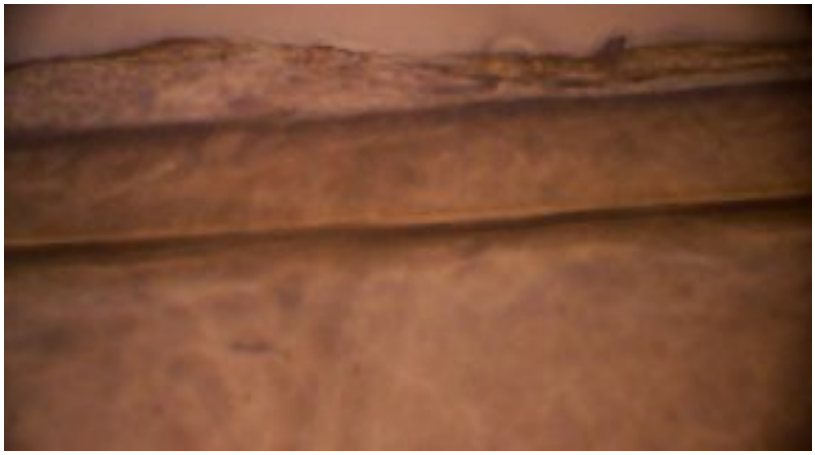

Figure 5.8. PAN membrane coated with the combination of fibronectin and poly-d-lysine. Seeding with cells at a density of 500,000 cells/cm^2.

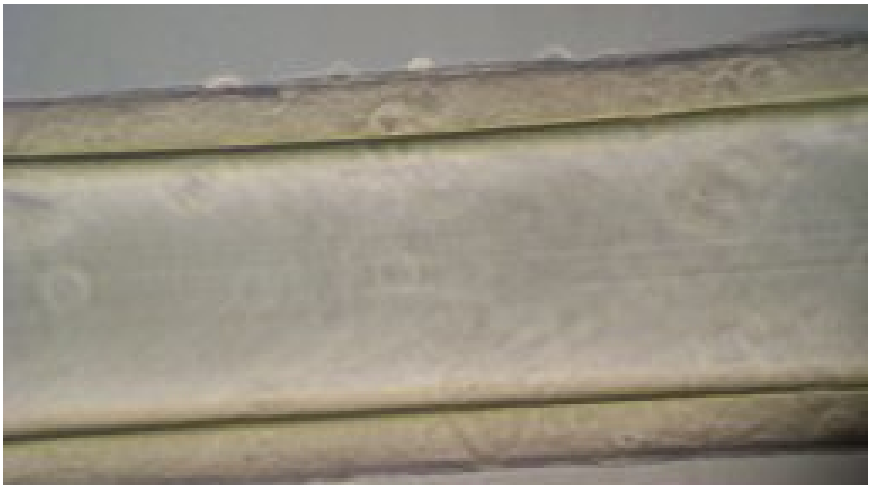

Figure 5.9. PAN membrane coated with the combination of fibronectin and poly-d-lysine. Seeded with cells at a density of 150,000 cells/cm2 for two days.

value for a cell coated microdialysis probes with a fibronectin, poly-d-lysine coating was 8.4 MΩ ± 1.7 MΩ or 1.38 MΩ·cm^2. These results show no increase in electrical resistance compared to the plain PAN membrane indicating poor integrity of the cell monolayer.

5.5.4 Investigation of Perfusion of PBS through the Microdialysis Probe

Although an appropriate sterilizing method, a membrane coating that allowed for agitation of the media and transfer across campus and a suitable seeding scheme that allowed for a uniform monolayer of cells to be coated on the microdialysis fiber were developed, the TEER values demonstrated the cell monolayer was not confluent and intact. To measure the TEER the linear microdialysis probe must be first perfused with phosphate buffered saline. Perfusing the probe caused the microdialysis fiber to shed the BeWo cells (Figure 5.10). A sudden surge of fluid going across the membrane could produce an added force on the membrane causing it to swell and compromise the cell monolayer.

Several perfusing methods were optimized to maintain cell adherence to the microdialysis fiber. First the cell-coated probe was perfused at low flow rates (0.1 μL/min) and incremented step-wise until the flow rate of 1.0 μL/min was achieved. As seen in Figure 5.11, better cell adhesion was obtained using this step-wise perfusion method. Following perfusion individual cells were distinguishable, which was not previously observed, and only small areas without cells were noted. The TEER was monitored after the initial low flow rate and when the maximum flow rate

Figure 5.10. PAN membrane coated with the combination of fibronectin and poly-d-lysine. Probe was seeded with Bewo cells at a density of 150,000 cells/cm^2 on day one and day two. Probe was perfused with PBS at 2 μL/min.

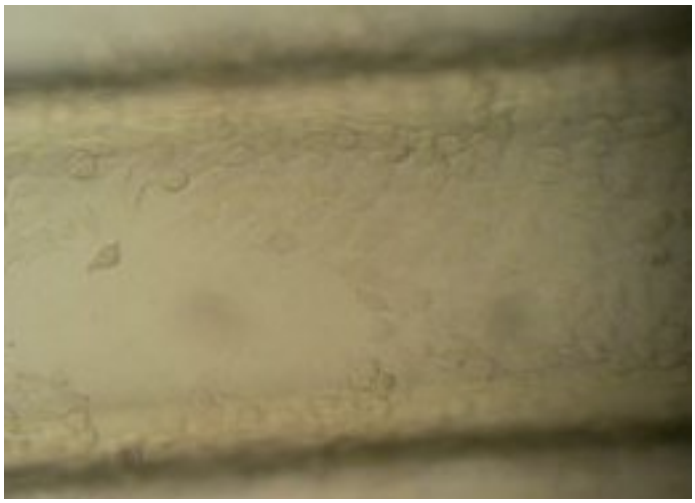

Figure 5.11. PAN membrane coated with the combination of fibronectin and poly-d-lysine. Probe was seeded with BeWo cells at a density of 150,000 cells/cm2 on day one and day two. Probe was perfused with PBS starting at 0.1 μL/min and increased by 0.1 μL/min until reached flow rate of 1 μL/min.

was obtained. A higher TEER value was initially measured (~13.6 MΩ, 2.24 MΩ·cm^2) at low flow rates and was found to decrease after higher flow rates were achieved (~10.6 MΩ, 1.75 MΩ·cm^2), indicating the integrity of the cell monolayer was degrading throughout the perfusion process. So even though the step-wise perfusion helped the cell adhesion, the monolayer still was compromised at the higher perfusion flow rates.

5.5.5 The Use of Caco-2 Cell in Monolayer Adherence to Microdialysis Fibers

Initial method development work was completed using the BeWo cell line since the time to confluency is within 4 – 6 days. Alternatively, the Caco-2 line requires 20 – 24 days for complete differentiation in order to establish appropriate transport characteristics. Therefore, the optimized sterilization technique and cell seeding density and frequency were utilized for the Caco-2 cell line while traditional coating techniques were explored.

As seen with the BeWo cells, Caco-2 cells seeded on bare PAN membrane were found to have minimal cell adhesion. Next, the use of commercially available rat tail collagen (type 1) was used to coat the PAN membrane. Using the previously developed protocol the probes were seeded at 150,000 cells/cm^2 for two days. By day 13 a confluent monolayer was observed on the membrane. When transferred, the cells remained adhered to the membrane. Perfusion of Hank's balanced salt solution was completed incrementally as previously described. The majority of the cells remained adhered to the probe with very minimal points of detachment. However,

the TEER measurement was 4.4 ± 0.8 MΩ (0.73 MΩ·cm^2), lower than a plain PAN membrane, indicating the cell-junctions between cells was not tight and the integrity of the monolayer was weakened.

Furthermore, a microdialysis recovery experiment was completed using acetaminophen as described in Chapter 1, Section 1.4.3.1. The average percent of acetaminophen recovered using microdialysis probe with an uncoated PAN membrane was previously determined to be 87.27 ± 1.51 %. With the addition of the Caco-2 cells coating the probe, a decrease in the percent acetaminophen recovered was determined to be 62.0 ± 7.21 %, a noticeable drop in the permeability of the membrane. However, examination of the individual recovery plot indicated a deterioration of the monolayer integrity as the percent acetaminophen recovery continued to increase throughout the experiment (Figure 5.12). Extended perfusion of the microdialysis probe caused a continual weakening of the tight-junctions between cells.

5.6 Conclusions

The development of a cell coated linear microdialysis probe for the use of cell permeability was explored. During the course of this study, several cell culture parameters were investigated that included sterilization techniques, cell adhesion to a substrate, seeding density and frequency, perfusion parameters, and cell types.

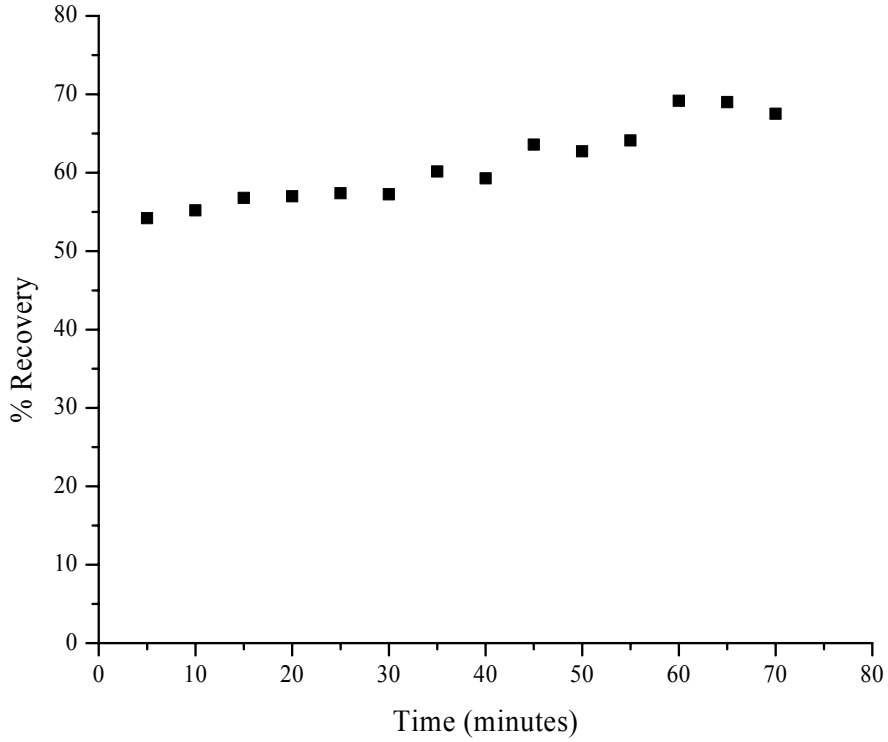

5.12. Recovery of acetaminophen using a Caco-2 cell coated microdialysis probe.

Optimal sterilization was found to be exposure to UV light for two hours prior to coating of the linear microdialysis probe. In addition, the linear probe was perfused (2 μl/min) with sterile water during the sterilization procedure and throughout coating until seeding and placement into the media. The best substrate coating for PAN membrane was found to be a combination of poly-d-lysine and fibronectin. The microdialysis fiber was dipped in a poly-d-lysine solution (25 mL of 1 μg/μL poly-d-lysine to 5 mL of 30% ethanol solution), allowed to dry for five minutes, re-dipped in the same solution and again allowed to dry for 3 hours under fluorescent lighting. The probe was sterilized for the final 45 minutes under UV lighting. Next the probe was dipped twice into a fibronectin solution (50 μg/mL) allowing 10 minutes drying time between applications. The ideal seeding density and frequency was two applications of 150,000 cells/cm^2 over two days. These conditions resulted in a uniform monolayer on the dialysis fiber. However, cell integrity was greatly affected when perfusing solution through the microdialysis probe. This was not only visually evident but confirmed by TEER measurements and recovery experiments.

In conclusion, appropriate parameters were determined for the growth of a cell monolayer on a microdialysis fiber. However, the integrity of the monolayer was not sustained following perfusion of the microdialysis probe. Therefore, the use of a cell coated microdialysis probe is not an ideal method for permeability studies.

5.7 References

1. Balimane, P.V. and S. Chong, *Cell Culture-Based Models for Intestinal Permeability: A Critique.* Drug Discovery Today, 2005. **10**(5): p. 335-343.

2. Hillery, A.M., A.W. Lloyd, and J. Swarbrick, *Drug Delivery and Targeting*. 2001, New York: Taylor and Francis.

3. Alberts, B., et al., *Molecular Biology of the Cell*. 3rd ed. 1994, New York: Garland Publishing, Inc.

4. Liu, F., M.J. Soares, and K.L. Audus, *Permeability Properties of Monolayers of the Human Trophoblast Cell Line BeWo.* The American Physiological Society, 1997: p. C1596-C1604.

5. Young, A.M., C.E. Allen, and K.L. Audus, *Efflux Transporters of the Human Placenta.* Advanced Drug Delivery Reviews, 2003. **55**: p. 125-132.

6. Utoguchi, N., M. Magnusson, and K.L. Audus, *Carrier-Mediated Transport of Monocarboxylic Acids in Bewo Cell Monolayers as a Model of the Human Trophoblast.* Journal of Pharmaceutical Sciences, 1999. **88**: p. 1288-1292.

7. Chandorkar, G.A., et al., *Peptide Transport and Metabolism across the Placenta.* Advanced Drug Delivery Reviews, 1999. **38**: p. 59-67.

8. Enders, R.J. and T.N. Blankenship, *Comparative Placental Structure.* Advanced Drug Delivery Reviews, 1999. **38**: p. 3-15.

9. Utoguchi, N. and K.L. Audus, *Carrier-Mediated Transport of Valproic Acid in BeWo Cells, a Human Trophoblast Cell Line.* International Journal of Pharmaceutics, 2000. **195**: p. 115-124.

10. Krishna, G., et al., *Permeability of Lipophilic Compounds in Drug Discovery Using in-Vitro Human Absorption Model, Caco-2.* International Journal of Pharmaceutics, 2001. **222**: p. 77-89.

11. Wirth, M., E. Bogner, and F. Gabor, *Parameters Influencing the Transport Rate of Marker Compounds across Caco-2 Monolayers.* Scientia Pharmazeutica, 2001. **69**: p. 91-104.

12. Yamashita, S., et al., *Optimized Conditions for Prediction of Intestinal Drug Permeability Using Caco-2 Cells.* European Journal of Pharmaceutical Sciences, 2000. **10**: p. 195-204.

13. Larger, P., et al., *Simultaneous LC-MS/MS Determination of Reference Pharmaceuticals as a Method for the Characterization of the Caco-2 Cell Monolayer Absorption Properties.* Analytical Chemistry, 2002. **74**: p. 5273-5281.

14. Hidalgo, I.J., T.J. Raub, and R.T. Borchardt, *Characterization of the Human Colon Carcinoma Cell Line (Caco-2) as a Model System for Intestinal Epithelial Permeability.* Gastroenterology, 1989. **96**: p. 736-749.

15. Macklis, J.D., R.L. Sidman, and H.D. Sine, *Cross-Linked Collagen Surface for Cell Culture That Is Stable, Uniform, and Optically Superior to Conventional Surfaces.* In Vitro Cellular and Developmental Biology, 1985. **21**(3): p. 189-194.

16. Freshney, R.I., *Culture of Animal Cells*. 3rd ed. 1994, New York: Wiley-Liss. 485.

17. Vleggeert-Lankamp, C.L.A.-M., et al., *Adhesion and Proliferation of Human Schwann Cells on Adhesive Coatings.* Biomaterials, 2004. **25**: p. 2741-2751.

Chapter Six

Conclusions and Future Work

6.1 Dissertation Overview

Appropriate techniques for monitoring drug delivery are important as it aids in drug screening and is used in the determination of proper dosing regimens. Current *in vivo* dermal sampling techniques are not optimal for drug delivery studies as they are not able to provide continual sampling in the same skin region, are extremely invasive, and do not determine true dermal concentrations. In addition, traditional *in vitro* drug penetration designs require large volumes of drug making its use limited for drug discovery. The focus of this research has been to utilize microdialysis sampling for the determination of drug delivery following dermal applications and as a novel *in vitro* drug transport design.

Microdialysis offers several advantages over traditional dermal techniques that make it ideal for drug delivery studies. This was initially illustrated by using multi-probe microdialysis which allowed the determination of concentration differences in a 1 cm^2 skin region. One of the main drawbacks to microdialysis sampling is the requirement of the test subject to be located in a laboratory setting. This research explored alternative sampling methods that allow the test subject to be in its natural environment. In particular, dermal ultrafiltration sampling and the use of the Alzet® osmotic pump as the pumping device for microdialysis sampling was

explored. Alternatively, as microdialysis sampling requires small sampling volumes its use for drug permeability studies was investigated.

6.2 Individual Study Summary and Future Work

6.2.1 Drug Delivery by Iontophoresis Monitored by Microdialysis

Microdialysis was a successful tool for the understanding of drug movement under iontophoretic conditions around a surgical incision. Traditional dermal sampling techniques have been limited in the amount of data provided due to their inability to continually monitor drug concentrations at specific regions.

Iontophoresis was found to enhance the amount of drug driven through an incision. This was verified by both the suture concentrations and the changes in the dermal concentrations. Lidocaine concentrations in the dermis 5 - 10 mm medial to an incision were 10 times less than dermal lidocaine concentrations in intact skin. The presence of a sutured incision did not affect the total free lidocaine concentration when the drug was delivered by iontophoresis. This demonstrates that total drug concentration is independent of the direction of drug flow and a function of the iontophoretic current of the patch.

Future work on the use of an iontophoretic patch in a region with a suture incision would involve a more in depth look of the concentration gradients around the incision. This would entail the development of a side-by-side microdialysis probe with a short spacer between the membranes. This probe would be implanted within the incision and would provide important information on the change in drug

concentration at different depths within the incision. Another interesting study would be to determine if there is a change in dermal concentration at different distances from the incision.

6.2.2 Dermal Sampling by Microdialysis and Ultrafiltration

An evaluation of cutaneous microdialysis and ultrafiltration sampling was completed in both the Göttingen minipig and the Sprague Dawley rat. Dermal ultrafiltration sampling in the Göttingen minipig allowed for consecutive sampling while the animal was freely moving. Microdialysis sampling required the animal to be restrained during sampling which limited the number of consecutive hours sampling could occur. The dermal penetration results obtained from the two sampling techniques were found to be different. Penetration results acquired from ultrafiltration sampling were delayed and lower than microdialysis data. A further investigation ensued in the Sprague Dawley. These results confirmed that the extracellular fluid extracted by ultrafiltration when sampling in the dermis comes from both the dermal regions and the subcutaneous regions, resulting in lower dermal concentrations. Therefore, microdialysis was found to be a superior dermal sampling technique compared to ultrafiltration

Future work for the dermal sampling in the Göttingen minipig project involves a more complete comparison between the dermal penetration of the Göttingen minipig and humans. This would involve the application of several high, medium, and low penetrating compounds.

6.2.3 Evaluation of the Alzet® Osmotic Pump as a Pumping Device

An assessment of the Alzet® osmotic pump as alternative pumping device for cutaneous microdialysis was completed. The flow performance of the osmotic pump was unaffected by the addition of a linear probe. When used for cutaneous sampling, the average flow rate of the osmotic pump had a much greater variation than an infusion pump. An internal standard was utilized that accounted for flow rate variations and resulted in variations comparable to the infusion pump. Sampling at shorter time increments produced similar results to the infusion data. The osmotic pump was found to be a successful pumping device for cutaneous microdialysis sampling.

Future investigations in the use of the Alzet® osmotic pump could include demonstrating its use in a larger animal such as the Göttingen minipig. Its use could also be expanded by either exploring different regions of the body, such as looking at the free blood concentration, or using a different pump size which would allow for multiple pump implantations.

6.2.4. Microdialysis for Drug Permeability Screening

This research explored the capabilities of a cell cultured microdialysis probe for drug permeability studies. Several cell culture conditions were optimized including sterilization parameters, coating techniques, and seeding density and frequency. A uniform cell monolayer consisting of either BeWo cells or CaCo-2 cells was grown on a microdialysis fiber. However, the integrity of the monolayer was not

sustained following perfusion of the microdialysis probe. The use of a cell coated microdialysis probe for permeability studies was proven to not be an ideal method.

Future work on the utility of the microdialysis probe for drug permeability screening could include finding methods to improve cell adhesion to the microdialysis membrane. Previous studies have cultured cells onto a capillary bed for the production of tissue-like structures *in vitro* [1-3]. These culture designs continually perfuse media through the capillary bed. By continually perfusing the microdialysis probes, the cells would grow under similar conditions as drug permeability screening. In order to apply this setup for microdialysis probes, a miniature perfusion circuit would need to be developed.

6.3 Future Directions

Overall, these studies exemplified the importance of microdialysis and explored alternative methods for cutaneous sampling. This acquired knowledge, allows for exploration into several crucial health issues. For instance, an understanding of the damaging effects caused from direct sunlight could be assessed with the techniques explored in this dissertation. The use of an osmotic pump implanted within a pig model would allow the pig to be exposed to direct sunlight within its natural setting. Exposure to ultraviolet radiation has been reported to have several detrimental affects that ends in the release of several mediators that include prostaglandins, nitric oxide, several interleukins and also depletion in antioxidant defenses such as ascorbic acid [4-7]. Microdialysis would be an ideal sampling

technique for this particular study as it would allow for the analysis of multiple analytes.

6.4 References

1. Gullino, P.M. and R.A. Knazek, *Tissue Culture on Artificial Capillaries.* Methods in Enzymology, 1979. **58**: p. 178-184.

2. Knazek, R.A., et al., *Cell Culture on Artificial Capillaries: An Approach to Tissue Growth in Vitro.* Science, 1972. **178**: p. 65-66.

3. Redmond, E.M., P.A. Cahill, and J.V. Sitzmann, *Perfused Transcapillary Smooth Muscle and Endothelial Cell Co-Culture- a Novel in Vitro Model.* In Vitro Cellular and Developmental Biology, 1995. **31**: p. 601-609.

4. Haywood, R., *Relevance of Sunscreen Application Method, Visible Light and Sunlight Intensity to Free-Radical Protection: A Study of Ex Vivo Human Skin.* Photochemistry and Photobiology, 2006. **82**: p. 1123-1131.

5. Leveque, N., et al., *Evaluation of a Sunscreen Photoprotective Effect by Ascorbic Acid Assessment in Human Dermis Using Microdialysis and Gas Chromatography Mass Spectrometry.* Experimental Dermatology, 2005. **14**: p. 176-181.

6. Rhodes, L.E., et al., *Ultraviolet-B-Induced Erythema Is Mediated by Nitric Oxide and Prostaglandin E_2 in Combination.* The Society for Investigative Dermatology, 2001. **117**: p. 880-885.

7. Shindo, Y., E. Witt, and L. Packer, *Antioxidant Defense Mechanisms in Murine Epidermis and Dermis and Their Responses to Ultraviolet Light.* The Society for Investigative Dermatology, 1993. **100**: p. 260-265.